Design and Simulation of an Efficient Hybrid Plasmonic-Photonic Waveguide

A Thesis

Submitted in fulfillment of the requirement for the award of the degree

Of

Doctor of Philosophy

Submitted by

TARUN SHARMA

Regd. No. 951106002

Under the guidance of

Dr. Mukesh Kumar

Assistant Professor

DEPARTMENT OF ELECTRONICS & COMMUNICATION ENGINEERING

THAPAR UNIVERSITY

PATIALA-147004, PUNJAB, INDIA

2015

Certificate

I, Tarun Sharma hereby declare that the work which is being presented in the thesis entitled **"Design and Simulation of an Efficient Hybrid Plasmonic-Photonic Waveguide"** is an authentic record of my own work carried out toward the partial fulfillment for the award of degree of Doctor of Philosophy in Electronics and Communication Engineering Department, Thapar University, Patiala, under the guidance of Dr. Mukesh Kumar.

The matter presented in this thesis is not submitted in any other university or institute for the award of any degree.

Tarun Sharma

Dated 11/04/16 signature of student

This is certified that the above statement made by the candidate is correct to the best of my knowledge and belief.

Dr. Mukesh Kumar
Assistant Professor
Electrical Engineering,
Indian Institute of Technology, Indore

Dated 11/04/16

ii

Abstract

Hybrid Plasmonic Waveguiding (HPW) is emerging as a tool which has the potential to realize low modal propagation loss with larger propagation length at nanoscale mode confinement. In this work, a detailed analysis is carried for the HPW for the low loss with deep subwavelength confinement. The improvement in the propagation length with low loss and mode coupling character of the hybrid plasmonic mode is obtained with various designs. The mode character for the hybrid mode and effect of high index layer on the waveguiding performance is also analyzed. The HPW with their deep-subwavelength mode sizes and long propagation lengths can be promising for applications in on-chip nano-scale devices such as nanolasers, biosensing and signal modulation for optical communication and optical interconnects.

In this work some of the novel designs of HPW are proposed one of which is hollow HPW. In our hollow design, long range propagation length obtained by optimizing the width and height of the air slice, sandwiched between metal and silicon leads to the confinement of Hybrid Plasmonic (HP) mode in the air. It is found that the introduction of air to confine the HP mode in the nanoscale can increase the propagation distance and can reduce the mode area, which done to reduce the effective index and the lateral optical spread. The analysis of optical mode confinement and propagation characteristic provides us low loss with nano scale confinement in the Hollow HPW.

The hybrid plasmonic mode is formed by the mode coupling between plasmonic and optical mode is shown. Mode hybridization of photonic and plasmonic modes in HP waveguide is proposed to achieve low-loss sub-wavelength (nano-scale) optical-confinement with variable optical nonlinearity. The coupled -mode-theory is used to calculate the coupling between the SPP and photonic- mode for the estimation of mode character. The high-index region under the (confinement) dielectric layer also plays a significant role in controlling the mode hybridization across the dielectric layer. It is found that beyond a certain thickness of high-index region evanescent filed into dielectric begins to lose its coupling with SPP mode

which disables the mode hybridization; the guided mode now becomes leaky photonic mode with larger field in the high-index region.

Further, some engineered structures of HPW by introducing the periodicity in HPW are proposed. Effect of different grating parameters like, (grating period, duty cycle, width, depth, grating length) on the waveguide characteristics is also studied. The garting shows the significant improvement on the propagation length with low loss and high nonlinearity.

A nanophotonic coupler based on HPW is proposed which shows long propagation length with high-speed coupling because of ultra-short coupling length. The introduction of a Lateral Subwavelength Grating (LSG) into the high-index layer in the HPW results in efficient coupling characteristics. The lateral resonances in the LSG modify the vertical coupling of HP modes providing us an ultra-short coupling length resulting from large phase difference between even and odd HP modes. Further the proposed coupler exhibits acceptably large propagation lengths for odd and even modes. In addition, the broadband nature of the LSG pushes the proposed coupler to show broadband coupling where coupling length remains acceptably small and the coupling performance remains high over a broad range of wavelength. The proposed work on the design, analysis and simulation of the HPW can be used to realize a nanophotonic platform with long range propagation with acceptably low-loss and nanoscale confinement.

Acknowledgement

First of all I would like to thank my Guru ji **Nirbhay Maharaj** for his grace, for providing an opportunity to pursue a Doctoral Degree. I would like to use this opportunity to express my sincere gratitude to my supervisor, **Dr. Mukesh Kumar** for providing me the research opportunities, his superb guidance and consistent support that enabled me to achieve all goals to complete this research to the best of my standard. Without his help, I would have never imagined that I could go this far.

I would like to show my granitite to the Head of the Department, **Dr. Sanjay Sharma** ECED, Thapar University for his encouragement, support and providing all the facilities for the completion of my research work. I would also like to thank my committee members for taking time to consider my work.

I would like to thanks my colleagues in HIET, Shahpur for their support and help and HOD ECE of DIT University. I would also like to thanks my friends Mr. Varun Mehta and Mr. Ajay Kumar for their help and suggestion.

My profound love and appreciation goes to my parents who have been the ultimate source of support not only during my studies but also throughout my life. Also, special thanks go to my dearest wife, Ms. **Priyanka Verma**, for her continuous encouragement, ever-lasting love and care. I am also very thankful to my beloved Son Adhrit Sharma who always remains the source of energy for me. I also take this opportunity to express my gratitude to Mr. Ranjeet Singh Punia, Mr. Abhishek Dwivedi and Mr. Yograj Rana and Mr. Vikram Chaudary for the help.

Last but not least; I would like to thank the Almighty, who has always guided me to work on the right path of the life.

Tarun Sharma

Table of Contents

List of Figures

List of symbols

dB	Decibals
λ	Wavelength
Ag	Silver
Au	Gold
Si	Silicon
SiO_2	Silica
h_{si}	height of silicon
h_{au}	height of gold layer
h_{air}	height of air slice
w_{air}	width of air slice
E	Electric field
n	Refractive Index
ε	Permittivity
ε_{si}	Permittivity of Silicon
ε_{SiO_2}	Permittivity of Silica
ε_{Au}	Permittivity of Gold
I	Laser Intensity
w_d	width of dielectric
h_d	height of dielectric
n_{eff}	effective refractive index
A_m	Mode area

$L_{prop.}$	Propagation length
L_m	Modal propagation loss
Λ	grating Period
C	Duty Cycle
t_d	Thickness of dielectric
γ	nonlinear coefficient
β	Propagation constant
A_{eff}	effective mode area
a	Mode character
Ψ	wave function
κ	Coupling coefficient
K	wave vector
t_g	Grating thickness
t_m	Metal thickness
L_c	Coupling Length
R	Coupler performance
f_{odd}	odd mode power

List of Acronyms and Abbreviation

EM	Electromagnetic
UV	Ultraviolet
nm	nanometer
mm	millimeter
µm	micrometer
THz	Terahertz
PC	Photonics crystals
IR	Infrared
LED	Light Emitting Diode
TE	Transverse Electric
TM	Transverse Magnetic
TEM	Transverse Electromagnetic
1D	One dimensional
2D	Two dimensional
3D	Three dimensional
1DPCs	One dimensional Photonics crystals
2 DPCs	Two Dimensional Photonics crystals
3 DPCs	Three Dimensional Photonics crystals
TIR	Total Internal Reflection
SP	Surface Plasmonics
SPPs	Surface plasmon polaritons

SERS	Surface Enhanced Raman Scattering
HP	Hybrid Plasmonic
HPW	Hybrid Plasmonic Waveguide
MMI	Multimode Interference
SOI	Silicon on Insulator
CMOS	Complementary metal oxide Semiconductor
PL	Photo-luminance
WG	Waveguide
HPSW	Hybrid Plasmonics slot waveguide
ER	Extinction Ratio
HDLW	Hybrid Dielectric Loaded Waveguide
HPMMI	Hybrid Plasmonic multimode interference
FDTD	Finite Difference Time Domain
FEM	Finite Element Method
MIM	Metal Insulator Metal
IMI	Insulator Metal Insulator
HPPs	Hybrid Plasmon polaritons
LRSPP	Long Range Surface Plasmon Polaritons
MSHPW	Metal strip hybrid plasmonic waveguide
WPPs	Wedge Plasmon Polaritons
CPPs	Channel Plasmon Polaritons
CyPPs	Cylinder Plasmon Polaritons

MMIM	Metal Metal Insulator Metal
LSG	Lateral Subwavelength Grating
GWD	Grating With Disordered Length
WDM	Wavelength Division Multiplexing

Chapter 1

Introduction to Nanophotonics

1.1 Introduction

The desire of access to information on the click of a button, to communicate without time and space constraints, the ability to stay connected is no longer a dream it is all possible due to advances in communication technology to the extent that the current era is known as the information age. What allows the information travel across long distances or who carries the information or how communication is possible with peers in distant places or how any or all these possible within a fraction of second? Is this possible at all? Yes, this all became reality, and yes, it is due to the hair-thin optical fiber which functions as waveguide to transmit light in this information age. Light the carrier of information signal in today's optical fiber links electromagnetic radiation in the waveguide. With the advent of Optical fiber came the need of a coherent light source that could revolutionize the communication industry and other challenges. In 1960, Theodore Maiman at Huges research laboratries, Malibu California worked out first operating laser[1], which created powerful flashes of red color light with unique properties such as temporal coherence and high spatial with very high brightness. Since then new developments in the field of laser with special properties have been revealed and drastic improvements have been made in terms of their costs, performance and viability. Over the last couple of years, it is the semiconductor laser which has received wide attention and has lead the way for compact and very efficient optoelectronic devices that are also know as semiconductor optical devices paving way for faster and more reliable communication systems. The other challenge was for obtaining optical fibers with very low propagation losses, new fabrication techniques were introduced which is also considered as the last push in this field [2-3]. However integration of fabrication with several photonic components on common planar substrate, the building blocks to fabricate the planar devices which are much more complex took us to field of integrated photonics.

1.2 Integrated Photonics

Since the invention of transistor, electronics provided the framework and formed the basis of information transmission. Electronics based systems used semiconductors devices for directing and controlling the electron flux. However, due to the urge for faster, reliable and more efficient systems as well as with the advent of (1980's) optics based systems the electronics gradually was partially replaced and largely supplemented by optics, as the frequency of light is high (200 THz), it permits large bandwidth for the purpose of managing and transporting a huge sum of information at faster rates of transmission. For the carrier of information photonics was substituted for electronics. Photonics is a mixed discipline which has appeared with the association of new developments with technologies such as electronics, gave birth to new as well as complex devices like light modulators, semiconductor detectors and lasers. These devices must be explained in terms of electronics as well as of optics these cannot be explained solely either by electronics or by optics. While electronics is discipline that deals with flow of electrons, photonics describes the control of photons. However, both of these two disciplines in many cases clearly overlap, for example in the case of detectors flux of electrons is controlled by photons, and for semiconductor lasers or electro optics modulators, properties of light propagation is dependent on the by constituent electrons .

Over the past couple of years new areas have been felt more relevant and have given birth to far more complex devices and newer fields of interest to the research community for example optoelectronics, waveguide technology, quantum electronics, electro-optics etc. when dealt collectively in light of existing devices like light modulators, lasers [4-10] and semiconductor detectors gave birth to the new family of devices which were much more complex than earlier devices, these new devices were not only complex but also improved performance of the system. Another significant contribution of these theories is the emphasis on need of treating light as flow of photons rather than electromagnetic waves in optical amplifiers and semiconductor devices as has been the case over the years. The advent of close relation between electronics and optics gave rise to novel photonic devices for example the semiconductor-based detectors (photodiodes)[11-12] and light-emitting diodes (LEDs)[13] are based on opto-electronics and quantum optics, some types of lasers or electro-optic modulators are based on acousto-optics and electro-optics, the optical amplifier that is based on non-linear optics & quantum optics, optical sensing, systems involving display and image, optical communications and optical computing as optical sensing is another applied disciplines that has grown out of these areas, systems and devices used in optical sensors, communication and optical computing are largely based on waveguide technology .

Integrated photonics [14-15] is the area of integrated optics come up as an growing branch of optics which integrates disciplines explained above. Figure 1.1 is depicting the integration of waveguide technology with disciplines like acoustic-optics, electro-optics and opto-electronics and non-linear optics which constitutes integrated photonics. It would be worth mentioning that silicon-based photonics has risen as a promising technology to become a standard platform for on-chip optics.

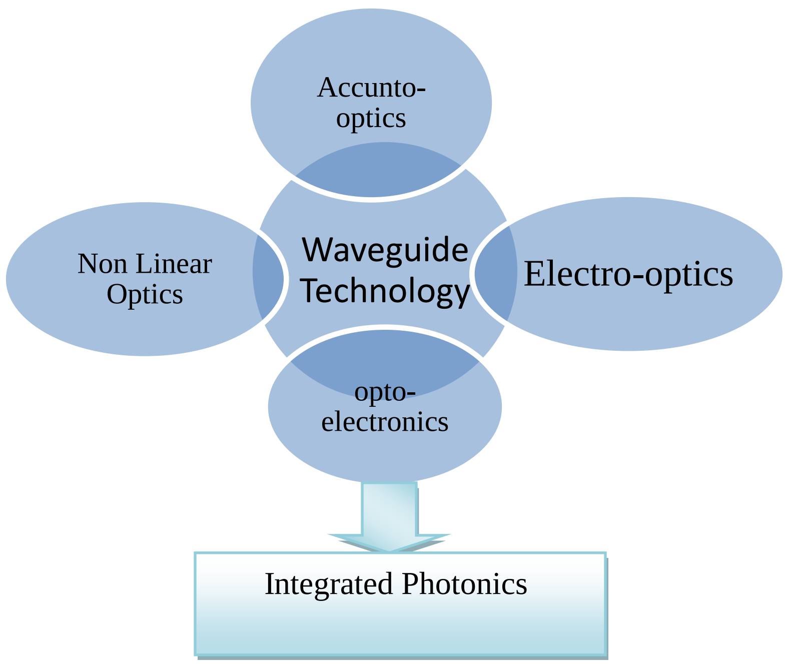

Figure 1.1 Convergence of many different fields into integrated photonics

The similarity between the integrated micro-electronics and planar optical circuits technology was first signified by S.E. Miller in 1960 and termed it as “integrated optics”. For Miller by using a process of integrating, interconnecting and combining a range of elements, may be active or passive and small optical transmission lines called waveguide [16] in a single substrate, fabrication could be done of integrated optical circuits was the way out presented by Miller.

It is obvious that in order to reduce the expenses of superior optical systems including the optical communication networks, integrating several optical functions in a single photonic device or on-chip photonics is the key. The basic optical components for the generation, isolation, modulation, light detection, splitting, junction, switching, focusing, coupling, polarization control, filtering and preferably all of them should be included and has been integrated on a single optical chip. The integrated photonics circuit is used for the optical interconnect applications. This type of the circuitry is used for the CMOS with the hybrid plasmonic waveguide. An example of this type of system is shown in figure 1.2.

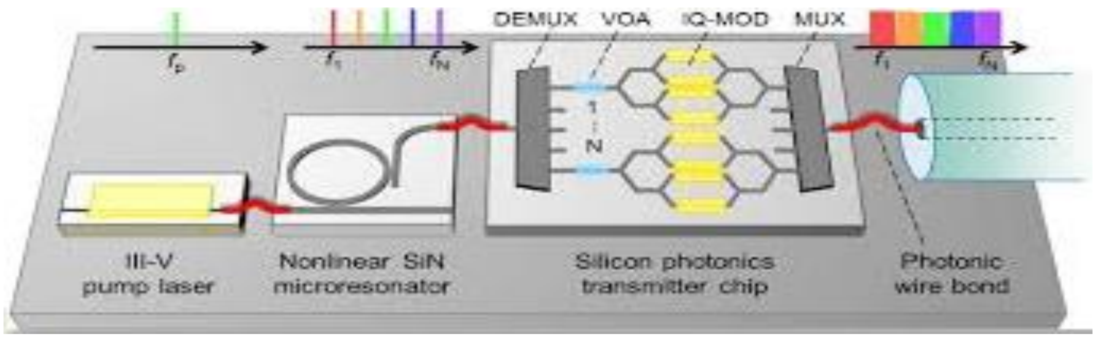

Figure 1.2 Chip Scale terabit optical transmitter [17]

Further for the interconnection of the variety of optical elements channel waveguides are used. Therefore the miniaturization of optical systems is the chief target pursued by integrated photonics. It is alike the way where electronic devices were miniaturized by integrated electronic circuits. Small wavelength of the light makes it possible only, as with sizes of the order of micron it permits the compact photonic devices and fabrication of circuits.

1.3 Nanophotonics

A novel technology that works with optical near field and mediates the interaction between nano metric particles is known as nanophotonics. It utilizes optical near field as electromagnetic field, located in close proximity to each other. The real character of nanophotonics includes realization of fabrication techniques, qualitative advancement in photonic systems and devices by using the novel phenomena and functions which happened due to optical near field interactions. Till conventional propagating light is used, its function and phenomena are almost impossible. Although in recent years plasmonics, photonic crystals, quantum dot lasers [18], silicon photonics and meta materials have remained as popular subjects to study whereas diffraction-limited wave optics [19] has been the base of them.

1.3.1 Photonic Crystals

A Photonics crystal generally possessing photonic band gaps and are periodically structured electromagnetic media [20-21].This periodicity is the electromagnetic analogue of a crystalline atomic lattice whose length scale in the band gap is in proportion to the wavelength of light. The periodic dielectric function (or equivalently a periodic index of refraction)[22-23] replaced periodic potential whereas macroscopic media took place of atoms or molecules having differing dielectric constants in the optical analogue, which is the photonic crystal. When the minimum absorption of light done by the materials and the dielectric constants of the materials in the crystal are adequately distinct, the reflections and refractions of light from all of the variety of interfaces can generate many of the phenomena alike for photons (light modes), created by atomic potential for electrons. Therefore to find out solution for the difficulty of manipulation and optical control the photonic crystal periodic with low-loss is found as the one way out. With specified frequencies in certain directions, photonic crystals are framed using photonic band gaps to avoid light from propagating. A photonic crystal permits propagation in a typical and in useful way. If for any polarization moving in some direction from a source for frequency range the photonic crystal restricts the propagation of electromagnetic waves, the crystal would be having a complete photonic band gap. To be periodic, dielectric lattice may be arranged along with three axis for creating a complete photonic band gap constituting a three-dimensional photonic crystal. The schematic illustrations of 1DPCs, 2DPCs and 3DPCs are depicted by figures 1.3(a), 1.3(b) and 1.3(c) respectively. Lattice constant is the spatial period of the stack; which corresponds to the lattice constant of ordinary crystals that are composed of regular array of atoms. The scale of lattice constant is one of the huge difference between ordinary crystals and photonic crystals.

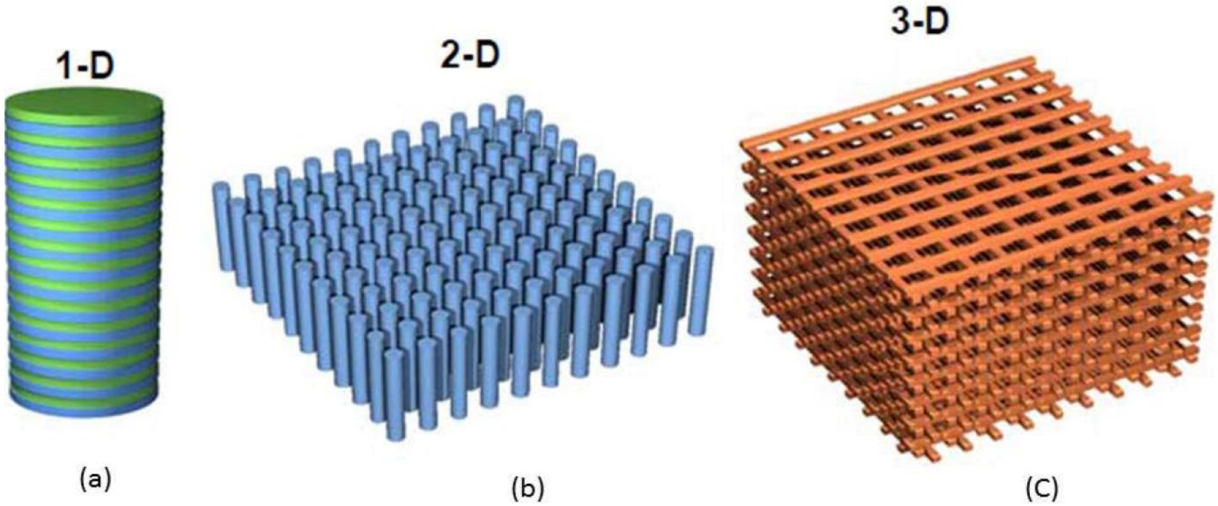

Figure1.3 Schematic illustrations of photonic crystals (a) 1D (b) 2D and (c) 3D [20].

1.3.2 Photonic Crystal Slabs

Photonic-Crystal slabs as shown in figure 1.4, consisting of two-dimensionally periodic index contrast are mainly introduced into a high-index guiding layer as an important class of photonic crystal structures. Without any coupling to radiations outside, the structures that support in-plane guided modes are completely confined by the slab. Inside the layer at the scale of wavelength, it is the guided mode that permits the control of light. Thus basic substrate may be provided by the slab structure for integration of large-scale and on-chip circuits and photonic components. With in-plane waveguiding, there is also a possibility of interaction of photonic crystal slabs with external radiation. The existence of guided resonances that takes place in the structures is particularly more important here. Just like the guided mode, electromagnetic power that strongly confined inside the slab is owned by the guided resonance. Light can be channel from inside the slab to the outside environment by using guided resonances because in contrast to the guided mode, the resonance can be coupled to the external radiation. Directional output couplers and lasers the very property has been exploited in designs of novel photonic light-emitting diodes which are crystal-based. Additionally, for filter applications the guided resonances can also influence the reflection and transmission of incident light leads to the complex resonant line shapes. To a minimum index contrast right from nontrivial brillion zones upto topological sensitivity the two dimensional photonic crystal systems[24] contains the majority of the chief features of photonic crystals and could be utilized to show the main proposed photonic-crystal devices. In all spatial directions, the possibility to manipulate electromagnetic radiation is one of the grand reward of photonic crystals. The realization of the fields by symmetry in 2-dimensions can be separated in two different polarizations: TE (transverse electric), where the magnetic field is perpendicular and the electric field is in plane and TM (transverse magnetic), where the electric field is perpendicular (z) and the magnetic field is in the (xy) plane, is the mean for understanding photonic crystals having two dimensions. Photonic-crystal slabs are hybrid Structures with two-dimensional periodicity but a finite thickness. They are not "two dimensional" photonic crystals, despite the resemblance: the finite thickness in the vertical (z) direction introduces qualitatively new behavior, just as the periodic dielectric waveguides differed from photonic crystals in one dimension.

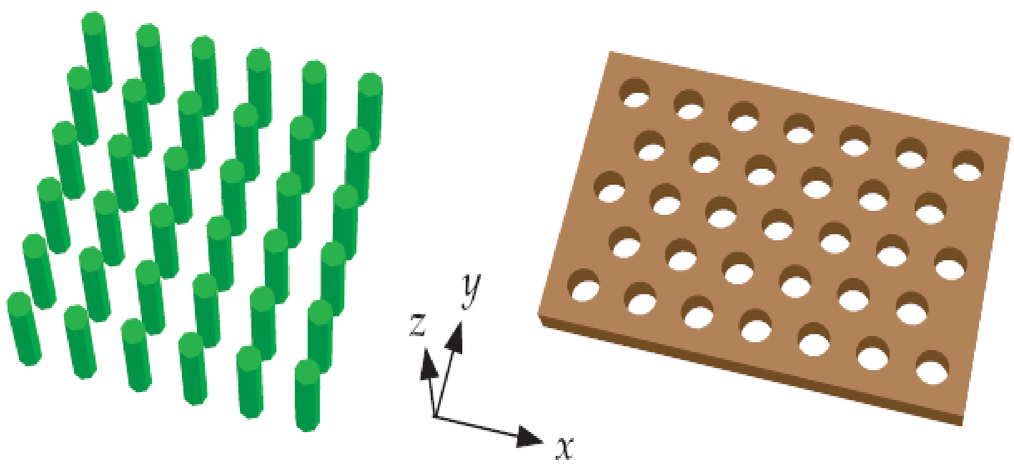

Figure 1.4 Photonic-crystal slabs combining two-dimensional periodicity (in the xy directions) and index-guiding in the vertical (z) direction. (a) The rod slab, a square lattice of dielectric rods in air. (b) The hole slab, a triangular lattice of air holes in a dielectric slab [24].

Photonic crystal slab has been utilized to realize number of photonics functionalities which includes band pass filters, super prisma effect, waveguide and cavity, communication, biosensors, light extraction in light emitting diodes (LED), spontaneous emission control and sensors dependent upon the photonic crystal slabs. Even with nanostructure of photonic crystal, it is difficult to confine the light in really nano region because of diffraction limit.

1.3.3 Slot Waveguide

The Progress in integrated optics by using the optical devices have reflected the ability to filter, split, bend and guide light on chips. The basic building block for the photonic integrated circuit is the integrated optical circuits they distribute the light among the various devices such as modulators, add-drops, filters polarizer, attenuators and switches with the use of the photonic wire.

Slot-waveguide alike the optical fiber has the ability to confine and guide light in a low index material which is nanometric-sized by making use of Total Internal Reflection(TIR). A slot-waveguide includes two strips which is comprise of high index material and is separated by using a sub-micrometer that have low index region [25]. The discontinuity of the electric field at high index contrast interface is the basic principle of operation of this structure.

Figure 1.5(a) depicts an electromagnetic wave propagating in the z direction and aligned in x direction, the electric field component of the quasi-TE mode shows a discontinuity which is proportional to the square of the ratio between the refractive indices of the high-index material that is the silicon nitride and the low-refractive-index slot material that is the silicon oxide. Upon comparing the high-index rails with the low index rails, it is observed that the field is very much intense in the low-refractive-index slot region. In comparison to the decay length of the field and the width of the slot, the electrical field remains almost high across the slot, which results in a power density in the slot which is much higher as in the high index regions. figure 1.5 (a) demonstrates the optical field distribution of the structure whereas the quasi-TE mode is depicted in figure 1.5 (b) which exemplifies the field improvement that takes place in the slot region. As there exist no involvement of interference effect and TIR mechanism is employed, very low level sensitivity is exhibited in the slot-structure [26]. High performance, ultra-sensitive sensors and active devices are possible applications of devices which are built with slot-waveguides, where high light matter interaction is desired.

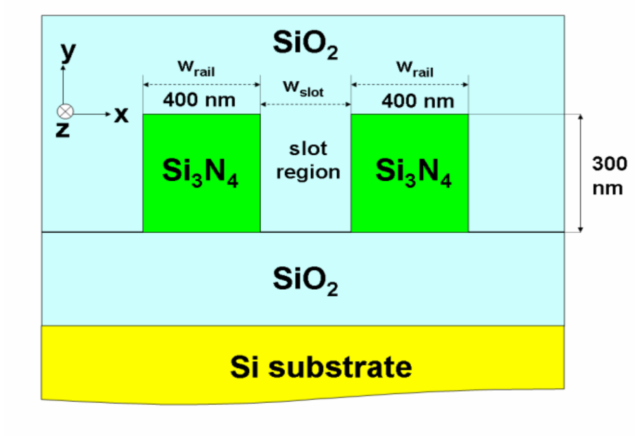

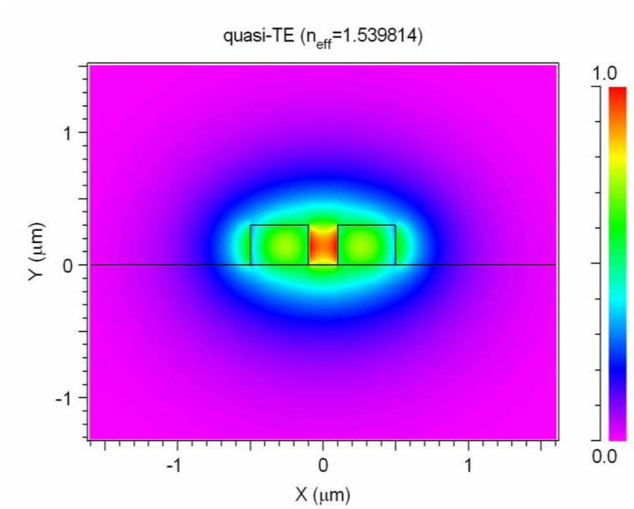

Figure 1.5 (a). Schematic cross-sectional view of a silicon nitride/silicon oxide vertical slot waveguide. b) Calculated electric field ($|E^2|$) distribution of the quasi-TE mode of the slot waveguide shown in Fig. 1.5 (a) [26].

1.3.4 Silicon Nanowire Waveguide

For the applications which range right from biosensing, telecommunications and to chip-to-chip interconnections in past years, the silicon photonics has presented various optoelectronic way outs which are low in cost. A range of devices such as modulators, four-wave mixers optical amplifiers and optical switches which have been demonstrated on silicon, the majority of the demonstrated devices make use of cross-sectional dimension based silicon strip waveguides in order to increase the optical confinement. This permit for designing of the waveguide bends with diameters that are reduced and also with increment in the diffusion of carriers in optical switches which lessen down the effective carrier for lifetime [27]. Because of scattering from sidewall roughness and for lowering down the loss, the process in the fabrication which is etch less of such waveguides has also been shown. These devices within the core of the waveguide take benefit of the increased optical fields. But in this regime the fundamental material properties which silicon contains do not change. Additionally below certain dimension there is loss in optical mode's confinement. Therefore, it is not possible to reduce the dimensions of the silicon core. An extension to these works by going to the regime of nanowire is promising because it is seen that different optical-carrier interactions are improved in the nanowire regime because of the quantum confinement and increase in the optical intensity [28]. Due to confinement in the quantum and increment in the optical intensity in the nanowire regime various optical–carrier interactions get enhanced. That is why going to the regime of nanowire and making extension to these works is quite promising.

Figure 1.6 is depicting the structure proposed. A SOI wafer as starting substrate and can be etched into an array of nanowire. Whereas on moving towards the vertical direction, transverse guiding of the optical signal is permitted by the refractive index difference that takes place between the insulator substrate and silicon.

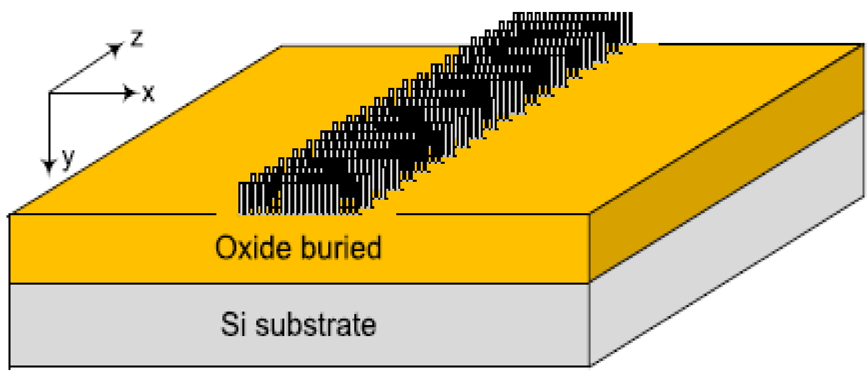

Figure 1.6 3-D diagram for arrays of SiNWs on SOI rib waveguide [28].

The guidance of light and applications in devices is considered as a significant standard of nano wires that are covered in optoelectronics devices. It is also demonstrated that nano wires which are semiconducting can also work just like nanoscale lasers, where lasing contrast in high refractive-index between the surrounding media and nanowire gives a optical cavity. The majority of the works regards nano wires of numerous 100 *nm* in diameter. Moreover in SiNWs as described above the increased material features are observed only for diameters which are less than 100 *nm*. A main difficulty of SiNWs is the lack of optical confinement particularly when the diameter is less than 100 *nm* . The low optical confinement as well as the low coupling efficiency suffers from two issues mainly. Even after correcting the low coupling efficiency by making use of tapers, the still devices suffers from critical alignment tolerances which leads to make the practical application of them a suspect for photonics

1.4 Plasmonics

Plasmonics, the density waves of electron, are produced on the surface of nano metal when light interact with it [29]. It is one of the electromagnetic properties of nano metals. Actually light will not interact with any matter which is less than its wavelength because of its property of diffraction [30]. But it goes entirely wrong because it is capable of interacting with metals at nano scale. When light falls on the surface of nano metal, excitation of electron results in producing large number of electrons (Plasmons), which converts that light energy in electrical pulse which has only short life span , eventually converts back into light . Presently, research is going on continuously using this plasmon for high speed data transmission. More over the sub wavelength is so small that it occupies only less space; so if it is to be developed, this would replace optical fibers. But the greatest disadvantage is that it is not stable, not even in millimeters.

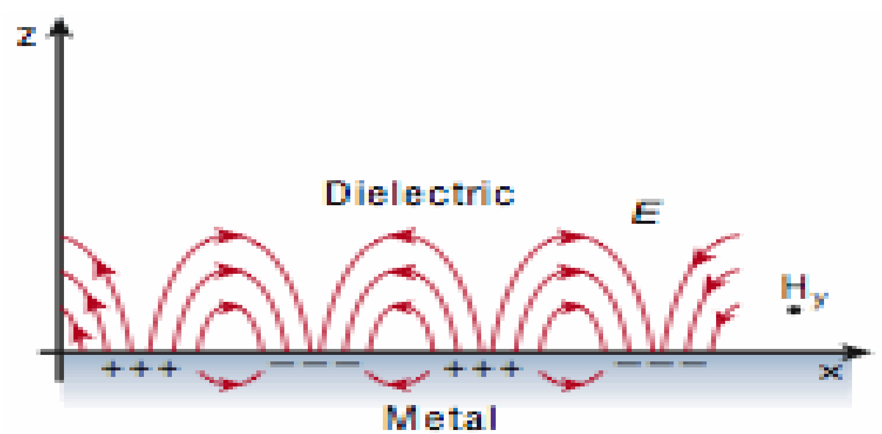

Figure1.7 Surface Plasmon [29]

In the field of fiber optics, optical data transfer requires bulky "wires" with reflective interiors which allows high bandwidth. Electronic data transfer requires tiny wires and operates at frequencies inferior to fiber optics. Plasmonics which is also known as light on a wire, regardless of the fact that besides photons the data moves in the form of electron density distributions along with the surface of a tiny metal wire that permits the data transmission at optical frequencies.

As discussed above Plasmons tend to dissipate after a few millimeters, thus resulting as the main limitation of plasmonics which is shown in figure 1.7. which makes them too short-lived to serve as a base for computer chips, that are just few centimeters across. Plasmonic waveguide technology would need even more improvement for sending data over longer distances. For this a material ideally negative with a low refractive index is used in such a way, that electromagnetic energy which is incoming is transmitted along its length as far as possible and reflected parallel to the surface of the material. For fabricating plasmonic devices which are efficient there must be make use of nanostructure materials as no natural material exists having negative refractive index. Therefore plasmonics is frequently associated with nanotechnology.

1.4.1 Plasma Physics

Surface wave plasma is "a bounded plasma" which "may support such (EM) waves which are guided along the boundary structure, their energy flux being concentrated in the vicinity of this surface". In short, the plasma guides the waves, which in turn provide energy to sustain the plasma. Simply, this is a type of plasma that is sustained by evanescently decaying electromagnetic surface waves, typically provided via a wave launcher such as a surfatron, surfaguide or microwave slot exciter/coupler. Initially, such plasmas were only possible in long, narrow tubes – which made them useful as a diagnostic tool, rather than a viable processing tool. However, recent developments have seen the generation of surface wave plasmas larger than 1 m^2 (supported by a dielectric plate, rather than a tube), which makes them particularly promising for large-area processing [31]. The physical foundations for surface plasmons consist of a few major milestones including, but not limited to: Mie theory for absorption and scattering of light by spherical particles and the Drude free electron model for metals etc. It should be noted that Mie theory, by itself, is geometric – the effect of a plasma is taken into account when the Drude Model is used to describe the dielectric function of the metal.The optical frequency is given by bulk plasma frequency which is obtained by Drude Model.

1.4.2 Surface Plasmon Polariton

The Modern photonics industry and research has gained number of significant developments in the recent years. For photonic circuits patent advantages in the data storage and delivery are there as compared with conventional electronic circuits. Therefore photonic devices such as waveguides, resonators and their integrations with electronic devices [32] have been gaining more and more attention at present times. Although miniaturization of photonic devices which are superior in the potential of signal delivery is always difficult. The optical fiber can efficiently deliver signals about three orders of magnitude larger than that of electronic devices, as a widely used optical interconnect, meanwhile its dimension is several hundred times larger than that of electronic devices[33-34]. This is mainly due to diffraction limit, as it reduces the dimension of a photonic device to be smaller than half wavelength (typically several hundred nanometers in optical telecommunication regime) that becomes a challenge. The realization of high density integration of these two technologies i.e. photonic and electronic devices is blocked due to huge mismatch between the photonic and electronic devices. To resolve such a problem, in recent years by utilizing the so-called plasmonic devices [35-45], a potential method has been proposed. These plasmonic devices have the capability of confining light in a deep sub wavelength scale by guiding the electromagnetic wave at a dielectric-metal interface. Therefore plasmonics simultaneously could have the advantages of both the electronics with miniaturized dimension and photonics with high-speed data delivery. Another than excellent mode confinement, plasmonic devices have another significant advantage which is the strong enhancement of the electromagnetic field. Optical gradient forces, Surface Enhanced Raman Scattering (SERS)[44] etc are such a special physical properties which are followed by it and widely applied in nonlinear optics, optical trapping etc. Metallic wire or stripe waveguides, metallic nano particle chain waveguides, wedge waveguides or plasmonic channel [36], dielectric-loaded plasmonic waveguides [41], plasmonic slot waveguides [40], hybrid plasmonic (HP) waveguides [46-49], etc are the various kind of waveguides which have been proposed in recent past years. The sub diffraction limiting guiding of the Surface plasmonic is achieved at very high loss. In the slot waveguide high loss is there with very low propagation length. Similarly the metal insulator and metal have tight confinement with very high loss. On the whole, these plasmonic waveguides have a trade-off between the mode confinement and propagation length. Figure 8, shows the various types of plasmonics waveguides, For example, the metallic wire or stripe waveguides have relatively large propagation lengths of various hundred micrometers or even several millimeters, however it is difficult for them to realize sub wavelength mode confinement; and for plasmonic channel or slot waveguides with deep-sub wavelength mode confinement, the propagation lengths are usually only several micrometers.

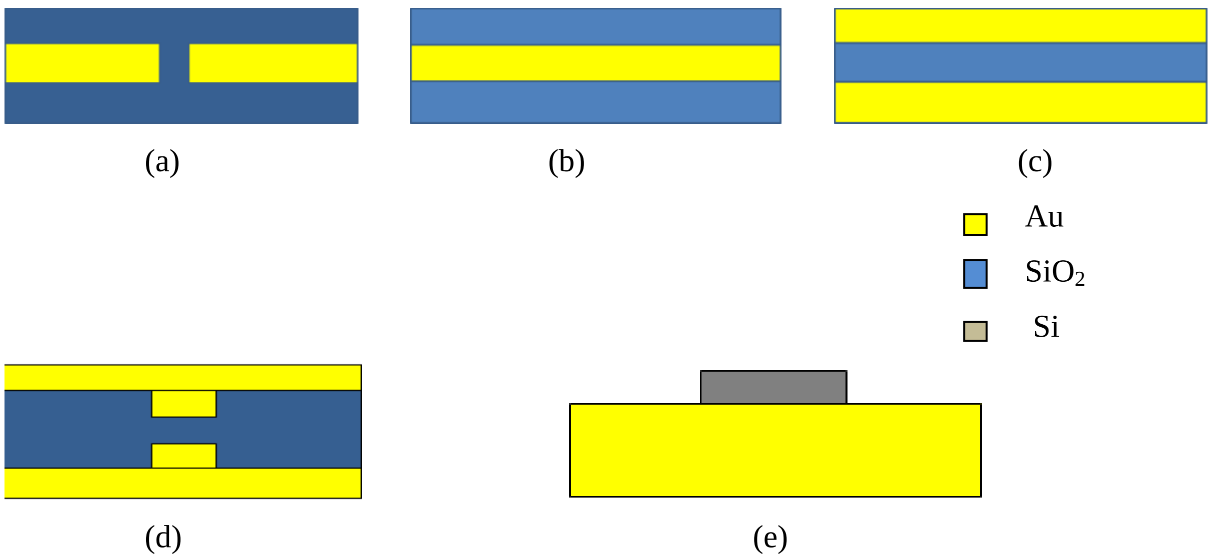

Figure 1.8 Various type of plasmonic waveguide (a) Plasmonic slot waveguide (b) Insulator Metal Insulator (c) Metal Insulator Metal (d) Plasmonic Wedge waveguide (e) Dielectric loaded Metal Waveguide

The surface-plasmon polaritons (SPPs) also known as short surface plasmon (SPs), are the respective modes which occurs at the interface between a dielectric and a metal and over the last number of years it has been observed that the outburst of research interest arouse in the field of nanoscale metallic structures sustaining both localized and propagating SPs. Surface Plasmon Polaritons (SPPs) refers to electromagnetic oscillations at the interface between a metallic layer [38, 43, 48] and dielectric layer. The electromagnetic fields can be well confined at the interface due to the existence of metal which can be exploited for sub wavelength mode confinement. The propagation length of a surface wave is relatively smaller than normal electromagnetic waves due to the large ohmic loss in metal leads to a large propagation loss. The SPP geometry for two-dimensional structure is shown in figure 1.9 and by making use of SPPs which propagates at a particular interface in between a thick dielectric and metal film for producing a wave guiding infrastructure, a lateral confinement of the SPP mode is required. By modifying the SPP dispersion relation by making local changes in the metal surface topology like holes and bumps and by creating a designer photonic surfaces we can achieve this. The SPPs at single interface leads us to the short range propagation of the mode occurring at the metal dielectric interface.

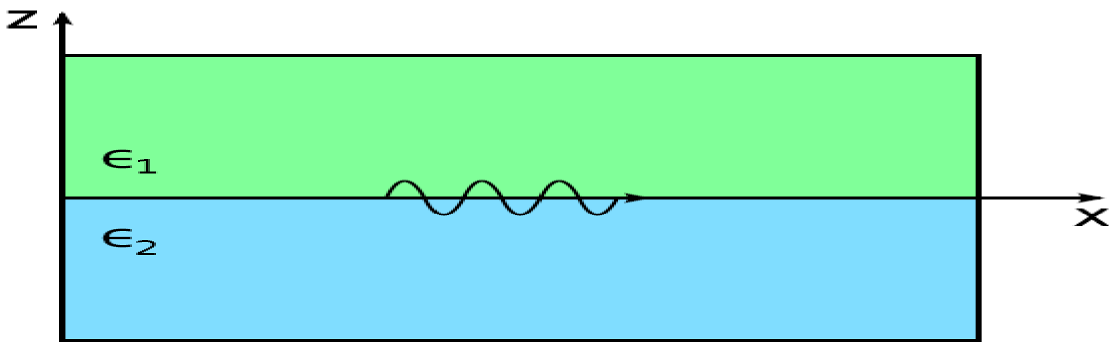

Figure 1.9 An electromagnetic wave propagating along the interface of two media [43].

When the metal film thickness (t) is small enough in order that the evanescent tails of the modes demonstrates significant overlap respectively, the field within the thin metal film which is decaying, the one surface giving support, the SPPs can couple with the SPP mode at the interface other than that, which will establish the two guided as well as leaky waves of opposite parities. The SPP frequencies used for a metal film which is thin and embedded in such a environment which is symmetric dielectric will be equal for the both top as well as bottom surface .There exists two way outs for coupled SPP modes which are purely bound: a high-frequency odd mode for infinitely wide metallic thin film which shows that in the direction of propagation, an asymmetric distribution of the component of the electric field which is longitudinal component and is associated with the collective electron oscillations as well as a low-frequency even mode. A marked difference was observed as due to the different symmetries of the spatial field distributions, both the modes demonstrate the obvious differences in the respective behaviors. The symmetry plane comprise of the three-layer based system the odd mode depicts a node of the longitudinal electric field component and for decreasing thickness it gets penetrated very less into the metal. However the limit of very much thin film, allowed by the distribution that is symmetric and the perpendicular component of the electric field evolves into the fundamental TEM mode that propagates in the homogeneous embedding material. Therefore, with decrease of the film thickness and concomitant decrease in confinement there exists a considerable decrease in attenuation. Thus the mode can be named as a long-ranging SPP. Further meant for the surface plasmons, the low attenuation of the bound odd mode and the small metal core thickness of IMI multilayer systems allow the propagation distances ranging from first to second orders of magnitude longer as compared to those which are having a thick metal film. However for metallic films ($t \approx 10$ nm) which are sufficiently thin besides from propagation length which is the multi-centimeter, its mode profile lends itself to effective end-fire excitation schemes. On the other hand, the bound even mode reflects the opposite behavior relating to attenuation and propagation constant both — with decreasing film thickness the field gets increasingly confined to the metal, as a mode having an asymmetric transverse electric field component could not have existence in a homogeneous background material [50-52]. For symmetric environment the bound modes don't demonstrate a cutoff thickness. Because of the mismatch in the surface plasmon frequency among the high- as well as the low -index interfaces that takes place for thin metal films which are embedded in an asymmetric environment, the situation becomes further complicated, that leads to a cut-off height in favor of the mode depicting decrease in the attenuation by film thickness, which goes on increasing with increase in the dielectric mismatch and reduction in the propagation length.

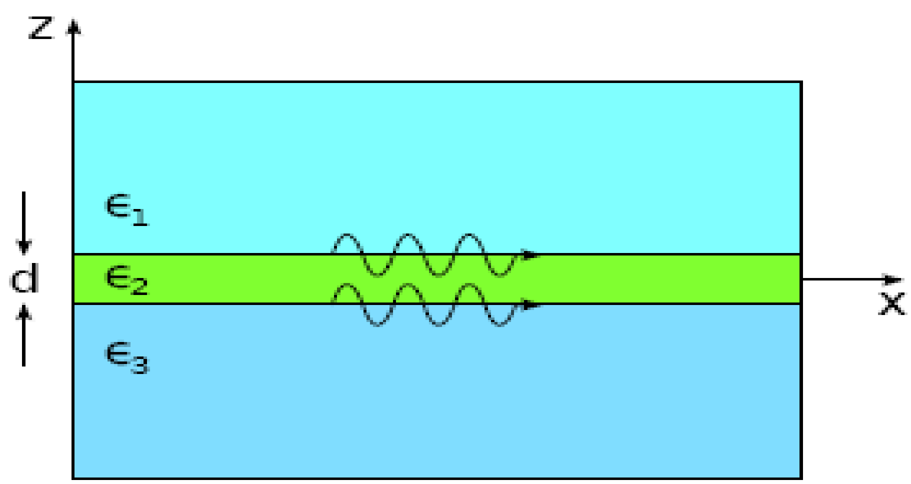

Figure 1.10 Surface Plasmon Polaritons Propagating along both sides of a film [50]

As shown the significant possibility for long-range wave guide which is based on SPPs via large propagation lengths of electromagnetic modes that are sustained by the Insulator Metal Insulator (IMI) stripe waveguides, the geometries are not appropriate to create sub wavelength photonic waveguides as per given reasons: first of all, in the regime of long-range guiding (corresponding to t<20 nm), with an evanescent tail which penetrates the adjacent dielectrics over the distances that corresponds to multiple wavelengths in the dielectric mode and still 2-D in nature, is just weakly confined normal to the plane of the waveguide. It is a consequence of the abovementioned tradeoff in between loss and localization: long-range guiding takes to weak localization. Therefore it is difficult to achieve the sub wavelength confinement that mainly limits the packing density of IMI waveguides. Also long ranging SPP modes have therefore been seen in stripe waveguides with $w/t >> 1$, and for the mode confinement a considerable decrease for stripe waveguides sustains a long-range mode that for the regime w<1 μm has been observed. More recently in IMI stripe geometries the work theoretical in nature that focus on analysis of various waveguide experiments has established the observed considerable increment in modal loss in regard to small-width regime. Both the width w and height t of the metal structure have to be selected of sub wavelength dimensions for providing a truly sub wavelength confinement of the optical mode by making use of a single metallic film that embedded in a dielectric: the ultimate scaling down of the metal stripe waveguides therefore outcome in metallic nano wires with a cross section considerably smaller than that of the diffraction limit of light. More recently it has been showed that for electromagnetic energy nano wires can act as waveguides with a mode confinement just below the diffraction limit and unidirectional propagation has been reported in bimetallic nanowire systems [28, 30]. The typical propagation lengths of sub wavelength confinement leads to the order of a couple of micrometers.

Surface plasmon polaritons are one of the most promising candidates for sub wavelength optical confinement. However studies mainly demonstrate the optical confinement similar to conventional dielectric waveguides of long-range surface plasmon polaritons due to practical reasons includes optical losses and stringent fabrication demands. Here a latest approach is followed that combine plasmonics with dielectric wave guiding. By nanoscale dielectric gap the hybrid optical waveguide consist of a dielectric nanowire and separated from a metal surface. The coupling that takes place between the waveguide modes and plasmonic across the gap makes ‘capacitor-like’ energy storage and permits the efficient sub wavelength transmission in non-metallic regions.

The Hybrid Plasmonic Waveguide (HPW) is relatively superior among these plasmonic waveguide. It is having a large propagation length with a sub wavelength mode confinement. In the integrated nanophotonics system, the waveguides are most important components that can be applied to interconnect all the other components. Figure 1.11 (a) demonstrates the schematic for the HPW.

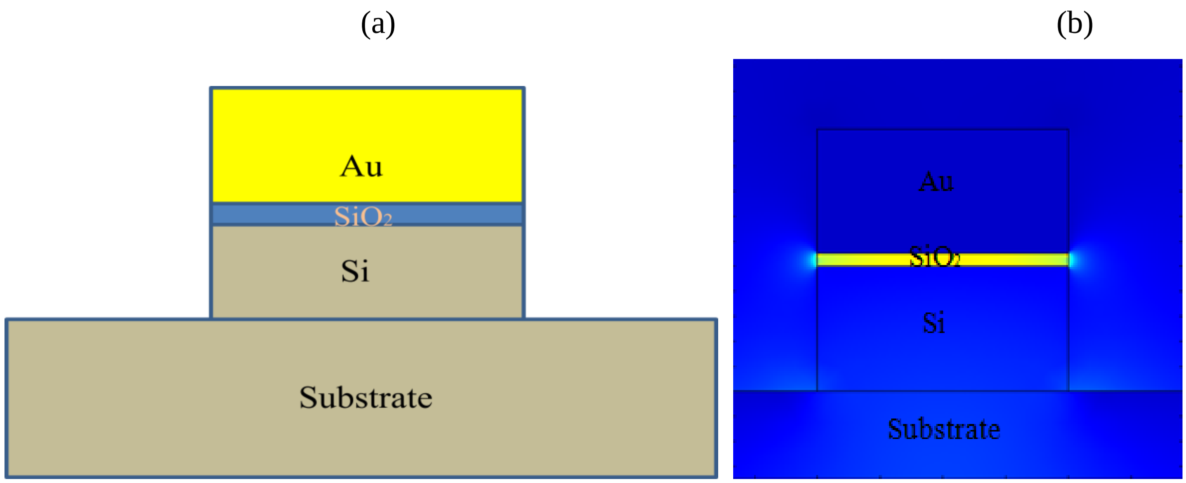

Figure 1.11 (a) A simple Schematic of the HPW, where low index region is sandwiched between metal and semiconductor (b) Field distribution of Fundamental TM mode with E_y field profile for HP mode.

For an efficient couple optical signals from a dielectric waveguide to a plasmonic waveguide as an extension, many other devices may also be referred which are based on waveguides in order to significantly a tapered structure or a directional coupler is required and to split light from one dielectric waveguide to several plasmonic waveguides, a Y-splitter or a multimode interference (MMI) may be a good choice. Meanwhile, the resonators are also important components in nanophotonics which are widely utilized as modulators or light sources. Although similar to other nanophotonics devices, there is a prominent difference in plasmonic devices as the existence of the propagation loss (Ohmic loss) which should be carefully considered in the design of plasmonic devices. On the other hand, with the excellent mode confinement there are many special functions which can only be realized in plasmonic devices such as extremely high purcell factor for laser cavity designs. For another advantage of the strong enhancement of the electromagnetic field of plasmonic devices, there are also many important applications, such as bio-sensor, SERS, optical trap

Chapter 2
Literature Review

2.1 Introduction

There have been significant developments in the field of photonics research and industry in recent years. There are patent advantages in the data storage and delivery for photonic circuits as compared to conventional electronic circuits. Therefore, photonic devices, such as resonators [57-60] and waveguides [53-56] and their integrations with electronic devices, have been the focus of research receiving high attention from the research community.

2.2 Literature Review

The huge mismatch, with respect to their sizes, between the electronic and photonic devices blocks the realization of high density integration of these two technologies. To overcome this drawback much has been proposed in recent years by utilizing the so-called plasmonic devices [35-45]. At the dielectric-metal interface, plasmonic devices having the capability of confining light in deep subwavelength scale by guiding the electromagnetic waves. Thus plasmonic simultaneously could have the advantages of both, the electronics with miniaturized dimension and the photonics with high-speed data delivery. The strong enhancement of the electromagnetic field is another significant advantage in plasmonic devices besides the excellent mode confinement.

Among the various Plasmonic Waveguide, a Hybrid Plasmon Polariton (HPP) concept is being proposed to overcome challenges associated with such a plasmonic waveguide such as high loss. HPW from by separation of metal surface by a nanoscale low dielectric regular gap, high dielectric constant semiconductor strip is used by this approach. This novel method offers reduced optical loss when compared to a metal–semiconductor interface design and simultaneously allows ultra-small mode confinement ($\lambda^2/400$) over a broad range of frequencies, as the hybridized Plasmon energy is concentrated in the low-loss gap. In addition to this, another advantage of the HPP mode, over other non-resonant plasmonic schemes, is the reduced optical loss by allocating most of the optical energy in the dielectric gap instead of inside the metal. This hybrid plasmonic waveguide is better in terms of loss and nanoscale mode confinement. Therefore HP waveguides are chosen as the major research area.

G.R. Bhatt et al -2012[61] studied the SOI waveguide device for the polarization sensitivity. He shows induced attenuation of TM polarized light with surface plasmon in the metal clad. The extinction ratio of TE vs TM is also studied.

Jing Xiao et al - 2011 [62] proposed and investigated the broadband hybrid plasmonic waveguide based on grating based Hybrid Plasmonic Slot Waveguide (HPSW) structure which consist of a vertical dielectric-slot structure. This is Sandwiched between the silicon rib and metal substrate and used as broadband filter near telecom wavelength. The grating propagation length is improved, optimizing cross-sectional structure, resulting in an enhancement in the optics confinement. A light reflective efficiency of 75% can be achieved by the Bragg grating, at telecom wavelength of 1550 nm with effective mode area 0.06177 μm^2. While revealing the design dependency this grating duty cycle has a major effect on the grating reflection spectrum.

Yao Kou et al -2011 [63] proposed a hybrid plasmonic waveguide with higher-order plasmonic modes of Ag nano wires by coupling the photonic modes of a Si waveguide. It was demonstrated that obtained HP modes possess reduced mode areas with longer propagation length with efficiency up to 90%,when compared to the conventional dielectric modes. They further projected a different model of HPW constructed by embedding SiO_2 covered Ag nano wires into a Si waveguide because metal nano wires build integrated optical circuits due to their small size and flexible shapes. Crosstalk between two parallel waveguides is calculated by using the coupled mode theory, is an attempt to assess the show of the present waveguide in integrated circuits. The calculations also demonstrated that he had obtained better coupling efficiency as compared to others. This type of structure is used as high-density photonic integration by these properties.

Volker J. Sorger et al -2011 [64] demonstrated experimentally, the deep sub-wavelength scales optical wave guiding with low loss. For nano scale photonics, because of the property that the wavelength can be scaled down below diffraction limit, a potential solution was proposed as Surface Plasmon Polaritons and collective oscillations of electrons at metal-dielectric interfaces. However the direct experimental demonstration for low-loss propagation with deep sub-wavelength nano scale optical modes, which pushes the electromagnetic field into the metal, could not been realized, owing to the rapid increase in the optical mode's propagation loss on scaling down the optical mode. As a result, in particular, for optical interconnects, the use of plasmonics for integrated photonics remains uncertain.

Yu Wakabayashi et al -2011 [65] studied a polarizer based on TM-Pass/TE-Stop on a Surface Plasmon Resonance by (Finite Difference Time Domain Method) FDTD method. His design consisting of a dielectric grating in which metal film is placed. High reflectivity of TE wave, with a subsequent high Extinction Ratio (ER) and a high transmission for the TM wave, appropriately chose the thickness and width of the dielectric grating. The case of an oblique incidence with respect to the grating plane, was considered by him. Calculations at normal incidence show that a transmission of more than 94% for the TM wave was obtained at λ = 1.55 μm. A high ER of more than 17 db over a wavelength range of 1.50 μm to 1.75μm was obtained and at λ = 1.55 μm, the TM-pass/TE-stop operation was achieved with a transmission of more than76%.

Later on, different types of hybrid plasmonic waveguides, for calculation of field confinement, effective refractive index and the propagation length were proposed by many researchers for nano-photonics circuits. The hybrid dielectric loaded plasmonic nano waveguide was proposed by **Hong-Son Chu et al -2011 [66].** It was shown that a good choice between field intensity confinement and the propagation length than a MIM nano slot waveguide could be achieved by HDLW

Yi-Song et al-2011 [67] Conducted theoretical investigation of multimode interface power splitters, based on HPW for efficient realization of power splitting with optimally structured parameters for MMI. It is a widely implemented device and the corresponding1x3 and 1x2 SOI-HPMMI.

The Coupled mode theory used for study of modal properties of hybrid plasmonic waveguide were investigated by **Lin Zhu-2010 [68]** by applying Finite Element Method (FEM). The normalize mode areas, subwavelength confinement factors, dispersion relations and thresholds of different super modes were calculated. Lowest threshold mode is determined by the hybrid waveguide and there is a reign where the maximum energy of hybrid mode is confined by the nanowire–metal hybrid waveguides. Nano scale laser is design with such type of devices. Nanowire radii is reduced to such an extent to obtain the deep sub-wavelength scale plasmonic laser and here symmetric hybrid mode is the only confined optical mode. The mode with larger area know as perturbed super mode act as lasing mode when the nano wire radii is not sufficiently small.

Yi-Song et al-2010 [69] investigated theoretically a broadband coupling of light between a hybrid plasmonic waveguide and dielectric waveguide. Plasmonic linear taper is used as to connect to types of waveguide which act as coupler. Mode mismatch between two waveguide and interface reflection is the main reason for the coupling loss.In this way the coupling competence is improved from 60% to 70% as compared to direct coupling.

Using Bragg grating and integrated Plasmon waveguides there has been much research carried out on the FDTD method. Much work is going on regarding low absorption loss, low scattering losses and long range propagations. One of the paper in this field is proposed by **Jian-wei et al -2009 [70],** who, theoretically studied the IMI surface plasmonic waveguide for a low-loss Bragg grating structure. The power reflectivity, transitivity and loss depends on metallic strip thickness was studied by them. The peak reflection and the transmission pit decreases with the increase in the thickness of the metal strip. The refractive index difference between the dielectric media on the reflection and transmission spectra on the gratings with the increase in the thickness of the strip is also studied .Comparison was made between the loss of the current structure and reflection with the SPP's voltage grating structure in order to further illustrate performance of the proposed structure.

A out-of-plane optical coupler based on a tapered hollow waveguide based optical coupler with out of plane characteristic was proposed by **H. Dalir –et al 2014 [71].** The modeling of the entire C-band is done with low polarization and wavelength dependences at 35 nm wavelength window (C-bands). The relative lateral displacements per spot size of the vertical output were less than 0.13 and 0.38 for TE and TM input modes respectively. The polarization-dependent insertion loss for TE and TM mode was below 1.35 dB.

Qin Zhang et al -2009 [72] studied MIM optical filter using novel sub wavelength Surface Plasmon Polaritons and numerically simulated using the FDTD with perfectly matched layer absorbing boundary conditions. Electromagnetic energy in a subwavelength limit can be confined and propagated due to the interaction between the free electrons in metals and photons the Surface Plasmon (SPs) trapped propagating on the surfaces of metals. The power dissipating from the cavity segment decreases when the coupling strength of the MIM coupler decreases and increasing the gap. By enhancing the asymmetry of the coupler the segment width increases and thus the coupling strength decreases. By using simulation he showed that the device has typical characteristics of a wavelength filter. Fabrication difficulties could be reduced with the help of simple structure with sub wavelength size when compared to previous grating-like hetero structures of a few micrometers in length. The new structure may have applications in ultrahigh nanoscale integrated photonic circuits on flat metallic surfaces. Conditions for compact photonic integration could be achieved by use of SPP waveguides, metal-insulator-metal (MIM) devices. Low radiation loss with ultra-high-intensity electromagnetic modes gives transmission of optical signals around sharp bends. The intrinsic ohmic loss in metal produces large loss in the MIM waveguide. When EM mode are highly confined to the metal surface, high coupling losses create problems for construction of integrated optical devices with MIM waveguides with low energy transfer efficiency.

Dmitri K. Gramotnev et al -2009 [73] proposed plasmonic beyond diffraction limit. Owing to significant mode mismatch, efficient coupling of input radiation delivered either by an optical fiber into a nanoscale SPP waveguide or freely propagating from a laser source is a challenge. A coupling scheme with generic coupling used for the excitation of the SPP mode with the help of tapered configuration similar as used for plasmon nanofocusing.

A hybrid plasmonic waveguide configuration that shows the coupling between optical waveguide and bound SPP mode was proposed by **Oulton et al -2008 [74]**. These hybrid plasmonic waveguide have advantages of SPP waveguides with the high-index-contrast semiconductor waveguides. These HP mode gives the volume 100 times smaller than that attainable at the optical diffraction limit in comparison to conventional MIM modes with reduced propagation losses. With help of these devices, design and development of deep subwavelength photonic integrated systems is possible. A new approach for low-loss with deep-subwavelength light confinement by controlling the hybridization of the fundamental mode of a dielectric cylinder, with the SPP of a dielectric metal interface while simultaneously achieving nano scale confinement and long range propagation. While keenly manipulate truly nanoscale optical fields, realization of waveguide loss compensation techniques with other schemes could be achieved as a consequence, would use this hybrid approach for integration of high gain semiconductor materials and plasmonics.

R F Oulton et al-2008 [75] studied the nano scale confinement and modal propagation characteristic of the subwavelength plasmonic modes for different type of the plasmonic structures like WPPs, CPPs CyPPs, HPPs. Out of these structures, Hybrid Plasmon polaritons structure is compatible with integrated photonics systems such as SOI-based photonics architectures. For nano-scale focusing HPPs are capable of overall energy confinement as well as strong enhancements of spontaneous emission. With the same size of nanoscale confinement in other waveguides HPPs have good propagation characteristics which show improvement in propagation length.

Georgios Veronis et al -2007 [76] proposed a structure using the plasmonic slot waveguide for subwavelength confinement. The modal properties for 3-D sub wavelength plasmonic slot waveguides were investigated by him. The fundamental mode is always a bound mode which is supported by a symmetric plasmonic slot waveguide with a thin metallic film with subwavelength slot embedded in an infinite homogeneous dielectric for waveguide parameters and operating wavelength with any combination of these. Modal fields are confined in wavelength range from zero frequency to ultraviolet. In this design asymmetric plasmonic slot waveguide is characterized for study of cutoff wavelength above which the mode becomes leaky and also study of cut off metal thickness and slot width by the surrounding dielectric media above and below the metal film, above which the mode becomes leaky. He calculated the eigen modes of plasmonic waveguides at given wavelength using a full-vectorial FDTD mode solver. The characteristic of the symmetric slot waveguide of supported mode by the variation of the parameters is also studied. It was thus found that as the metallic film thickness approaches zero, its propagation length decreases, while effective index of the fundamental mode increases and an asymptotic nonzero value is approached by its modal. The fringing fields of the mode are shown by this behavior.The fundamental mode characteristic support by the plasmonic slot waveguide are pretty tolerant to variation on the sharpness of the slot corners connected with the fabrication process.

SPP excitations by interfaces between metallic and insulating media at near infrared frequencies for the waveguiding applications, was proposed by **Stefan A. Maier – 2006 [77].**He showed that in order to provide a truly subwavelength confinement of the optical mode, using a single metallic film embedded in a dielectric both the height *t* and width *w* of the metal structure have to be chosen of sub wavelength dimensions and the eventual scale down of the metal stripe waveguides with metallic nanowire with a cross section geometry beyond diffraction limit of light. It was further concluded that since field penetration into the metallic media is a necessary requirement for the occurrence of SPPs there exists a general tradeoff between localization and loss. Hence a judicious choice of wave guiding geometry is necessary for particular applications such as a long-range (and thus low-confinement) propagation and a high confinement (and thus short-range) wave guiding for achieving a high packing density of waveguides on future optical chips.

Plasmonic Bragg reflector structure with low loss and nano scale confinement was proposed by **Amir hosseini et al -2006 [78]**. He shows that with Periodic changes in the dielectric materials of the MIM waveguides which was utilized to design effective filtering around the Bragg frequency. Realistic material parameters results with FDTD simulation were with the transfer matrix approach for utilizing the effective indices associated with subwavelength waveguides.

Xiang-Tian Kong et al -2012 [79] Researched in the field of plasmonic waveguide and moves towards the structural variation of plasmonic devices. He shows that the unique properties of plasmonic modes supported by MMIM that could not be observed in the MIM structures. The MMIM Structures give substantial insight into the guided plasmonic modes in them and are helpful for supple designing of MIM type waveguides and MIM-based devices. Depending on the index distribution or the geometric parameters, MMIM structures can posses either larger propagation length or better energy confinement as compared to the corresponding MIM structures. By this the Modal properties of hybrid plasmonic- photonic waveguide can be improved further.

Recent Research in the field of HPW for low material gain have opportunity to use the plasmonic devices in lively application such as amplifiers, sources, and modulators. One of the papers in this field as proposed by **Linfei Gao et al -2012 [80]** by using active metal strip hybrid plasmonic waveguide (MSHPW) for gain materials and low loss compensation. With tuning ability waveguide dimensions gives low propagation loss and tight mode confinement of the waveguide are efficiently controlled. From the simulation it is observed that at metal strip width 350 nm both nanoscale compact confinement and low-loss propagation length is obtained.

To address the problem of coupling, a research paper on this field as given by **T. P. H. Sidiropoulos et al- 2012[81],** who studied an antenna consist of two metallic nanoparticle with efficient low dispersion light coupling, into a silicon waveguide for the efficient efficiency. For comparable efficiency with low dispersion over a much broader spectrum, conventional grating couplers with sub-wavelength optical coupler is designed. It was found that coupling of pulses at 500 nm bandwidth near infrared telecom bands as shot as 50fs, with low group delay dispersion.

A novel HPW with two identical dielectric nanowire Symmetrically placed on each side of a thin metal film was studied by **Lin Chen et al -2012 [82]**.Deep-subwavelength mode confinement upto subwavelength scale with strong interaction between LRSPP mode of a thin metal film and dielectric cylindrical waveguide mode. The strong coupling is achieved between the gaps of dielectric nanowire and metal film with simultaneously achieving deep subwavelength optical field in between dielectric cylinder waveguide mode and long-range SPP mode. Enhanced optical forces with increased propagation length can be expected as a combination of ultra-low loss and strong coupling strength between the dielectric waveguide mode and plasmonic mode. At the same time there is a gap on the mode hybridization of two uncoupled mode using couple mode theory in this paper.

2.3 Relative Issues

Large propagation loss & weak confinement:- While designing of hybrid plasmonic nanophotonic device(s) low loss and strong confinement is required. Various plasmonic devices are reported in literature but low loss and strong confinement is by default achieved simultaneously. Nanoscale optical confinement with low loss is the biggest issue with the plasmonic waveguide due to ohmic loss of metal. In order to avoid such problems to some extent there is a need to design HPW devices. For practical applications in plasmonic devices low loss and strong confinement are desirable.

Coupling efficiency of coupled waveguide devices:-Coupling efficiency of coupled waveguide devices is required to be calculated for coupling performance assessment of the waveguides in photonics devices. This results in improving the packing density. It has been shown through literature survey that during coupling of plasmonic waveguide with dielectric coupling loss, there is mode disparity between two. Interface refraction and the mode mismatch between the two waveguide is the main cause of the coupling efficiency. The coupling efficiency is determined by the energy losses caused by mode mismatch. In hybrid plasmonic- photonic devices, plasmonic waveguides is used for miniaturized devices whereas dielectric waveguide used for longer propagation of the optical signal. So there is a need to study the efficient coupling between dielectric waveguide and plasmonic waveguides, to realize hybrid plasmonic- photonic devices.

Analysis of propagation characteristic of hybrid waveguide:-A nano- scale optical waveguide is the basic element for photonic Integrated circuit. SPP waveguide provides us nano confinement of light with nanoscale waveguide. It has been shown, through literature survey that nano scale plasmonic waveguide has issue with large loss and propagation distance is usually on a scale of several micrometers. Thus there is a need of HPW which integrates dielectric waveguide with plasmonic. They support photonic plasmonic-hybrid mode which offers tight mode confinement with low propagation loss. So there is a need to analyze the propagation properties of hybrid waveguide, such as mode area, propagation length, and propagation of mode energy that propagates with in the mode area and normalized energy density.

Simulation of hybrid nano devices:-Grating based devices act as narrow band stop filters. Bragg grating has been intensively studied as waveguiding characteristics can be tailored using grating structure optimization. Optical systems have application using the grating based devices. It has been shown through literature survey that SPP- Bragg reflector, crystal based on IMI geometry, subwavelength confinement in these devices is not obtained for photonic devices. This is due to much longer penetration depth of the SPP fields penetrate into dielectric medium larger in comparison to that into metallic medium at the SP interface. The cross sectional geometry of metal insulator metal (MIM) constitutes the long range SPP mode which have lower loss. So there is a need of insertion of nanostructured Hybrid Plasmonic Photonic grating waveguide devices which can provide an ultra high mode confinement & reduce propagation loss. These devices are the promising candidates for future integrated photonic circuits.

2.4 Research Gaps

1. The performance evaluation (based on various propagation characteristics) of hybrid plasmonic- photonic waveguide for Integrated photonic devices has not yet done [90, 73-74].

2. Less work has published so far on hybrid plasmonic waveguide based on coupler with broadband coupling efficiency [81, 67- 68].
3. Less work has done on insertion of nanostructured grating in hybrid plasmonic waveguide [81, 65].

4. There is a scope of improvement in the propagation characteristics of hybrid plasmonic waveguide for efficient integrated devices [79, 66].
5. Less work has done on the mode hybridization of two uncoupled hybrid plasmonic modes [81, 71-72].

2.5 Research Objectives

On the basis of the understanding established from the initial study and literature survey the following objectives are proposed:

1. Optimization of hybrid plasmonic-photonic waveguide parameters.
2. To study the effect of grating parameters like (grating period, width, depth, Length) on the waveguide characteristics.
3. To propose an efficient design of hybrid plasmonic-photonic waveguide with Improvement in propagation characteristics.
4. Design and simulation of coupler based on proposed hybrid waveguide.

2.6 Methodology

1 Hybrid plasmonic-photonic waveguide will be designed in the Finite element method (FEM) based on COMSOL Multiphyscics.

2 Optimization of Hybrid plasmonic waveguide parameters like various modal characteristics (Dispersion relation, Normalized mode area, confinement factors, propagation loss, and effective mode index) will be done on Finite element method (FEM) based on COMSOL Multiphyscics.

3 The effect of grating parameters like (grating period, width, depth, Length) on the waveguide characteristics(Propagation length, normalized optical power, effective mode area) will be done on Finite element method(FEM) based on COMSOL Multiphyscics.

4 The improvement in propagation characteristics of hybrid plasmonic –photonic waveguide will be steadying by varying the geometrical cross sectional parameter in the proposed structure in eigen value solver of Finite element method (FEM) based on COMSOL Multiphyscics.

5 The FEM will be used for the simulation of eigen modes of hybrid waveguide.

2.7 Thesis Organization

The thesis has been organized into seven chapters. The content of each chapter is briefly described below:

Chapter 1: This chapter comprises of introduction regarding major theoretical concerns. In this chapter a brief introduction of Plasmonic Waveguide is also given.

Chapter 2: After the introduction of the Plasmonics in chapter1, chapter 2 will cover the literature review related to area and objectives of the study.

Chapter 3: This chapter will mainly deal with the parametric study of hybrid plasmonic-photonic waveguide parameters and will present the proposed novel hollow hybrid plasmonic waveguide and its various modal characteristic: like Modal Propagation Loss, Effective Mode Area, Propagation Length and Nanoscale Confinement of the Hybrid plasmonic mode.

Chapter 4: This chapter will show proposed efficient design of hybrid Plasmonic-photonic waveguide with improvement in propagation characteristics. In this chapter mode hybridization will be explained by using the couple mode theory and the significant role of high-index region, silicon in controlling the mode hybridization across the dielectric layer will also be explained.

Chapter 5: This chapter is confined to study the effect of grating parameters like (grating period, width, depth, Length) on the waveguide characteristics. This chapter will cover the effect of grating period and duty cycle on the propagation length, effective mode area, nonlinearity, modal propagation loss.

Chapter 6: This chapter comprises of design and simulation of the coupler based on the proposed hybrid plasmonic waveguide. Further a new design in with coupling length, odd mode power loss, coupling efficiency by the even and odd mode beating of the hybrid plasmonic waveguide will also be shown.

Chapter7: This chapter draws the conclusion, and more importantly recommendations on the basis of results obtained for the future scope.

Chapter 3

Novel Hybrid Plasmonic Waveguide for Longer Propagation

3.1 Introduction to Hybrid Plasmonic Waveguide

With the introduction of the integrated photonics and plasmonic waveguide in chapter 1 and further with the literature review for the plasmonic waveguide in chapter 2, in this chapter hollow core hybrid plasmonic waveguide design is proposed. Hollow waveguide have many applications in the integrated photonics. It gives the tight control on the optical confinement to the nanoscale. Its application includes the Bragg reflector, optical switches etc [83-84]. As a solution to the issue of propagation loss of SP, a new waveguide, which we designate as a Hybrid Plasmonic Waveguide (HPWG) is proposed [46, 73-74]. HPWG offers a number of advantages: a better compromise is presented between loss and confinement as compared to purely plasmonic waveguides, and this is more well-matched with silicon on insulator technology. TE and TM modes power in such a guide are intense in two dissimilar layers, controlling of their properties can be done in different manners by altering their material properties and the dimensions of waveguide layers- a property that can be used to design new kind of photonic components. Because of these attractive features the proposed guide has grasped the attention in current years. Many different variations of HPWG have been investigated by different groups and many different applications have been suggested [45-46, 62-64, 73] here.

The advantages and limitations of plasmonic and dielectric waveguides are in some ways complementary. Dielectric waveguides can be practically lossless but the mode size in such guides is limited by diffraction. Plasmonic guides on the other hand can squeeze light far below the diffraction limit but at the cost of large propagation loss. An interesting query arise which has to be questioned that: what will be the outcome if one attempts to unite both guiding mechanisms? The response is the Hybrid Plasmonic Waveguide (HPW), and this is the topic of investigation in this dissertation. It has been explained in the previous chapter that a metal-dielectric interface for example the silver-silica crossing point supports a SP mode. A silicon slab surrounded by silica can support a dielectric waveguide mode. When the two guides are brought close to each other, ss in guide 1 which supports SP mode coupled with the

TM type dielectric waveguide mode which in turn is supported by guide 2 and forms a hybrid mode. Nanoscale confinement of the power for the HP mode in medium is low index contrast between metal and dielectric slab (an area which is selected as *spacer* in the whole work). Since the SP mode is TM in nature, the hybrid mode is also a TM mode. The hybrid plasmonic waveguide which was first proposed by Outlon [66], hybrid plasmonic waveguide states about plasmonic waveguide configuration and a electromagnetic mode which is coupled between the optical waveguide mode bounded with SPP mode. This concept of hybrid is revolutionary because it highlights the advantages of the high-index-contrast dielectric waveguides i.e. SPP waveguides. The mode area of hybrid plasmonic modes is hundred time lesser beyond the diffraction limit of light as compared to conventional MIM modes, while significantly reducing propagation losses. Deep sub wavelength photonic devices for integrated systems will be facilitated by this. Figure 3.1 shows the hybrid plasmonic design proposed by them.

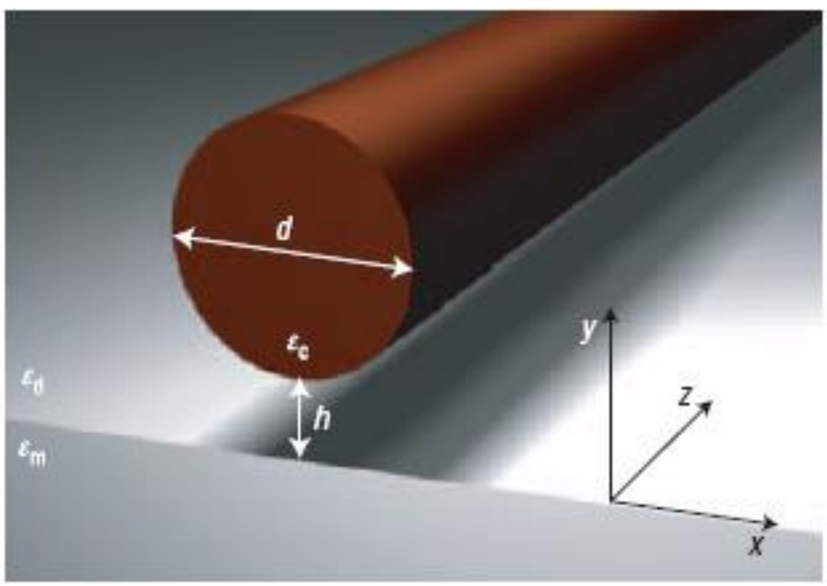

Figure 3.1 The hybrid optical waveguide [74]

Recent research in the field of HPW with material gain opens up the possibility of plasmonic devices for application in amplifiers, sources, and modulators. One paper in this field is proposed by **Linfei Gao et al -2012 [80]** in this paper he studied MSHPW with gain materials as loss recompense. The waveguide dimensions were controlled for propagation length and nano scale mode confinement of the waveguide by tuning. The width of metal strip with an optimum value is demonstrated to be 350nm for together compact confinement and propagation of low-loss in the passive case. The introduction of gain materials could be within the index within large contrast layer for or compensation of loss in low-contrast gap in the active case. Figure 3.2, shows the hybrid plasmonic waveguide proposed by them.

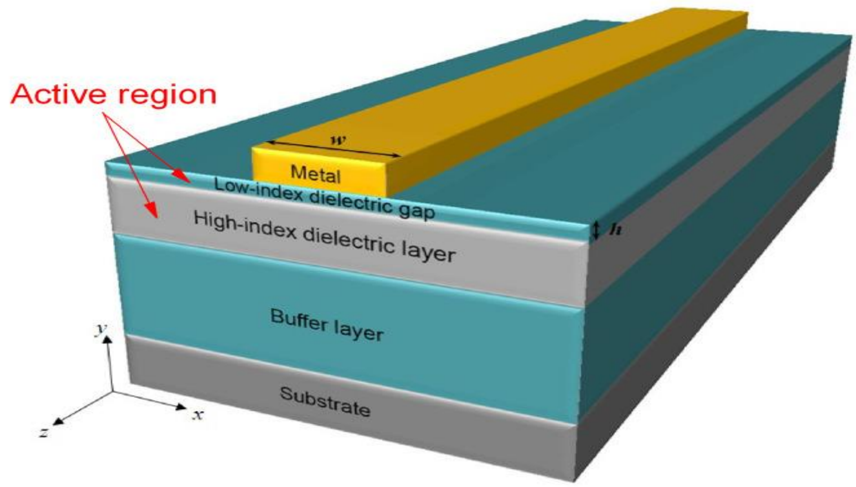

Figure 3.2 Hybrid plasmonic waveguide of active metal strip

3.2 Theory of HPW

A number of researches has been carried out within the field of the HPW is proposed recently. The comprehensive exploration to give details of the guiding mechanism of the HP mode guide is explained by alam et al [48]. A meticulous investigation of the modes sustained by the HP guide under a range of conditions will explain the physical nature in these structures of the guided modes and the enhanced understanding. Thus achievement may also be constructive for the drawing of future HP waveguide devices.

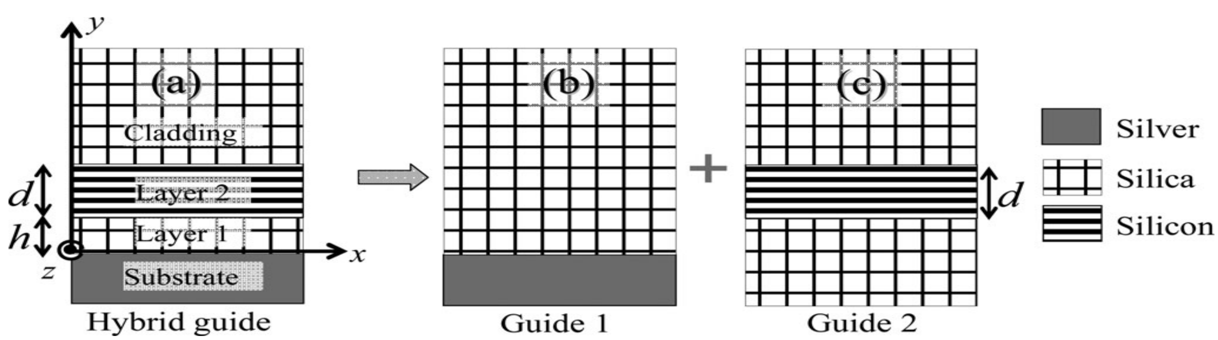

Figure3.3. HPW shown in (a) combination of two guides: guide 1 and guide 2. Guide 1 is a SP waveguide consisting of Ag–SiO_2 interface in (b), and guide 2 is a dielectric waveguide consisting of a Si slab surrounded by SiO_2 (c) [48].

In Figure 3.3 (a) a Ag –Silica interface can support a SP mode and b) a Silicon slab surrounded by Silica can support a dielectric waveguide mode. When the two guides are brought close to each other, the SP mode supported by guide 1 couple with the TM type dielectric waveguide mode supported by guide 2, and forms a hybrid mode. The "h" is the thickness of layer 1(silica) and "d" is the thickness of layer 2(silicon) and these are denoted as k_j. The power of the hybrid mode is highly confined in the low index medium between the metal and dielectric slab. Since the SP mode is TM in nature the hybrid mode is also TM mode. Transfer matrix method is used to study the modes supported by the structure as it provide accurate solutions for the modes supported by a 1-D multilayered structure. The method works by constructing the transfer matrix from enforcing boundary conditions between the adjacent layers as explained in detail in [85]. The propagation assumed in *z*-direction, the magnetic fields and electric fields can be expressed for the intermediate layer *j* (*j* = 1, 2) can be as [48]

$$H_j\ (\mathrm{y}, \mathrm{Z}) = \mathrm{x}\ H_j\ (\mathrm{y})\ \mathrm{exp.}\ [\mathrm{i}(\gamma \mathrm{z} - \omega \mathrm{t}) \tag{3.1}$$

$$E_j\ (\mathrm{y}, \mathrm{Z}) = \left[y\ E_{yj}\ (\mathrm{y}) + \mathrm{z}\ E_{zj}\ (\mathrm{y})\right]\mathrm{exp.}\ [\mathrm{i}(\gamma \mathrm{z} - \omega \mathrm{t}) \tag{3.2}$$

Here $\gamma = k_0\ (N_{\mathrm{eff}} + iK_{\mathrm{eff}})$ is the constant of complex propagation, $k_0 = (2\pi)/\lambda_0$ is wave number in the free space and λ_0 is free space wavelength of the free space. Real and imaginary parts N_{eff} and K_{eff} are of the effective refractive index. The electric and magnetic fields are related by Maxwell's curl equations.

$$\nabla \times E = i\omega\mu_0 H \tag{3.3}$$

$$\nabla \times H = -i\omega \varepsilon_0 \varepsilon_r E \tag{3.4}$$

Inserting expressions (3.1) and (3.2) into (3.3) and (3.4), the following equation can be derived for magnetic field in the intermediate layers.

$$\frac{d^2 H_{xj}(\mathrm{y})}{dy^2} + k_j H_{xj}\ (\mathrm{y}) \tag{3.5}$$

Here, k_j is the transverse wave number for the j^{th} layer (j = 1, 2) and is given by $k_1 = \sqrt{\mathcal{E}_{silica}\kappa_0^2 - \gamma^2}$ and $k_2 = \sqrt{\mathcal{E}_{Si}\kappa_0^2 - \gamma^2}$; $\mathcal{E}_{silica}$ and $\mathcal{E}_{Si}$ are permittivity of silica and silicon respectively. The corresponding electric field components are

$$E_{zj}\ (\mathrm{y}) = -\frac{i}{\omega\mathcal{E}_0\mathcal{E}_{rj}}\frac{dH_{xj}(\mathrm{y})}{dy} \tag{3.6}$$

$$E_{yj}\,(\mathrm{y}) = -\frac{\gamma}{\omega\mathcal{E}_0\mathcal{E}_{rj}} H_{xj}\,(\mathrm{y}) \qquad (3.7)$$

Here $\mathcal{E}_{r1} = \mathcal{E}_{silica}$ and $\mathcal{E}_{r2} = \mathcal{E}_{si}$. H_{xj} and its y –derivatives must be solution to the wave equation (3.5). For the intermediate layers we assume a sine and cosine dependence of the fields and after some algebra we may relate the fields at the bottom of one layer to the fields at the bottom of the layer above it through [85]

$$\begin{bmatrix} H_{xj}\,(\mathrm{y_j}) \\ \frac{1}{\mathcal{E}_{zzj}}\frac{\mathrm{d}}{\mathrm{dy}}H_{xj}\,(\mathrm{y_j}) \end{bmatrix} = \begin{bmatrix} \cos(k_j\,\mathrm{d_j}) & -\frac{\mathcal{E}_{zzj}}{k_j}\sin(k_j\,\mathrm{d_j}) \\ \frac{k_j}{\mathcal{E}_{zzj}}\sin(k_j\,\mathrm{d_j}) & \cos(k_j\,\mathrm{d_j}) \end{bmatrix}\begin{bmatrix} H_{xj+1}\,(\mathrm{y_{j+1}}) \\ \frac{1}{\mathcal{E}_{zzj+1}}\frac{\mathrm{d}}{\mathrm{dy}}H_{xj+1}\,(\mathrm{y_{j+1}}) \end{bmatrix} \qquad (3.8)$$

For a bound TM mode, the magnetic field in the cladding H_c and in the substrate H_s are exponentially decaying and hence can be written as

$$H_c\,(\mathrm{y, Z}) = \mathrm{x}\, A_c\ e^{-\kappa_c((y-(h+d))}\ \mathrm{exp.}[i(\gamma z - \omega t)] \qquad (3.9)$$

$$H_s\,(\mathrm{y, Z}) = \mathrm{x}\, A_s\ e^{-\kappa_s y}\ \mathrm{exp.}[i(\gamma z - \omega t)] \qquad (3.10)$$

where k_s is defined as the rate of attenuation in the substrate (silver) and k_c as cladding (silica) which are given by $k_s = \sqrt{\gamma^2 - \mathcal{E}_{Ag}\kappa_0^2}$ and $k_c = \sqrt{\gamma^2 - \mathcal{E}_{silica}\kappa_0^2}$. A_s and A_c are constants and only one of them is independent. A_s and A_c can be shown to be related by equation (3.8).

$$\begin{bmatrix} A_s \\ \frac{A_s \mathrm{k_s}}{\mathcal{E}_{Ag}} \end{bmatrix} = \begin{bmatrix} m_{11} & m_{12} \\ m_{21} & m_{22} \end{bmatrix}\begin{bmatrix} A_c \\ -\frac{A_c \mathrm{k_c}}{\mathcal{E}_{silica}} \end{bmatrix} \qquad (3.11)$$

$$\begin{bmatrix} m_{11} & m_{12} \\ m_{21} & m_{22} \end{bmatrix} = \begin{bmatrix} \cos(k_1\,\mathrm{h}) & -\frac{\mathcal{E}_{silica}}{k_1}\sin(k_1\,\mathrm{h}) \\ \frac{k_1}{\mathcal{E}_{silica}}\sin(k_1\,\mathrm{h}) & \cos(k_1\,\mathrm{h}) \end{bmatrix}\begin{bmatrix} \cos(k_2\,\mathrm{d}) & -\frac{\mathcal{E}_{Si}}{k_1}\sin(k_2\,\mathrm{d}) \\ \frac{k_2}{\mathcal{E}_{Si}}\sin(k_2\,\mathrm{d}) & \cos(k_2\,\mathrm{d}) \end{bmatrix} \qquad (3.12)$$

Eliminating A_s and A_c from (3.11) the dispersion relation or propagation constant for the multilayer structure can be obtained as

$$\frac{\mathrm{k_s}}{\varepsilon_{\mathrm{Ag}}}\mathrm{m_{11}} + \frac{\mathrm{k_s}}{\varepsilon_{\mathrm{Ag}}}\mathrm{m_{22}} - \mathrm{m_{21}} - \frac{\mathrm{k_s}}{\varepsilon_{\mathrm{Ag}}}\frac{\mathrm{k_c}}{\varepsilon_{\mathrm{silica}}}\mathrm{m_{12}} \qquad (3.13)$$

Solutions of (3.13) lay down precise information concerning the guided modes for any combinations of waveguide dimensions and material properties. The dispersion relation Eq. (3.13) to find the exact solutions for the guided modes but rely on the concept of coupling among the modes to provide a physical picture of the modes formation. This is the fundamental theory behind the research.

After the detailed study of the theory of the hybrid plasmonic waveguide by the different researchers, we propose a design of hybrid plasmonic waveguide for long range propagation with low loss. The upsurge of the width and height of the air slice that is sandwiched between metal and silicon leads to the captivity of HP mode in the air. The FEM is used for simulation of the waveguide. For confining of the HP mode in the nano scale the introduction of air can diminish the mode area and amplify the propagation distance, which are in that order due to reduction in the efficient index and in the lateral optical spread. The features of propagation announced for the proposed waveguide are improved over other easy-to-fabricate HP structures, which used dielectric materials like SiO_2 and Al_2O_3, for submission in the realization of nanophotonic devices [86-87]. The practicability in the guided wave devices will be boosted due to air presence in the waveguide [88, 80]. For the realization of long-range propagation of the HP mode, present work is focused on deliberately introducing an air gap in the guiding region. A thicker metal approximately up to 100 and 10 nm air gap, concerning the trade-off between propagation loss/propagation length and optical confinement is employed. The proposal of an air gap into the guiding region has formulated significant consequences [89]. The fabrication of the HPW will be exigent, and during fabrication a vigilant assessment of the metal and dielectric surface will be necessary. There can be formation of air gap by wafer bonding and/or selective wet etching with high selectivity. Various steps of selective wet etching can be performed to realize a defect-free and smooth air slice.

3.3 Hollow HP Waveguide

The anticipated design of the hollow HPW is shown in figure 3.4. It is composed of air, to guide the HP mode, as the dielectric between silicon and top metal layer. Silicon height, as depicted in figure 3.4, is h_{si} = 100 nm and h_{Au} = 100 nm is the thickness of the gold layer. W_{air} is the width of the air slice and the air slice height is denoted by h_{air}. For single-mode operation of the waveguide the width of the air slice should remain less than 240 nm (W_{air} < 240 nm) at an working wavelength of 1550 nm. The field for low loss and strong confinement has the minimum value of hair which is 10 nm, after this the rectangular geometry of the air slice is not supporting the HP mode and the mode will turn into pure SPP [73]. It is within the 10 nm air layer the confinement of electric field is strong. The dragging of optical mode can be in the direction of the metal–dielectric interface in order to turn it into the HP mode for attaining long-range propagation with sub wavelength confinement. On introduction of an air gap into the guiding regions it raises the characteristics of propagation [89].The material used have properties as the refractive index of Si, SiO_2, Air and Au is taken as n_{si} = 3.48, n_{SiO2} = 1.45, n_{air} = 1, n_{au} = 0 .55 – 11.5 i and the permittivity of the material taken as ε_{si} =11.7, ε_{sio2} = 2.25, ε_{au} = -114.9 -11.0918 i[90].

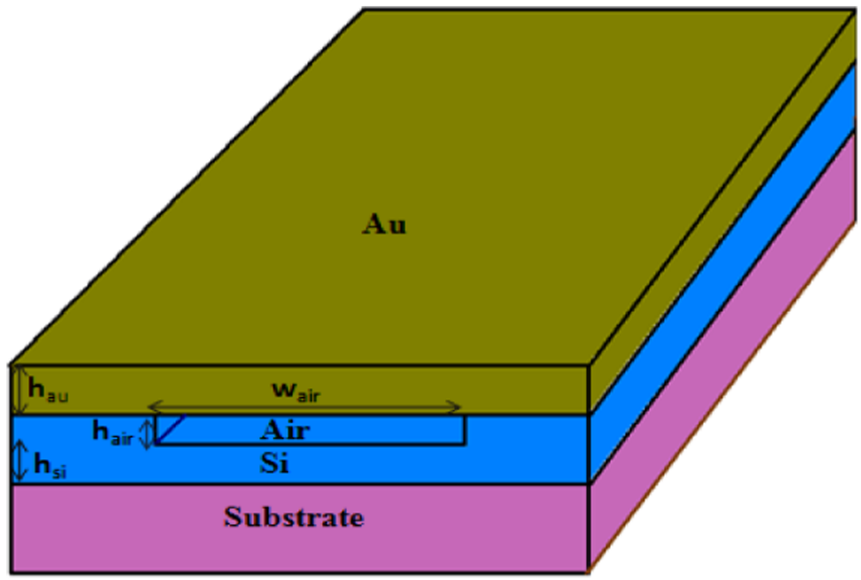

Figure 3.4 Representation of the projected design of the HP hollow wave- guide where an air slice has height of h_{air} and width W_{air} which is produced in silicon under the top gold layer with a thickness of 100 nm.

3.4 Modal Analysis of Hollow HP Waveguide

The field distributions E_y of the basic TM mode of the HPW, are demonstrated in line graphs as well as by pictorial graphs, in figure 3.5(a) and 3.5(b). Figure 3.5 (a) tells about the HP field confinement when SiO2 is sandwiched between metal (dielectric based) and silicon, while Figure 3.5(b) shows the HP field confinement of the dielectric between the metal and silicon (hollow) when the air slice is introduced in place. The responsibility for field leakage when the material- filled losses will be into the bottom Si in the first case and introducing of the air slice in position of the dielectric can avoid the condition to some extent. The value of effective index neff is 2.75 which is real part of refractive index for a dielectric-based HPW, however it is 2.64 for a hollow HPW with width W_d and height h_d of the dielectric/air is respectively 200 nm and 10 nm. Thus in the second case of the hollow HPW the field will travel much longer. Field distribution is formed by the sum of two exponential functions. When the air slice is very thin (even smaller than the evanescent penetration depth) the field of air-slice layer is enhanced significantly. The strong field enhancement in the air slice is obtained at the Au–air interface and the discontinuity in the E_y field at the Si–air interface due to the combination of the surface plasmon.

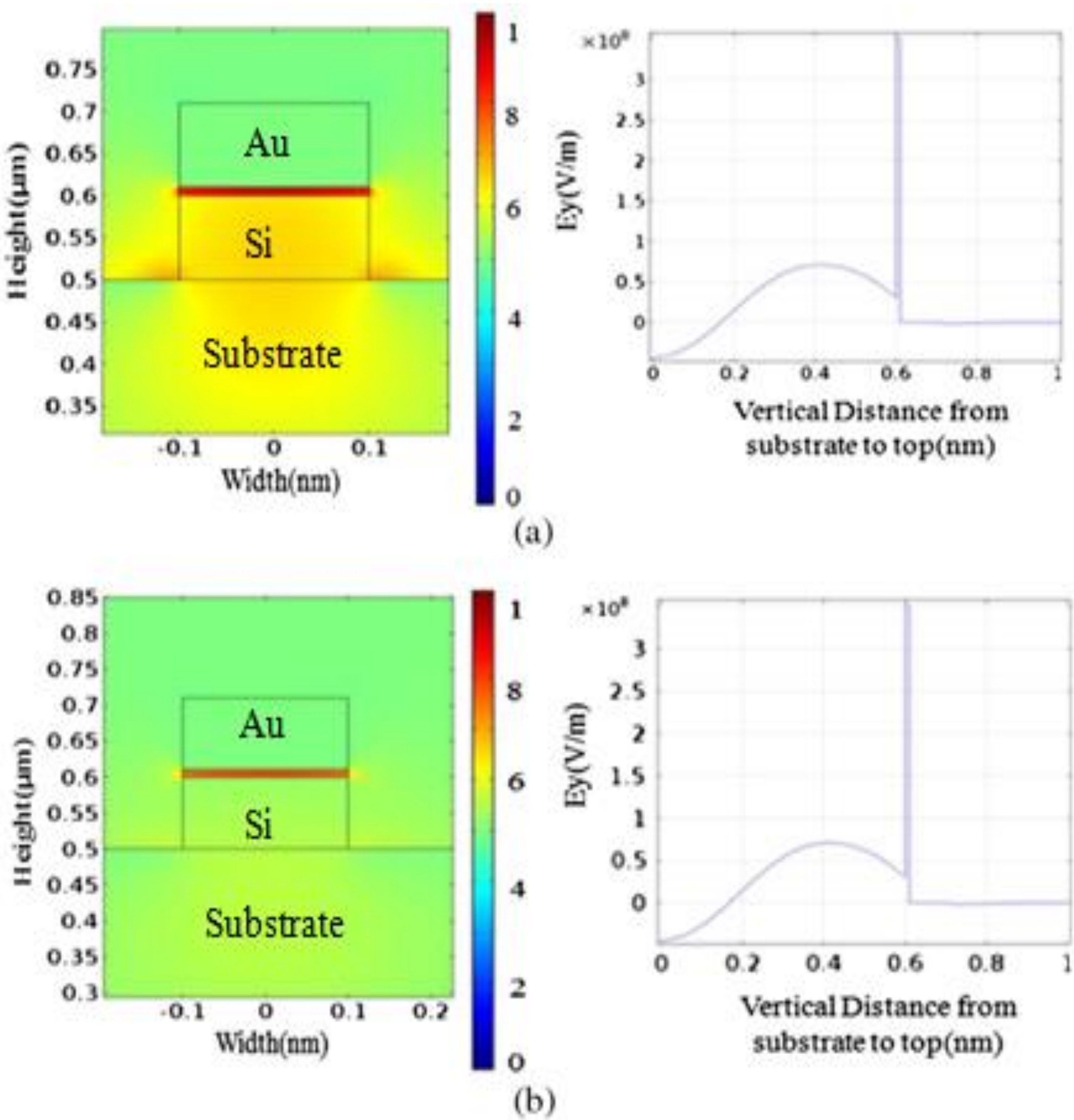

Figure 3.5 Field distributions Ey of the fundamental TM mode of the HPW (a) for a dielectric-based waveguide and (b) for a hollow waveguide

3.5 Propagation Characteristic of Proposed Design

Geometric parameters play a considerable control over the guiding performance of a waveguide. The guiding performance of the HPW is analyzed by observation of the effect of height h_d and width w_d of the air slice. With the increase in W there is increases or decrease in h and the effective index neff of the guided mode rises. FEM is used for the simulation of the guiding characteristics. The energy distribution in the waveguide is affected by the dimensions of waveguide especially n_{eff} will be larger for rigid confinement in some high-index cores. With a small value of n_{eff} the loss is caused in lower of the modal propagation cause. The guided HP mode propagation length is offered by $L_p\ (\mu m) = \frac{\lambda}{4\pi(neff)imaginary}$ [88] and the modal propagation is presented by L_m(db/um) = ($2K_0$(img.)n_{eff})×4.34 [80]. The modal area of the field confinement illustrate character of the guided mode[74]. The mode area of the guided fundamental mode a measure of the nature whether the localized field is HP or optical or pure plasmonic [74] and becoming the merit for confinement ability, which is known by $A_m(/\mu m^2) = \frac{\int_{-\infty}^{\infty} p(x,y)dxdy}{max[p(x,y)]}$ [80]. Figure 3.6 depicts the consequence of a change in the width w_{air} of air slice on the effective mode area A_m. The value of Am is known to be large for W_{air} < 100 nm. The achievement in the strong HP mode confinement for 100 nm < W_{air} < 250 nm is also shown as the effective mode area and remains acceptably small in this range. The value of effective mode area is $0.0685/\mu m^2$ at W_{air} = 100 nm which exhibits the HP nature of the confined mode.

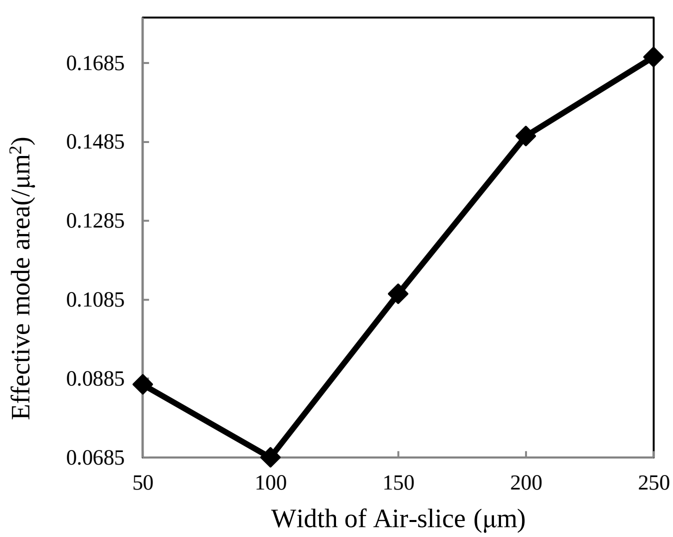

Figure 3.6 Variation in effective mode area with the width of air-slice at an air-slice height of 10 nm

Similarly the variation of the air slice height with the effective mode area at constant width of W_{air} = 100 nm is shown in figure 3.7. It shows that as we increase the air slice height with constant W_{air} = 100 nm the mode area increases. The smallest value of the mode area is obtained at h_{air} = 10 is A_m = 0.068/µm^2. At these values the lesser modal propagation loss L_m = 0.03 dB⁄µm with larger modal propagation length L_p = 142 µm is obtained.

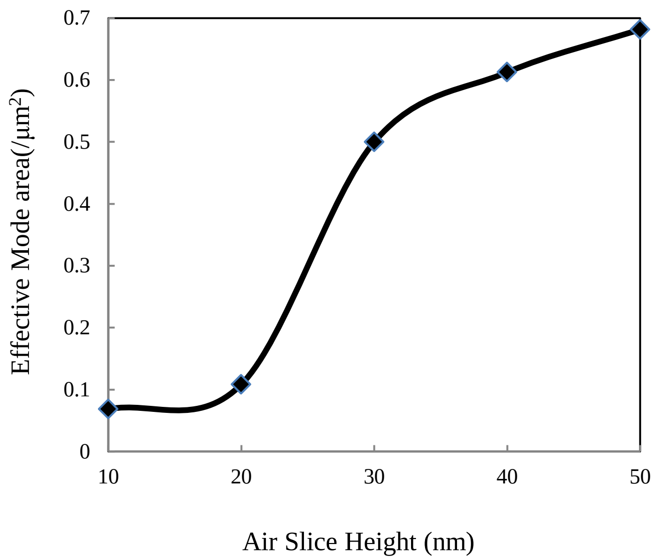

Fig.ure3.7 Variation in effective mode area with the air-slice height at an air-slice width of w_{air} = 100 nm

It is the height of the air slice which plays a chief role in considerably controlling the propagation characteristics of the guided mode. At w_{air} = 100 nm the effect of variation in the air slice height on the propagation length is depicted by figure 3.8. The HP nature of confined mode is lost as for values of h_{air} larger than 50 nm even though the propagation length is always larger for these values. At h_{air} = 10 nm the confined mode illustrates a strong HP nature, with a moderate value of the propagation length of 142 µm, while it is 28 µm for the SiO_2 (dielectric-based) waveguide at w_{air} = 100 nm as depicted by figure 3.8. However with air slice height, the propagation length further increases but we decided to fix it at h_{air} = 10 nm, as it exemplifies the tight confinement of the HP mode, the effective mode area at this height is 0.068⁄µm^2 as explained above.

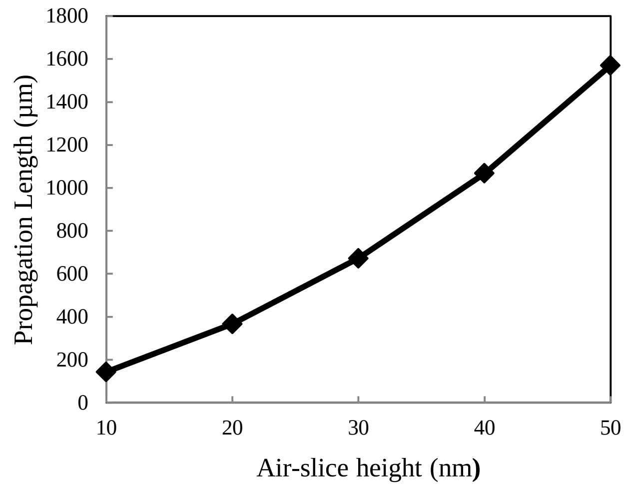

Figure 3.8 Consequence of height of air-slice on propagation length at an air-slice width of w_{air} = 100nm.Value of mode area with different air heights (0.068/µm^2, 10nm) (0.108447466/µm^2, 20nm) (0.49984863/µm^2, 30nm) (0.612370246/µm^2, 40nm) (0.1068157061/µm^2, 50nm)

Similarly in comparison to figure 3.8 the effect of height of SiO_2 with the propagation length is depicted in the figure 3.9. It demonstrates that as with increases of SiO_2 layer thickness the propagation length increases but in comparison to the air slice height at 10 nm , the very low value of the propagation length L_p = 29 µm with high modal propagation loss L_m = 0.15 dB/µm is shown.

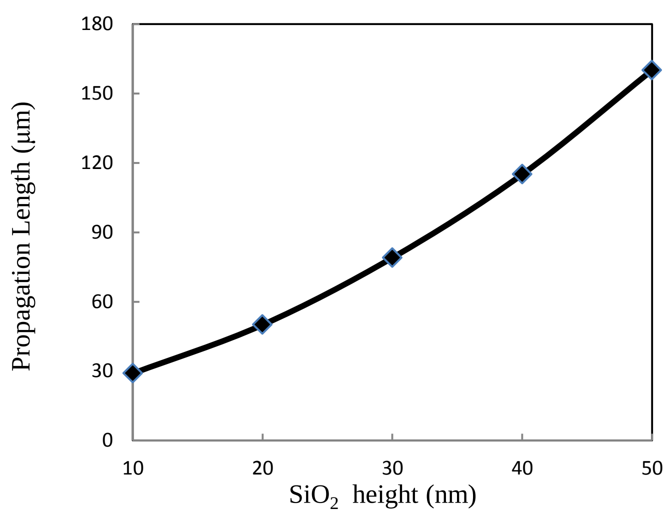

Figure 3.9 Effect of height of SiO_2 on propagation length at an SiO_2 width of w_{sio2} = 100nm.Value of mode area with different air heights (0.0003700799064/µm^2, 10nm) (0.0006683380099/µm^2, 20nm) (0.172640969/µm^2, 30nm) (0 .22018727/µm^2, 40nm) (0.265698469/µm^2, 50nm)

Fig. 3.10 illustrates the effectiveness of the width of the dielectric (SiO_2/air) on the propagation length. It is realized that at a constant dielectric height h_d of 10 nm, the dielectric width W_d increases with decrease in propagation length. The hollow HPW explains a propagation length larger than the dielectric- based (SiO_2 here) waveguide. Fig. 3.3 illustrates that at W_d = 50 nm for both of the cases the propagation length is largest, though the confinement of the HP mode will be poor due to the effective mode area in this case will be larger. To get the optimized structure that can strongly confine the HP mode and can guide it longer is our main objective here.

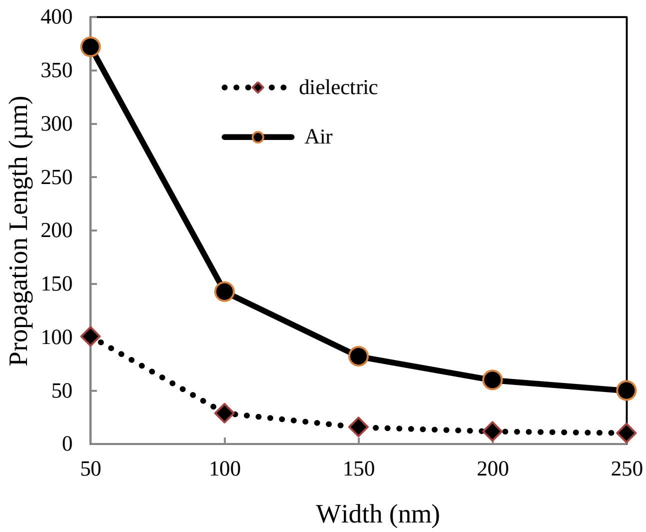

Figure 3.10 Variation of Propagation Length with SiO_2 (dielectric) and Air width at constant h_{air}, h_{SiO2} =10nm.Value of effective mode area for air and dielectric (SiO_2) with different width, 1. For air (.08745/μm^2,50nm),(0.0685/μm^2,100nm),(0.11031/μm^2,150nm)(.15041/μm^2,200nm),(0.17021/μm^2, 250nm).2 For dielectric (SiO_2) (0.03301/μm^2,50nm) (0.00037/μm^2,100nm) (0.000574003/μm^2,150nm) (0.000809439/μm^2,200nm) (0.001076068/μm^2,250nm).

For completing the results fully, the analysis of the modal propagation loss of the proposed hollow HPW is carried out, as shown in figure 3.11. The variation in the propagation loss with the air slice width is depicted at different values of the height of the air slice. The propagation loss decreases with decreasing w_{air}, and the loss increases with decreasing h_{air}. As discussed above, the optimized values of w_{air} and h_{air} are respectively 100 nm and 10 nm. The propagation at these values is 0.03 dB/μm. For low loss and strong field confinement the minimum value of h_{air} is 10 nm, below which the rectangular geometry of the air slice will not support the HP mode and the mode will become pure SPP [73], which will be seen as a smaller propagation length in the waveguide. To further increase the propagation length with tight confinement at smaller heights of the air slice, a circular air slice may be a potential candidate for long-range propagation.

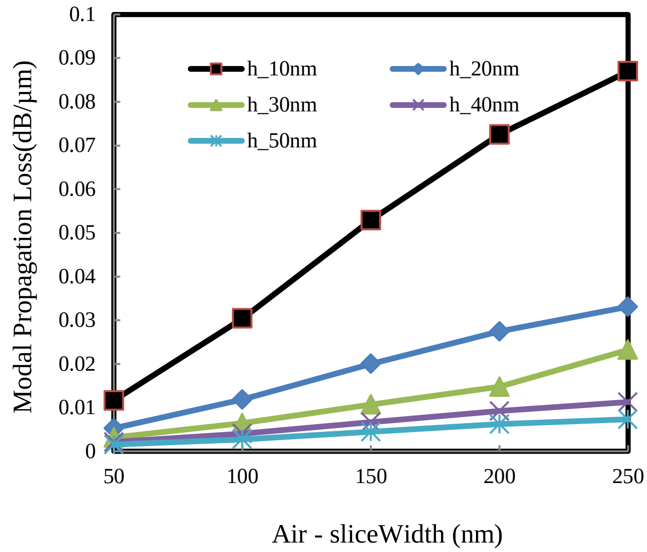

Figure 3.11 Change in modal propagation loss of the hollow HP waveguide with width of air-slice and heights of the air- slice

Similarly the change in modal propagation loss with SiO_2 width and thickness of the SiO_2 layer is shown in figure 3.12. Plot shows that with the increase of the SiO_2 width propagation loss is going to increase and with the decrease of thickness of the SiO_2 layer the modal propagation loss is going to be increased. But as figure 3.8 shows that the air slice lesser loss is obtained as compared to the SiO_2 as dielectric.

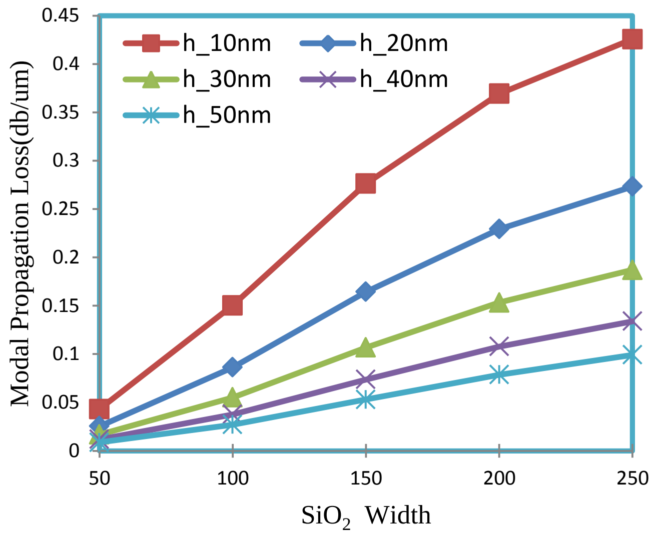

Figure 3.12 Change in modal propagation loss of the HP waveguide with width of SiO_2 and heights of the SiO_2 layer

3.6 Summary

A novel design of a hollow HPW for nanoscale optical confinement and long-range propagation is proposed. The propagation characteristics of the proposed waveguide are improved over other easy-to-fabricate HP structures. Optimized width and height of the air slice sandwiched between metal and silicon lead to a strong confinement of the HP mode in the air, with a small mode area. The introduction of air into the HPW can increase the propagation distance with acceptably small propagation loss. The air-confined hybrid mode exhibits a smaller effective mode area $A_m = 0.0685/\mu m^2$ and longer propagation distance L_p = 142 μm, with a low modal propagation loss of 0.03 dB/μm at optimized values of the width and height of the air slice as compared to the hybrid mode confined in the dielectrics. The proposed easy-to-fabricate design of the waveguide will be useful for the realization of integrated Nanophotonic devices with acceptably small losses. To further enhance the guiding performance, a circular air slice can be formed into the HPW for longer propagation and stronger field confinement. The presence of air in the guiding region may enable the application of the hollow HPW for low nonlinearity and efficient on-chip tiny sensors. To ease the fabrication process of the proposed waveguide, it is possible to achieve long-range propagation with larger air gaps by further engineering the waveguide structure, which will help in utilizing the waveguide to make functional nanodevices.

Chapter 4

Mode Hybridization and Coupling Performance of the HP Waveguide

4.1 Introduction

In this chapter we theoretically represent that how the mode coupling is between the plasmonic and optical mode which takes us to the HP mode. In the present chapter the effect of the high index layer has also been studied. Plasmonics is the important part of the rising field of the nanophotonics [43, 80, 91-92] which explores that how EM field can be confined on the scale much smaller as compared to the operating wavelength [73]. It is possible to guide and confine the light at real 'nanoscale' with the help of hybridization of the photonic mode and SPP mode. The hybridization is analytically decided by a parameter called mode character *a*, which defines the nature of the HP mode resulting from coupling of optical and SPP mode [74].

An integrated platform based on hybrid plasmonic-photonic waveguide can be promising for making photonic devices at real nano scales. In this chapter coupling and propagation analysis of SPP and photonic modes of HP waveguide are presented with the material system – Si/SiO_2/Ag. Low-loss sub-wavelength (nano-scale) optical confinement with variable optical nonlinearity is proposed as result of the mode hybridization of photonic and plasmonic modes in Hybrid Plasmonic Waveguide (HPW). The origin and analysis of coupling, guiding and confinement of HP mode are presented analytically as well by using Finite Element Method (FEM) [79]. Our analysis reveals that the photonic mode confined in a rectangular geometry in contrast to circular mode confined in a wire [74] can be efficiently pushed with longer propagation, towards metal-dielectric interface. This photonic mode can be coupled with SPP mode to give us HP mode with longer (than that in circular geometry) propagation length because of the leaky nature of the modes confined in rectangular geometries. In addition, the evanescent nature of the field confined in the high-index region under dielectric is introduced to understand the coupling of surface plasmon and optical field. It is shown that the modification in the nature of the coupling of surface plasmon and optical field is an important requirement to push the SPP longer into the waveguide. This coupling can be modified by increasing the evanescent field into dielectric to propagate the HP mode longer in the dielectric. The coupled mode theory is used to calculate the mode character and coupling between the SPP and optical mode [45, 91-92]. The coupling strength for $Si/SiO_2/Ag$ system is 52% and propagation length of HP mode with silicon is 154 μm at a 10 nm thick dielectric. The propagation loss for Si based HP waveguide is 0.028 *dB/μm* and modal area for silicon is 0.0009 /μm^2. Lower plasmonic losses in Si cause low-loss guiding of HP mode with stronger optical confinement and hence smaller mode area [40]. The thickness of high-index region and waveguide-width are shown to control the optical nonlinearity of the waveguide. It has been shown that the nonlinearity of the guided HP mode remains at par with that of photonic mode which can be considered low with nano-scale optical confinement.

4.2 Waveguide Design Proposed

Figure 4.1 is depicting the design of the hybrid plasmonic waveguide that is to be analyzed

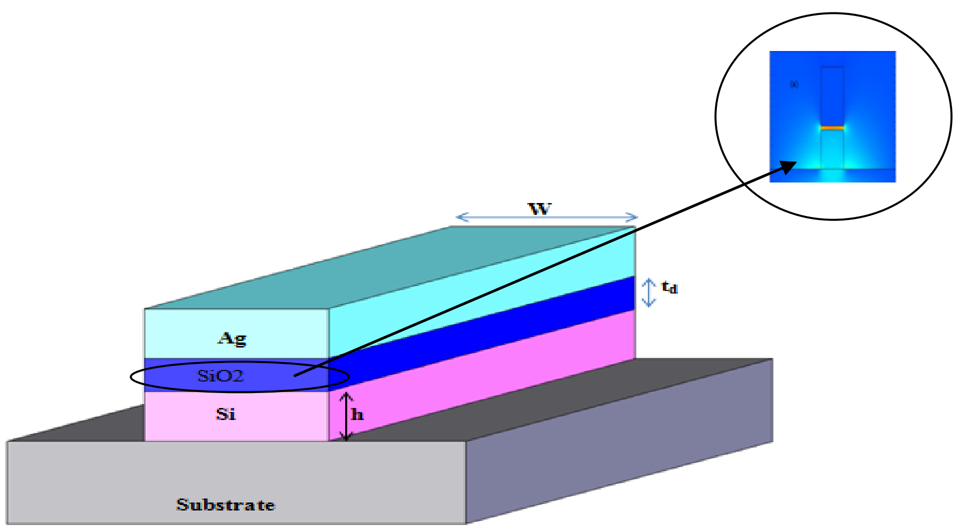

Figure 4.1showing the Schematic of the proposed design of hybrid-plasmonic waveguide with SiO_2 of thickness t_d and waveguide width of *w*. Optical mode (confined in Si) can be pushed towards metal-dielectric interface surface to couple it with SPP mode. The thickness of top Ag layer is 200 nm. The thickness of Si is denoted by *h*. *h* and *w* are taken to be equal to form a square optical waveguide. Inset shows the field distribution E_y of the HPW is shown in the pictographic form. The field confinement, when SiO_2 sandwiched between Ag and Si. The t_d is 10 *nm* and width is 200 *nm*. For this, mode area is 0.0009 /μm^2 and modal propagation loss is 0.028 *dB/μm*. We have largest propagation length L_p= 154 μm.

It consists of SiO_2 slice sandwiched between Ag and Si to guide and confine the HP mode. The waveguide width is w and the thickness of the dielectric (SiO_2) is t_d. The optical waveguide (Si) is taken to be a square waveguide with h = w where h is the thickness of the Si. The height of top Ag layer is taken to be 200 nm.To form an HP mode the coupling of field confined in the Si with SPP mode is controlled through the intermediate dielectric layer between metal and Si. At optimized coupling of optical and SPP modes, hybrid mode is formed for which mode character is 0.5 [74].

For the fabrication point of view we consider a rectangular geometry of the waveguide. The choice of the noble metal tells us that Ag supports longer propagation length with very low loss [91] and appropriate choice of the dielectric which enables us the induction of the gain, compensation of the loss in metal and increases the SPP signal propagation length. We choose Ag, which has highest conductivity among the metals in the wavelength range and Si and which have higher value of the relative permittivity thus help to enhance more electric field in the dielectric region. The strong field confinement in the SiO_2 is because of arrangement of SPP at Ag and SiO_2 interface and also due to the discontinuity in the field confinement E_y from at Si-SiO_2 interface.

4.3 Analysis of Mode Hybridization

With the coupled mode theory [74, 89], the eigen mode Ψ supported in the coupled waveguide system can be described as the superposition of the rectangular mode $\Psi_{react.}$ and SPP mode. If t_d is the thickness of the dielectric and h and w are thickness and width of Si based optical waveguide and if $a_+(h, w, t_d)$ is the field-amplitude in the rectangular waveguide and $b_+(h, w, t_d)$ is the field-amplitude of the SPP mode, the wave function of the symmetric eigen mode Ψ_+ can be written as [74, 89]

$$\Psi_+(h,w,t_d) = a_+(h,w,t_d)\Psi_{react.waveguide}(t_d) + b_+(h,w,t_d)\Psi_{SPP} \quad (4.1)$$

The square of the modulus of rectangular mode amplitude is the measure of the character of the hybrid mode known as mode character given by $|a_+(h,w,t_d)|^2$. It specifies the degree to which the guided mode is optical or SPP. A guided mode will be hybrid plasmonic if [74]

$$|a_+(h,w,t_d)|^2 = 0.5 \quad (4.2)$$

Field-amplitude of SPP mode will then be given by

$$b_{+}(h, w, t_d) = \sqrt{1 - |a_{+}(h, w, t_d)|2} \qquad (4.3)$$

As shown in eq. (2) and (3) field amplitudes are the function of h, w and t_d. The behavior of the typical coupled mode system the mode character is given as

$$|a_{+}(h, w, t_d)|^2 = \frac{[n_{hyb.(h,w,t_d\ )} - n_{SPP}]}{[n_{hyb.(h,w,t_d\ )} - n_{react.\ (h,w).} + n_{hyb.(h,w,t_d\ )} - n_{SPP}\ ]} \qquad (4.4)$$

Here n_{hyb} is the effective refractive index of the HP mode, n_{SPP} is the effective refractive index of the SPP mode and n_{rect} is the effective index of the optical mode in Si. The n_{hyb} is caused by the coupling of optical and SPP mode which is predicted by the real part of effective index and that is calculated by using FEM. For the prediction of mode character we calculate the effective index of the SPPs mode and that of rectangular waveguide mode as follows: The interaction of light at the metal surface leads to the confinement of the light beyond the reach of the dielectric photonic structure [74]. The interaction between the metal and the dielectric interface supports SPPs. These are the evanescent electromagnetic wave bound to the interface that is strongly coupled to the coherent oscillation of free electron charge at metal surface. The eigen mode of an interface between a dielectric and a metal are SPPs. We refer to them as the eigen modes in the sense that they are solution of the Maxwell's Equations that can be formulated in the absence of an incident field. In general, coupling of the HP mode may be either TE or TM type but since the Surface plasmonic mode supports in metal dielectric interface are TM in nature, the permittivity $\mathcal{E}$ only varies in one spatial coordinates $\mathcal{E} = \mathcal{E}(z)$. The interface is set to coincide with z = 0 and the wave propagation is taken in the x direction, showing the spatial variation in the plane y- direction. The propagating wave can be written as,

$$E(r\ ,\ t) = E(z)e^{i(\beta x - \omega t)} \qquad (4.5)$$

where β is the propagation constant of the travelling waves. It is given as

$$\beta = n_{eff}\frac{2\pi}{\lambda_0} \tag{4.6}$$

The Helmholtz equation for the propagation wave is written as

$$\frac{\partial^2 E(z)}{\partial z^2} + \left(\omega^2\ k_0^2 - \beta^2\right)E(z) = 0 \tag{4.7}$$

The two Maxwell's equations for this are

$$\nabla \times E = i\omega B \tag{4.8}$$

$$\nabla \times B = -i\omega\mu\mathcal{E}E \tag{4.9}$$

The wave vector is perpendicular to the interface in this medium for Z>0

$$\kappa_1^2 = \beta^2 - k_0^2\mathcal{E}_m \tag{4.10}$$

for Z<0

$$\kappa_2^2 = \beta^2 - k_0^2\mathcal{E}_d \tag{4.11}$$

In order to confine the surface wave on the interface, the real part of κ_1 and κ_2 must be positive, which in turn requires that the real part of the complex permittivity $\mathcal{E}_m$ and $\mathcal{E}_d$ are of opposite in sign.

$$\frac{\kappa_1}{\kappa_2} = \frac{-\mathcal{E}_m}{\mathcal{E}_d} \tag{4.12}$$

The interface between dielectric and metal satisfies the conditions. A confined surface wave propagating along such an interface is called SPP, which arises by coupling of the electromagnetic field to the surface plasmon. The dispersion relation for the SPP is given as

$$\beta = \frac{2\pi}{\lambda_0}\sqrt{\frac{\mathcal{E}_m\mathcal{E}_d}{\mathcal{E}_m+\mathcal{E}_d}} \tag{4.13}$$

where $\frac{2\pi}{\lambda_0} = \kappa_0$

$$\beta = \kappa_0\sqrt{\frac{\mathcal{E}_m\mathcal{E}_d}{\mathcal{E}_m+\mathcal{E}_d}} \tag{4.14}$$

and

$$n_{eff} = \frac{\beta 2\pi}{\lambda_0} = \sqrt{\frac{\mathcal{E}_m\mathcal{E}_d}{\mathcal{E}_m+\mathcal{E}_d}} \tag{4.15}$$

This relation gives the effective index of the SPP mode as

$$n_{SPP} = \frac{\beta 2\pi}{\lambda_0} = \sqrt{\frac{\mathcal{E}_m\mathcal{E}_d}{\mathcal{E}_m+\mathcal{E}_d}} \tag{4.16}$$

and similarly the wave vector for the SiO_2/Si is given as [45]

$$\kappa_3^2 = k_0^2 \varepsilon_{Si} - \beta^2 \tag{4.17}$$

$$\kappa_4^2 = k_0^2 \varepsilon_d - \beta^2 \tag{4.18}$$

and after solving that we obtained it as

$$\beta = \kappa_0 \sqrt{\frac{\varepsilon_{Si}\varepsilon_d}{\varepsilon_{Si}+\varepsilon_d}} \tag{4.19}$$

$$n_{eff} = \frac{\beta 2\pi}{\lambda_0} = \sqrt{\frac{\varepsilon_{Si}\varepsilon_d}{\varepsilon_{Si}+\varepsilon_d}} \tag{4.20}$$

This relation gives the effective index of the rectangular (optical) waveguide mode as

$$n_{rect.} = \frac{\beta 2\pi}{\lambda_0} = \sqrt{\frac{\varepsilon_{Si}\varepsilon_d}{\varepsilon_{Si}+\varepsilon_d}} \tag{4.21}$$

Plasmonic mode (SPP) confined at the interface between metal-dielectric does not propagate longer because of the high ohmic losses associated with the metal. The coupling of the SPP with the field confined in the dielectric is determined by the nature of the field in the dielectric which is controlled by the total internal reflection in the dielectric. To push the plasmonic mode longer in the waveguides, the coupling of the surface plasmon in the metal surface should be modified by introducing an enhanced evanescent field in the dielectric. It is a well known situation in leaky waveguides where leaky modes propagate longer in cladding regions [75]. In case of conventional metal-dielectric plasmonic waveguides, the vertical coupling is a measure of coupling between surface plasmon and optical field is proportional to skin depth z. Enhanced evanescent field in the dielectric causes longer propagation length into the waveguide [75]. In a high refractive index region given below, dielectric should be added to enhance evanescent field in the dielectric by modifying the coupling between surface plasmon and optical field. The waveguide structure thus becomes hybrid plasmonic waveguide [74]. The skin depth quantifies the confinement of the surface wave and is defined as the distance from the interface where the magnitude of the field has dropped to $\frac{1}{e}$

$$z = \frac{1}{|\kappa_i|} \tag{4.22}$$

For the larger decay length, the weaker confinement, L is the intensity of the propagating wave has dropped to $\frac{1}{e}$

so $$L_{SPP} = \frac{1}{2\mathrm{Img}(\beta)} \tag{4.23}$$

img.(β) deals with the loss of the waveguide.

The coupling strength plays most important role in dragging the optical mode to metal dielectric interface and the coupling strength (κ) between SPP and optical mode can be written as [85]

$$\kappa(h, w, t_d) = \sqrt{(n_{eff} - n_{SPP})(n_{eff} - n_{rect.})} \quad (4.24)$$

Using eq. (24), we obtained the coupling strength between the SPP and optical mode for the two material systems. The values for the n_{spp} and $n_{rect.}$ are respectively obtained from eq. (16) and (21). Our analysis indicates permittivity has a significant effect on the propagation length and mode area, the coupling strength for the Si/Ag is 0.52. Figure 4.2 depicts the results. The SPP mode shows a larger coupling with Si. Higher the coupling strength, stronger will be the mode confinement with longer propagation length. For the single mode operation of the waveguide, width of the SiO_2 should stay below 240 nm. For strong field confinement and low loss at an operating wavelength of 1550 nm with good coupling strength and larger propagation length, the lowest value of t_d =10 *nm* below which the rectangular geometry of the mode and the HP mode will turn into the pure SPP [74]. Therefore the Subwavelength optical confinement with strong mode confinement and lesser modal propagation loss is achieved at t_d=10 nm. Now the reduced equation according to equation (4) is given as to predict the mode character of the hybrid mode and SPP mode as

$$|a_+(h, w, t_d)|^2 = \frac{\kappa(h,w,t_d)^2}{[n_+(h,w,t_d) - n_{react(h,w)}] + \kappa(h,w,t_d)^2.} \quad (4.25)$$

The reduced form of the equation from coupled mode theory is given by

$$n_+ = n(h, w, t_d) + \Delta(h, w, t_d) \quad (4.26)$$

$$n(h, w) = \frac{n_{react.}(h,w) + n_{SPP}}{2} \quad (4.27)$$

$$\Delta(h, w, t_d) = \sqrt{\frac{(n_{react.}(h,w) - n_{PP})^2}{4} + \kappa(h, w, t_d)^2} \quad (4.28)$$

From equation (24) and (4) we found following equation

$$[n_+(h, w, t_d)] = [n_{hyb.}(h, w, t_d)] \quad (4.29)$$

Therefore for the calculation of the mode character eq. (4) can be written as given above and it gives us the mode character of the hybrid mode, SPPs mode and optical mode. Therefore by using eq. (25) we are able to calculate the mode character. These results match with our analytical and simulation, we obtained mode character which is approximately equal to the HPM i.e. $|a_{+}(h, w, t_d)|^2 = 0.50$ at t_d = 10 nm for Si/Ag with very low modal propagation loss, larger propagation length and tight field confinement.

From the above numerical analysis we have come to the conclusion that n_{eff} can be obtained for the hybridization of the optical mode and SPP mode.

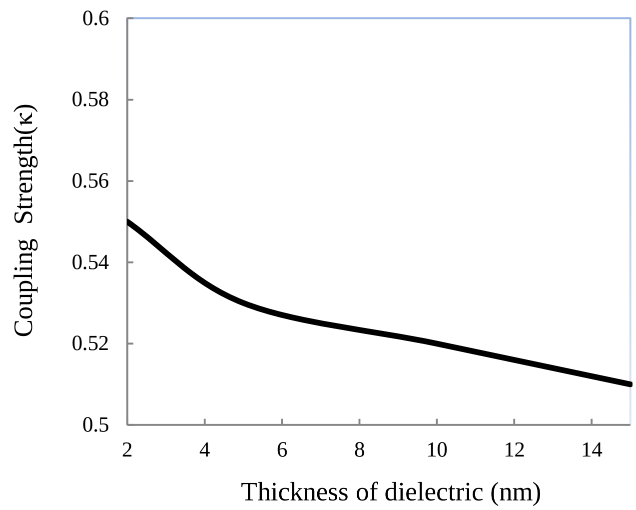

Figure 4.2 Effect of dielectric thickness on the coupling of optical and SPP mode at width = 200 *nm*, h = 200 *nm*. At t_d = 10 nm with the Lp = 154μm, Loss = 0.028 dB/μm, coupling strength = 0.52

Figure 4.3 tells us about the mode character hybrid plasmonic waveguide, and we observed that for width <200 nm, it is SPP mode and at width =200 nm, it is hybrid plasmonic mode and for width > 200 nm, it is optical mode. The similar behavior is shown upto t_d= 15 nm, after reaching this level mode indicates the optical behavior, here we shows only for t_d=10 nm. In Figure 4.3, we found that mode character is 0.5 at width 200 nm for Si which shows the hybrid plasmonic waveguide nature.

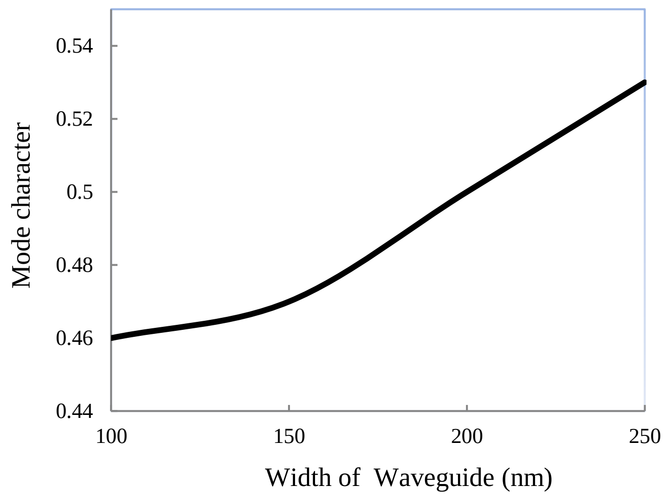

Figure 4.3 depicting the Variation of the mode character with the width of waveguide at constant t_d =10nm. As mode character approaches to HP mode at t_d = 10 *nm* and at width =200 nm for Si, we have largest propagation length L_p= 154 μm and mode area is 0 .0009 /μm^2 and modal propagation loss is 0 .028 dB/μm.

4.4 Propagation and Nonlinear Characteristics

By observing the effect of the width of the SiO_2 and the thickness geometrical parameters of the proposed waveguide design can be significantly controlled the guiding performance of the HPW. The effective index neff of the guided mode rises with the increase in width and decrease in t_d. The FEM is used for simulation of the guiding characteristic. The propagation length and modal propagation loss and effective mode area is calculated in the same way as we do in the chapter 3.By varying the waveguide-width and dielectric thickness t_d we obtained the tradeoff between the modal propagation loss and mode area.

We observed that strong mode confinement with lesser modal propagation loss and larger propagation length is obtained at w < 240 nm at t_d = 10 nm. The high-index region, silicon here also plays a significant role in controlling the mode hybridization across the dielectric layer. Figure 4.4 shows the effect of variation in silicon thickness on the propagation length (via coupling of SPP and photonic modes) with t_d = 10 nm and w = 200 nm. As we increases the thickness of the silicon, firstly upto 150 nm there is increase in the propagation length and from 150 nm onward upto 300 nm remains constant and for 300 onwards upto 500 nm it increases.

We observed that upto 100 nm of Si-thickness plasmonic (SPP) mode dominates which typically shows very high losses and hence short propagation length, from Si-thickness of 100 nm to 300 nm SPP and photonic modes got hybridized providing a mode character of 0.5 which shows long range propagation with subwavelength optical confinement. Beyond Si-thickness of 300 nm evanescent filed into dielectric begins to lose its coupling with SPP mode which disable the mode hybridization; the guided mode now becomes leaky photonic mode with larger field in the silicon. Thus the presence of high-index region under the dielectric is crucial and can be used to mould the coupling of the free electrons of metal with the optical fields. At value of the 200 nm for width and thickness of the Si waveguide we obtained proper tradeoff between modal propagation loss and mode area and in terms of the nonlinearity.

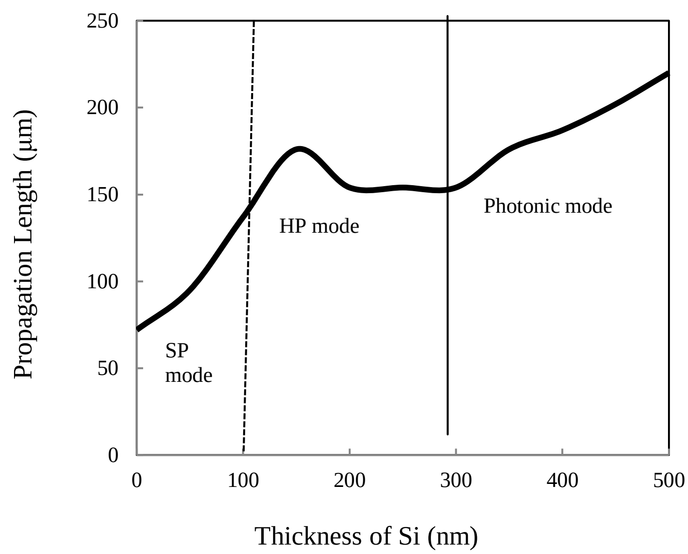

Figure 4.4 The effect of thickness of high-index region (silicon here) on the propagation length showing the journey of the guided mode from pure plasmonic to leaky photonic mode through hybrid plasmonic mode; the thickness of the Si at constant w=200 nm and t_d = 10 nm of the waveguide.

As we know that with raising the width of waveguide and with decreasing the thickness of the dielectric, the propagation decreases. Figure 4.5 depicts that with increasing the width the propagation length is decreased. As the thickness of the dielectric is reduced, the propagation length is also reduced. We have highest propagation length at 15 nm and lowest propagation length at 2 nm, but there is tradeoff between modal propagation loss and mode confinement. Thus with t_d = 10 nm and at w = 200 nm, we have proper tradeoff between modal propagation loss, with increase in the width and decreases in the thickness, the modal propagation loss increases. We observed that at the small value of dielectric thickness we have higher modal propagation loss. The modal propagation loss is 0.028 dB/μm and mode area is 0.0009 /μm^2 for Si. But we found a different type of the behavior in case of mode area.

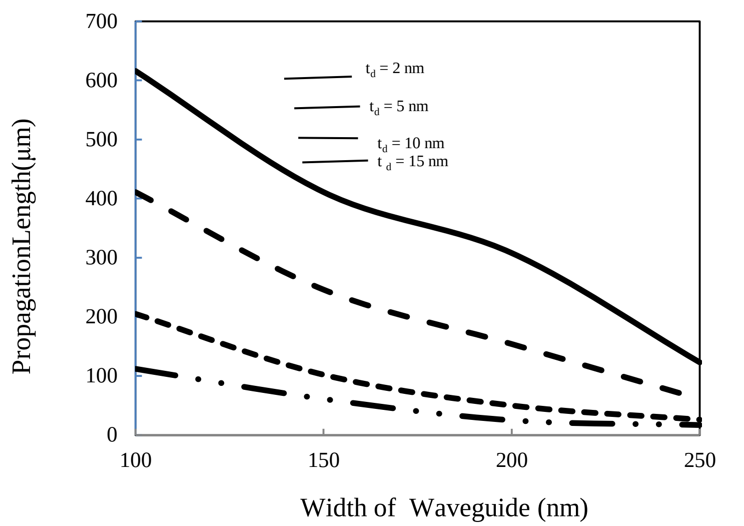

Figure 4.5 Variation of the propagation length with w at different thickness. The mode area at t_d= 10 nm and at width W = 200 nm, A_m = 0.0009 /μm^2 and modal propagation loss is 0.028 dB/μm. And coupling strength is 0.52.

On observing theses results closely we found that at w = 200 nm and t_d =10 nm, we have proper tradeoff between the modal propagation loss, mode area and propagation length. In figure 4.6 we have a plot for mode area and propagation length with thickness of dielectric at W = 200 nm. The solid black line shows propagation length and dotted lines shows mode area for the Si at W = 200 nm at different thickness. At t_d = 10 nm we have larger propagation length and lesser modal propagation loss and smaller mode area.

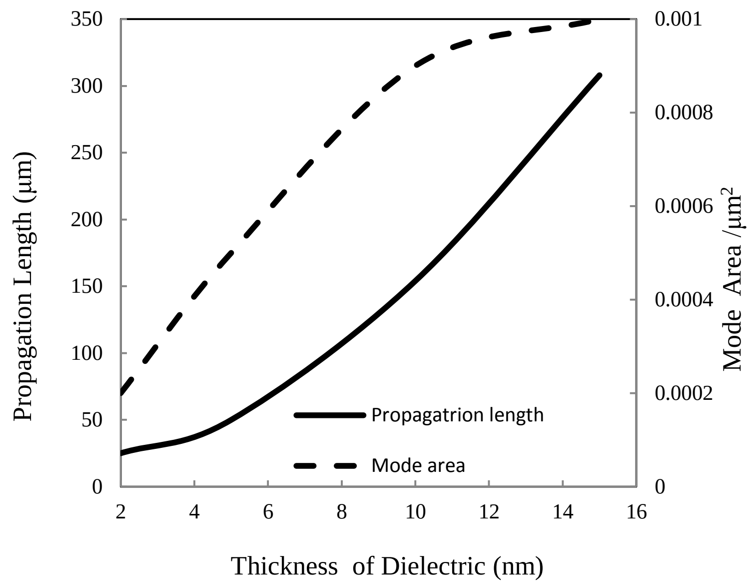

Figure 4.6 Variation of the propagation length and mode area with different t_d at constant width w =200 nm. At td = 10 nm we have L_p = 154 µm and mode area is Am = 0.0009 /μm^2 and the modal propagation loss is L_m = 0.028 dB/ µm.

The third order material plays a essential function in various application of nonlinear optics. The Third order response takes us to the process such as two photon absorption and third harmonic generation, but more notably takes us to the intensity dependent refractive index, i.e. the base of almost all of the nonlinear optical switching devices. The intensity dependence of refractive index is explained as [93-94] $n = n_0 + n_2 I$,where 'I'is the laser intensity and n_2 is the coefficient of the intensity dependent refractive index. This quantity can related to the nonlinear susceptibility by means of $n_2 = \frac{12\pi^2 \aleph^3}{n_0^2}$, where n_0 is the refractive index of the medium. This value of the refractive index for Si is 3.4 and for SiO_2 is 1.45 and third order susceptibility for Si is 2.0×10^{-10} and 1.8×10^{-14} for SiO_2 by putting these values, we obtained the value for the n_2. The value of third order nonlinear optical coefficient for Si is $2.7\times 10^{-16} m^2/W$ and $3.2\times 10^{-18}\ m^2/W$ for SiO_2. We obtained the nonlinearity as [95], $\gamma = \frac{n_2\beta}{A_{eff}}$, where n_2 the nonlinear index β is the propagation constant, and A_{eff} is the effective mode area. Figure 4.7 shows the nonlinear effect on the proposed design. The nonlinearity in hybrid plasmonic waveguide used in application such as nonlinear directional coupler, low power, all optical switching and in the nonlinear signal processing.

Here we start with the t_d = 2 nm and vary it upto 50 nm. At t_d = 2nm, 5nm, 10 nm and w_{Si} & h_{Si}= 200 nm, we have nonlinear coefficient $\gamma = 17.3 \times 10^7$ $km^{-1}w^{-1}$, 6.9×10^7 $km^{-1}w^{-1}$, 3.8×10^7 $km^{-1}w^{-1}$ .At w = 100 nm, 150 nm, 200 nm and 250 nm, at constant t_d = 10 nm we have nonlinearity varies from 11.2×10^7 $km^{-1}w^{-1}$, 5.6×10^7 $km^{-1}w^{-1}$, 3.8×10^7 $km^{-1}w^{-1}$ and 2.8×10^7 $km^{-1}w^{-1}$.

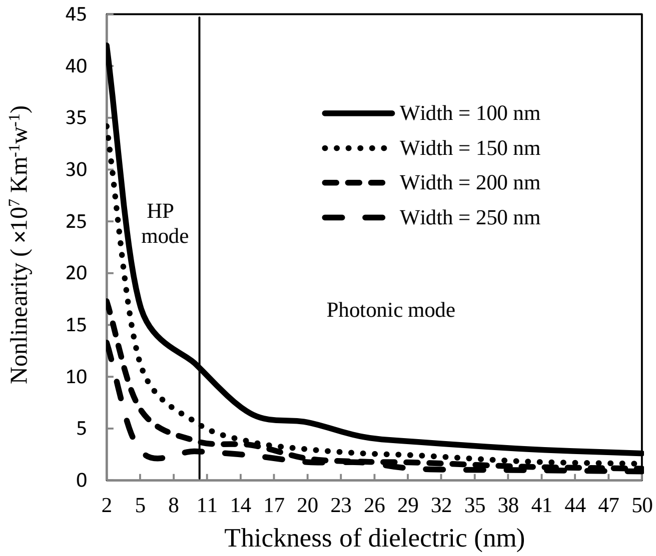

Figure 4.7 Variation of the nonlinear coefficient with the thickness of the dielectric. At t_d = 10 nm, nonlinear coefficient $\gamma = 3.8\times 10^7$ $km^{-1}w^{-1}$ with lesser modal propagation loss L_m = 0.028 dB/μm, larger propagation length L_p = 154 μm and mode area is A_m = 0.0009 */μm²* is obtained, where w is the width of the waveguide.

At t_d = 10 nm and w = 200 nm it slow down the light with lesser modal propagation loss L_m = 0.028 dB/μm, larger propagation length L_p = 154 μm with mode area A_m = 0.0009 /μm^2, as compared to other reported in the literature [96-98] with nonlinearity 3.8×10^7 $km^{-1}w^{-1}$. From [80] at t_d = 20 nm and at w_{Si} = 100 nm, nonlinearity is 4.7×10^8 $km^{-1}w^{-1}$. At this width of silicon and thickness of dielectric we have nonlinearity 5.6×10^7 $km^{-1}w^{-1}$. From [95] the obtained value for the nano shell plasmonic waveguide at the aspect ratio near to 1.33 is 4.1×10^7 $km^{-1}w^{-1}$ and for the hybrid plasmonic waveguide the value obtained is 3.8×10^7 $km^{-1}w^{-1}$, at unity aspect ratio.From [99-100] the nonlinearity for the slot hybrid plasmonic waveguide is 7.82×10^6 $km^{-1}w^{-1}$. We obtained the variable value of the nonlinearity for SiO_2. As we increases the thickness of the dielectric, nonlinearity decreases and at these values the mode area increases, the thickness of high-index region and waveguide-width can control the optical nonlinearity of the waveguide. The nonlinearity of the guided HP mode remains at par with that of photonic mode which can be considered low with nano-scale optical confinement. The origin and design analysis of long range propagation in a Hybrid Plasmonic (HP) waveguide and nano-scale optical confinement are described in this chapter. Material systems $Si/SiO_2/Ag$ are presented to analyze hybrid mode character and to realize an efficient design of the HP waveguide. The *mode character* predicts whether it is HP mode, pure-plasmonic (SPP) or optical mode. The coupled mode theory is used to calculate the mode character and coupling between the SPP and optical mode. The coupling strength to achieve *mode character* $a = 0.5$ (for HP mode) for $Si/SiO_2/Ag$ system is found 52%. It is shown that the modification in the nature of the coupling of surface plasmon's and optical field is an important requirement to push the SPP longer into the waveguide. This coupling can be modified by increasing the evanescent field into dielectric for to push HP mode longer in the dielectric. It is also found that the HP mode originated from the optical mode confined in a rectangular geometry can have longer propagation length. Propagation length of HP mode with silicon is 154 μm at a 10 nm thick dielectric. The calculated modal area of the proposed HP waveguide is 0.0009 /μm^2 and the modal propagation loss is 0.028*dB*/μm. The coupling and propagation characteristics of the HP waveguides are calculated analytically as well by using FEM. Our analysis shows that the optical mode confined in a rectangular geometry, in contrast to circular mode confined in a wire can be efficiently pushed towards metal-dielectric interface. This optical mode can be coupled with SPP be modified by increasing the evanescent field into dielectric to push HP mode longer in the dielectric. It is also found that the HP mode originated from the optical mode confined in a rectangular geometry can have longer propagation length. Propagation length of HP mode with silicon is 154 μm at a 10 nm thick dielectric. The calculated modal area of the proposed HP waveguide is 0.0009 /μm^2 and the modal propagation loss is 0.028*dB*/μm. The coupling and propagation characteristics of the HP waveguides are calculated analytically as well by using FEM.

4.5 Summary

Our analysis shows that the optical mode confined in a rectangular geometry in contrast to circular mode confined in a wire can be efficiently pushed towards metal-dielectric interface. This optical mode can be coupled with SPP mode to give us HP mode with longer (than that

in circular geometry) propagation length because of the leaky nature of the modes confined in the rectangular geometries. The high-index region under the (confinement) dielectric layer also plays a significant role in controlling the mode hybridization across the dielectric layer. It is found that beyond a certain thickness of high- index region evanescent filed into dielectric begins to lose its coupling with SPP mode which disables the mode hybridization. The guided mode now becomes leaky photonic mode with larger field in the high-index region. Thus the presence of high-index region under the dielectric is crucial and can be used to mould the coupling of the free electrons of metal with the optical fields. Lower plasmonic losses in Si cause low-loss guiding of HP mode with stronger optical confinement and hence smaller mode area. The thickness of high-index region and waveguide-width are shown to control the optical nonlinearity of the waveguide. It has been shown that the nonlinearity of the guided HP mode remains at par with that of photonic mode which can be considered low with nano-scale optical confinement. The proposed work can be useful to enable an integrated platform based on hybrid plasmonic-photonic waveguide which can be promising for making photonic devices at real nano scales with flexible and variable nonlinearity.

Chapter 5
Hybrid Plasmonic Waveguide with Engineered Structure

5.1 Introduction to Subwavelength High-index Contrast Grating

Nanophotonics is promising technology for on-chip data processing & transmission in large-scale integrated photonic circuits. It is key for various applications in sensing and optical communication. Plasmonic waveguides and devices have been attracting an ever increasing interest. Plasmonics addressed the major issues like confinement and controlling of light beyond the diffraction-limit. Further the attractive features for 'nanophotonics' come at a cost with the larger modal propagation losses and field penetration in the metal region. To reduce loss by plasmonic waveguide, considerable elaborate geometrical/material configurations used. The main issue with the plasmonic waveguide is to attain, at the same time larger propagation length with tight field confinement with low modal loss. As our topic of study on the Hybrid Plasmonic Waveguide, only this waveguide are able to address the issue of the plasmonic waveguide of high loss and low propagation length. In the chapter 3 and 4, we propose the new design of the Hybrid plasmonic waveguide. Both of these design is able to make the tradeoff between propagation length and loss. Moreover the device designed in chapter 3 act as a gas sensors and device designed in chapter 4 act as a variable nonlinearity device.

In the chapter 4, a novel design for hybrid plasmonic waveguide is proposed with long range propagation with nanoscale confinement. The effect of the high index layer was also studied in the chapter 4. The detail about the effect of high index layer on the mode confinement and nonlinearity is studied in chapter 4. The high index layer has a great role in controlling the mode hybridization between plasmonic and optical mode. In this chapter, hybrid plasmonic waveguide with different structure is engineered with the insertion of the grating [101-104]. The grating in the different types of the design is formed by the Si/SiO_2 (high index/low index). The different type of the structure with variable grating period and duty cycle gives us the long range propagation length with nanoscale confinement as compared to without grating insertion. We explained each structure step by step with their design specification, results, conclusion etc.

5.2 Engineered Design of HP Waveguide

In this chapter study of grating parameters like (grating period, width, depth, length) on the waveguide characteristics is done. This chapter will cover the effect of grating period and duty cycle on the propagation length, effective mode area, nonlinearity, modal propagation loss. In the recent years various garting based on hybrid plasmonic waveguide structure have been proposed [62, 70, 78, 105]. Grating plays a very important role in the enhancement of modal properties of the hybrid plasmonic waveguide.

5.3 Design and Analysis of various structures

5.3.1 Air-Slice and Dielectric-Slot Assisted HP Waveguide

In this design a HPW with subwavelength optical-confinement, large propagation length with low modal-propagation-loss is proposed. The low-loss guiding of hybrid plasmonic mode is reported by introducing an SiO_2 slot in the silicon under the air-slice. The reported results will be useful in realizing nanophotonic devices based on hybrid plasmonic waveguide for applications in large-scale photonic integration [63, 69, 80, 105].

The proposed waveguide design of the HPW is depicted in the figure 5.1. It consists of air slice sandwiched between Au and Si to guide and confine the HP mode. The waveguide width is w and the thickness of the dielectric (air) is t_d. To form an HP mode the coupling of field confined in the Si with SPP mode is controlled through the intermediate dielectric layer between metal and Si. The appropriate choice of the dielectric which enables us the induction of the gain, compensation of the loss in metal and increases the SPP signal propagation length. We chose Au, which have good conductivity among the metals in the wavelength range and Si, which have higher value of the relative permittivity which helped to enhance more electric field in the low index region. The height of Si, h_{is} = 100 nm and thickness of Au layer is t_{au} = 100 nm. The width of SiO_2 slot under the air slice is w_{SiO2} = 50 nm and height is 100 nm and these values are kept fixed. For strong field confinement and low loss the minimum value of thickness of air slice is t_d = 10 nm, below which the mode behaves as the SPP [80]. The material parameter is kept same as that for the structural design in the chapter 3.

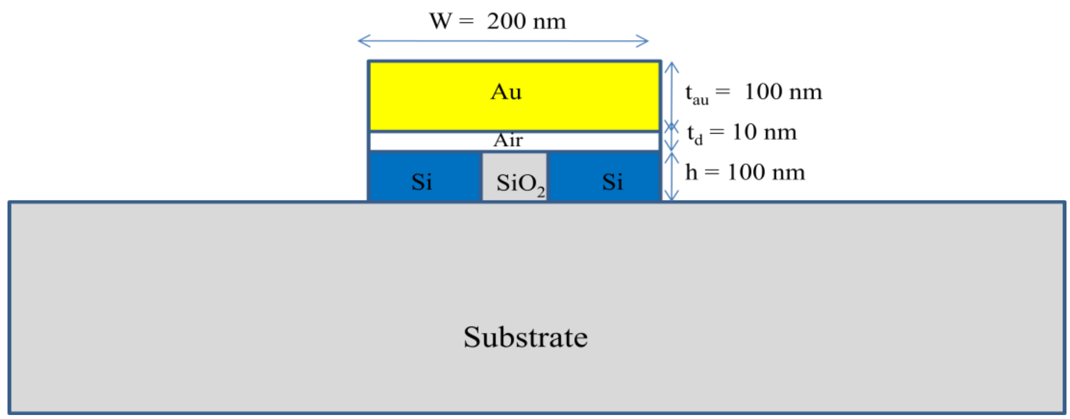

Figure 5.1 Proposed design of hybrid-plasmonic waveguide. The SiO_2 slot width= 50 nm and height = 100 nm is kept fixed under the air slice.

The E_y component of electric field, for fundamental TM mode of the HPW is shown by line graph as well as in the form of the pictorial graph in figure 5.2 (a) and 5.2(b). Figure 5.2(a) depicts HP field confinement where the air is there between the silicon and metal. Figure 5.2 (b) depicts the HP mode field confinement, while SiO_2 is introduced below air slice in Silicon. The refractive index for the real part is n_{eff} = 2.64 without air slice and it is 2.59 with the introduction of the SiO_2 slot below the air slice, where w_d is the width of the waveguide. The strong field confinement in the SiO_2 is because of the combination of SPP at Ag and SiO_2 interface and the discontinuity that takes place in the field confinement E_y from at Si-SiO_2 interface. With the introduction of the air slice field will travel longer.

(a)

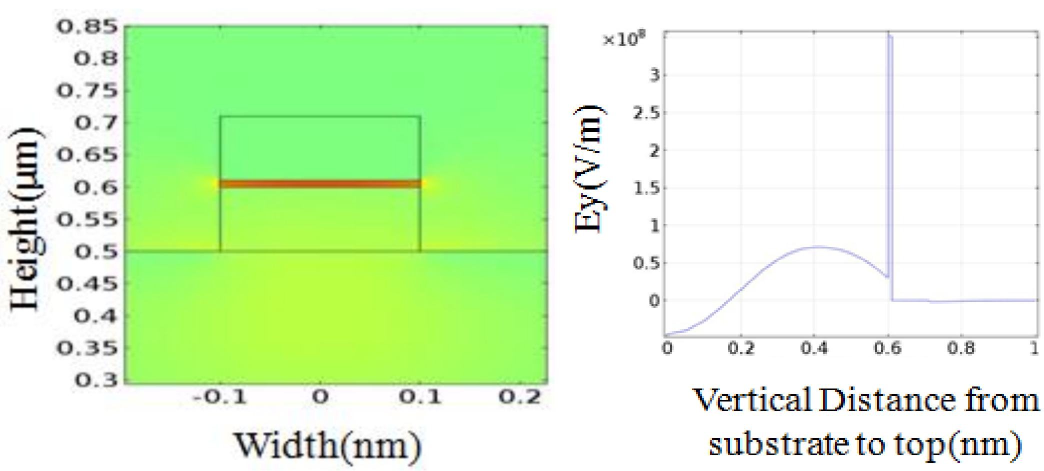

(b)

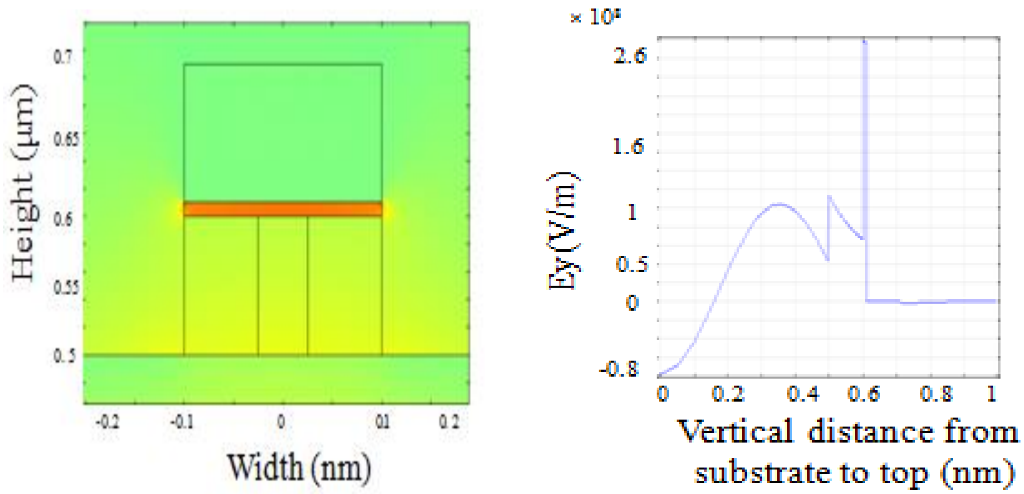

Figure 5.2 The electric field E_y of the fundamental TM mode of the hybrid plasmonic waveguide (a) for hollow waveguide (b) for SiO_2 slot below the air slice.

The effect of the thickness and width of SiO2 is studied. The geometrical parameters of the proposed waveguide design can be appreciably control the modal characteristic of the HPW. The n_{eff} of guided mode raised as width of the waveguide increases. Finite Element Method (FEM) is used for simulation of the modal characteristic. The propagation length for the guided hybrid HP mode, modal propagation loss and effective mode area is calculated by the same formula as we used in the chapter 3.

As we know that at t_d = 10 nm, we have tight mode confinement with lesser modal propagation loss with improved propagation length. Figure 5.3 Shows variation of propagation length with width of waveguide. It is observed that at constant dielectric thickness t_d = 10 nm, with increase in the dielectric width w_d there is decrease in the propagation length. At w_d = 50 nm both type of waveguide have same value of the propagation length. As we introduced the SiO_2 slot below the air slice the propagation length enhanced with the lesser modal propagation loss. At w_d = 100 nm the L_p = 142 µm for air slice and it is L_p = 224 µm when slot is introduced. The dotted line for the air slice propagation length and solid black line for the Silica slot based propagation length.

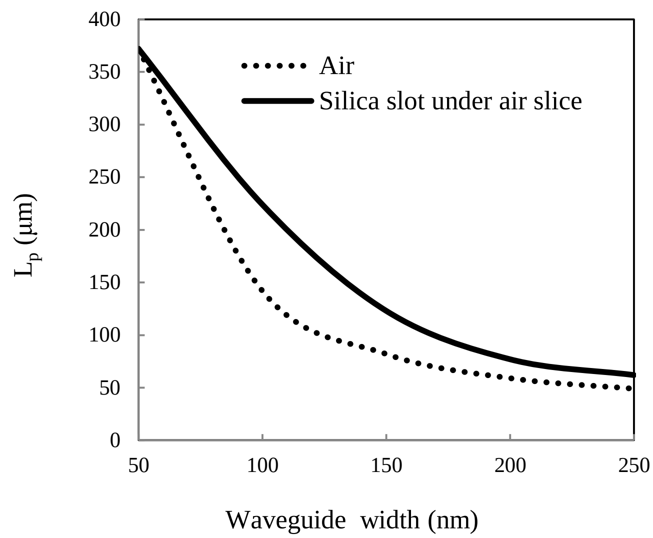

Figure 5.3 Effect of Propagation Length with width of air slice and with silica slot under air slice is shown. The silica slot height and width is kept constant h_{aio2} = 100 nm and w_{SiO2} =50 nm. We kept the air slice thickness t_d = 10 nm constant

Figure 5.4 shows the effect of the waveguide width on the modal propagation loss. Modal propagation loss is decreased with decreasing the width of the waveguide. At w_d = 100 nm we have modal propagation loss for air slice is = 0.03 dB/µm and it is 0.019 dB/µm for SiO_2 slot under the air slice.

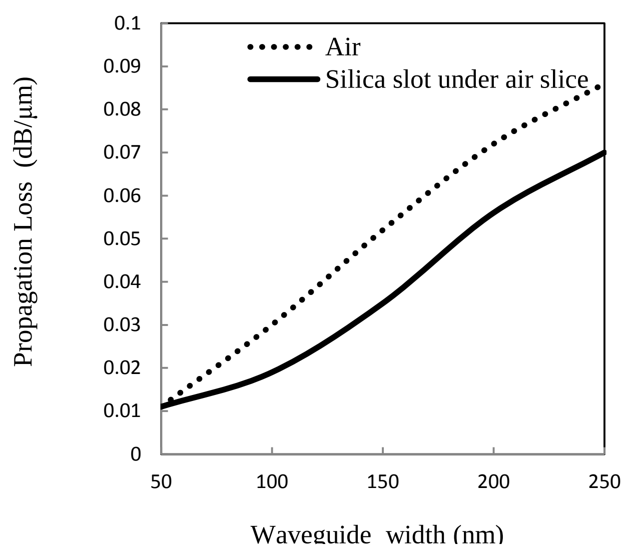

Figure 5.4 Effect of waveguide width for modal propagation loss, with width of air slice and with silica slot under air slice is shown. The silica slot height and width is kept constant h_{sio2} = 100 nm and w_{SiO2} =50 nm.

A nanophotonic waveguide for subwavelength optical-confinement is proposed here and the propagation characteristics of the proposed waveguide are enhanced by an innovative design. The introduction of the SiO_2 slot below the air slice increases the propagation length with acceptable small propagation loss in comparison to hybrid mode in the air slice. SiO_2 slot based waveguide have smaller mode area 0.00023 /μm^2, larger propagation length 224 μm and lesser modal propagation loss 0.019 dB/μm at optimized value of width and thickness.

5.3.2 Grating based HPW with High Nonlinearity

In this design, a grating based HPW for subwavelength long range propagation and optical confinement with high nonlinearity is proposed here. The grating formed in the high-index material, silicon under the core-dielectric (SiO_2) modifies the coupling of Surface Plasmonic Polariton (SPP) and evanescent field in the core-dielectric and causes a large propagation length of 1-mm with a low propagation loss of 4-dB/mm. The nonlinearity of grating based HPW is found to be $1.87 \times 10^8\ km^{-1}w^{-1}$ which is almost ten times higher than that of other nanophotonics waveguides. Evanescent-field confined in the high-index region under dielectric is modified by the introduction of the grating in this region which interacts strongly with surface plasmonic mode and with the optical field dragged from high index region to core-dielectric.

Hybridization of plasmonic and photonic modes has become a promising way of realizing nano-scale photonic devices beyond diffraction limits [73]. In HPW, the SPP mode confined in the metal-dielectric interface is dragged deeper into the dielectric where its nature becomes hybrid which is combination of plasmonic and photonic mode. The proposed grating based structure of HPW is shown in figure 5.5.The arrow indicates the Si and SiO_2 grating. The height of the Si is h_{is} = 500 nm and width = 2000 nm. The SiO_2 have thickness t_d = 10 nm and w_{sio2} = 200 nm, these are the optimized value. The top Au layer with thickness t_{au} = 150 nm and w_{au} = 200 nm all these values are kept constant. Here W_{sio2} and W_{au} are denoted as W (width of waveguide). The garting is formed in the Si with Si/SiO_2 at fixed duty cycle is C = 0.96 and from this the obtained the grating period = 260 nm and thickness of each SiO_2 grating based slot is 10 nm and height of the slot is same as that of Si height. The duty cycle 0.96 is obtained by varying the thickness of the SiO_2 slot in the grating region. We obtain the different value of the duty cycle by varying the thickness of the SiO_2 in grating region. But only at 0.96 the largest value of L_p = 342 μm with low loss 0.012 dB/μm, which makes us choice of this value of duty cycle. We also try different value of the duty cycle for variation of the garting period but only with duty cycle 0.96 and at grating period 260 nm largest value of propagation length with high nonlinearity is achieved. At this optimized value we obtained the larger L_p, nano scale confinement with very low loss. The electric field distribution of basic TM mode of the HPW is shown in figure 5.5 (b,c), in the form of pictorial graph and line graph. The real part of the n_{eff} is 2.45. The field travel upto L_p = 1 mm with grating insertion in Si as compared to without grating L_p = 224 μm. The strong field enrichment in the SiO_2 is because of the combination of SPP at Au and SiO_2 boundary and the discontinuity in the field confinement E_y from at Si-SiO_2 boundary [80].The garting help the strong field confinement in the SiO_2.

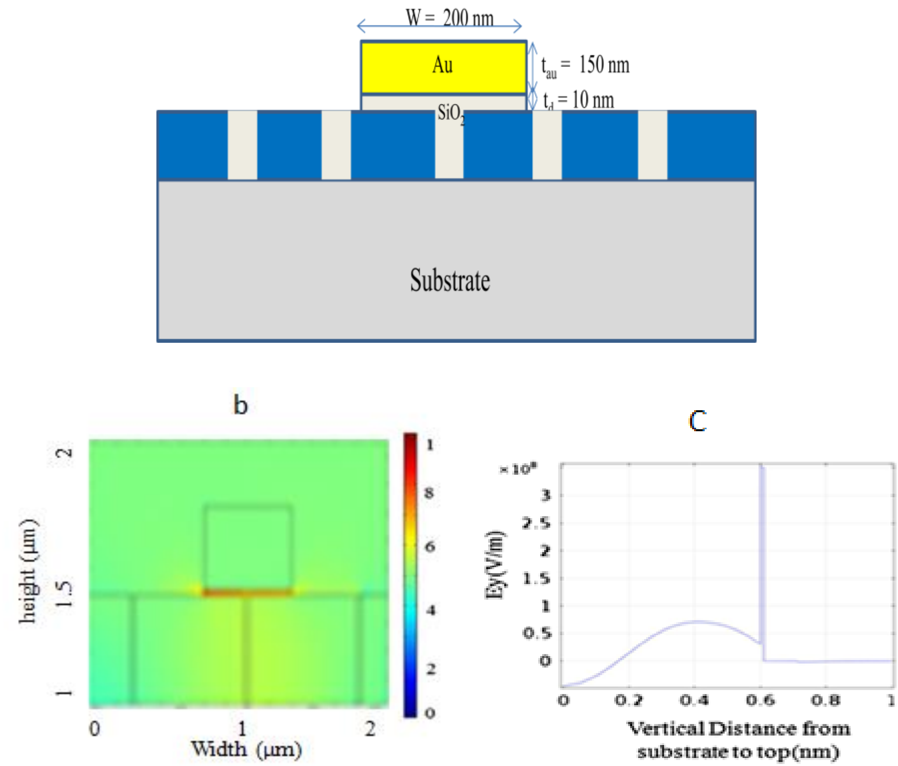

Figure 5.5 Proposed grating based hybrid plasmonic waveguide design with the duty cycle C = 0.96, thickness of SiO_2 under metal t_d = 10 nm, width of waveguide W = 200 nm; b) and c) electric field distributions respectively in pictorial and line graph forms of the fundamental TM mode of the HPW.

The propagation length used for the guided hybrid HP mode and modal propagation loss with effective mode area is calculated in the similar ways as we did in the chapter 3. The mode area should be lesser than the diffraction limit mode area in free space $A_0 = \frac{\lambda^2}{4}$, here strong mode confinement ranging from $\frac{\lambda^2}{4000}$ to $\frac{\lambda^2}{4oo}$. The nonlinearity given as $\gamma = \frac{n_2\beta}{A_{eff}}$ [99], where n_2 the nonlinear index, β is the propagation constant, A_{eff} is the effective mode area. As we know that at t_d = 10 nm, we have tight mode confinement with lesser modal propagation loss with improved propagation length.

The variation of the propagation length and modal propagation loss with the grating period at constant duty cycle (0.96) is shown in figure5.6. The left handed y-axis shows the propagation length and right handed y –axis shows the loss. The graph shows that with the increases of the grating period propagation length going to be decreased and loss going to be increased. But at grating period ʌ = 260 nm, we have largest propagation length L_p = 1 mm and highest nonlinearity $\gamma = 18.7 \times 10^7$ $km^{-1}w^{-1}$ and lowest loss L_m = 4 dB/mm with nanoscale optical confinement A_m = 0.00017/ μm^2 when we have grating in the Si layer as compared to the propagation length without grating is L_p = 224 μm and low nonlinearity $\gamma = 4 \times 10^7$ $km^{-1}w^{-1}$ loss is L_m = 18 dB/mm and larger mode area A_m = 0.00081 /μm^2.The solid black line is for the propagation length and dotted line is depicting the loss.

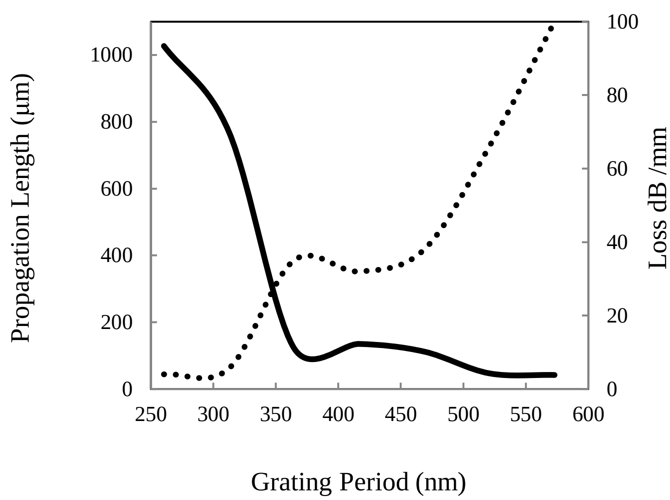

Figure 5.6 Variation of the propagation length and propagation loss with garting period with constant duty cycle of 0.96.

Figure 5.7 shows the variation of the garting period on nonlinearity and mode area. The grating is formed by Si/SiO_2. As in this figure garting varies from 260 nm to 600 nm and we obtain the different value of the nonlinearity and mode area at different grating period. As we know that in HPW the light is confined in the low index region. As we increases the grating period from 600 nm, there is no confinement of the light in the low index region. In fact after 573 nm grating period with this particular design, we are not able to obtain any mode area. The left hand axis indicates the nonlinearity and right hand axis indicate mode area. As the grating period increases mode area going to be increased and nonlinearity going to be decreased. At grating period 260 nm, smallest mode area = 0.00017/ μm^2 and highest nonlinearity γ = 1.87 x 10^8 $km^{-1}w^{-1}$ and these values shows largest propagation length and lesser loss. The solid blue line is for the nonlinearity and solid black line is for the mode area. So the reported result gives strong mode confinement with larger propagation length with low loss and ultra high nonlinearity.

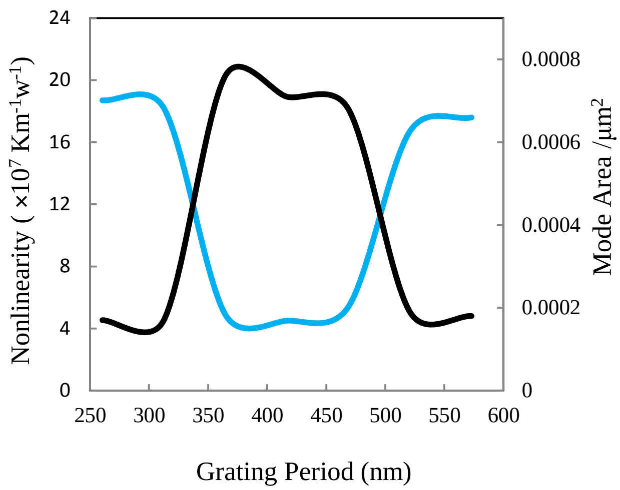

Figure 5.7 Effect of the grating period on nonlinearity and mode area. Gating thickness and duty cycle are respectively 10 nm and 0.96.

A novel nanophotonics waveguide for low-loss subwavelength optical confinement with ultra high nonlinearity is projected. The propagation characteristics of the projected waveguide are enhanced with the Si/SiO_2 grating formed in the high-index material silicon under the core-dielectric. The presence of grating under core-dielectric causes a large propagation length of 1-mm with a low propagation loss of 4-dB/mm. The strong subwavelength optical confinement is evidenced from a very small mode area of 0.00017/ μm^2. The nonlinearity of grating based HPW is found to be $\gamma = 1.87 \times 10^8\ km^{-1}w^{-1}$ which is almost ten times higher than that of other Nanophotonic waveguides. The obtained results indicate the possible utilization of the proposed hybrid plasmonic waveguide in high density photonic integration and potential application in efficient nonlinear signal processing.

5.3.3 Grating based Nano-Channel HP Waveguide

In the last two decades there have been a number of significant developments in the photonics industry and research. For conventional electronic circuits, photonic circuits have patent advantages in the data storage and delivery. Therefore, more and more attentions have been paid to photonic devices, such as waveguides [52], resonators [34] and their integrations with electronic devices.

Thus huge mismatch between the electronic and photonic devices blocks the realization of high density integration of these two technologies. To solve such a problem, a potential method has been proposed in recent years by utilizing the so-called plasmonic devices [37]. By guiding the electromagnetic wave at the interface of dielectric-metal, plasmonic waveguide based devices have the ability of confining light in a deep subwavelength scale. Thus plasmonics could have the advantages of both the photonics with high-speed data delivery and the electronics with miniaturized dimension simultaneously. Besides the better mode confinement, plasmonic devices have another significant advantage: the strong ability to enhance the electromagnetic field. Among them HPW is relatively superior with large propagation length and subwavelength mode confinement. These types of devices have ultra high mode confinement and reduced the propagation loss. We recently proposed a novel structure of the hollow HPW for nano-scale optical confinement and long range propagation [74]. There is a need to analyze the propagation properties of hybrid waveguide, such as mode area, propagation length, propagation of mode energy that propagates with in mode area and normalized energy density.

Figure 5.8(a) shows the block diagram for the proposed nanophotonics platform at duty cycle 0.57. (b) and (c) depicts field distributions, respectively in pictorial and line graph forms, of the fundamental TM-mode of the hybrid plasmonic waveguide. Above the substrate a crystalline Si is deposited with thickness t_{si} = 600 nm, width w_{si} = 4µm. Now in this layer by varying the grating period and duty cycle grating is formed of Si/SiO_2. By the optimization of the grating period and duty cycle at width of Si = 400 nm and SiO_2 = 300 nm, the best results for the propagation properties of the waveguide is obtained. Further formation of Si above the grating with Width = 1500 nm and thickness = 400 nm is studied to find out the effect of the high index layer. Above this a low refractive index region SiO_2 with width = 200 nm and thickness = 10 nm is fixed and at the top metal with thickness = 150 nm and width = 200 nm is fixed.

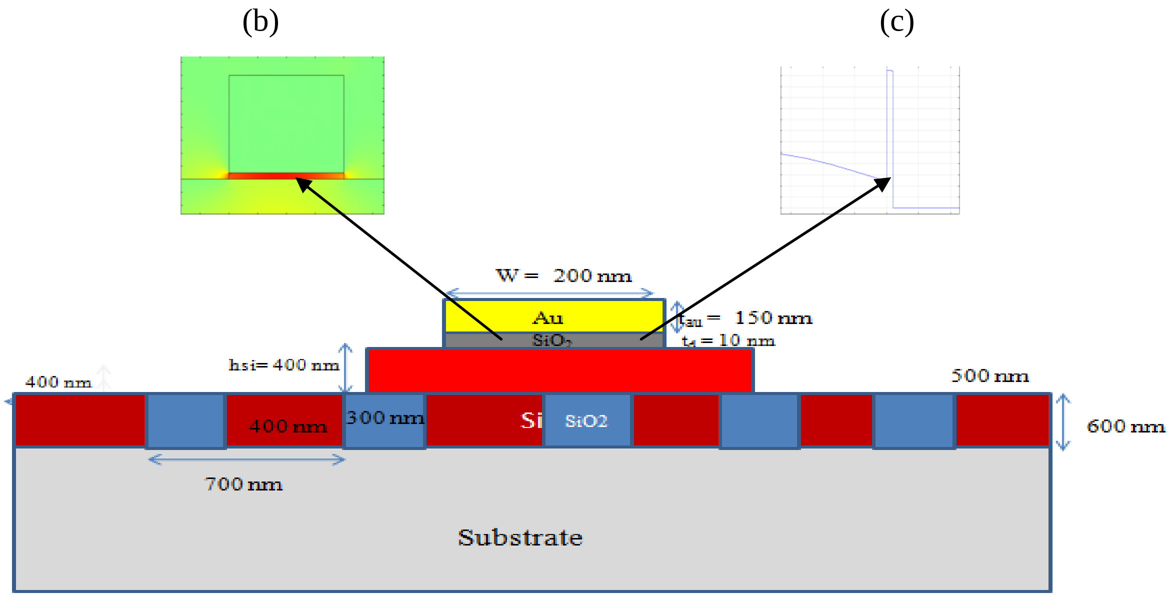

Figure 5.8(a) Shows the block Diagram for the Proposed Nanophotonics platform for HPW at duty cycle 0.57. (b) and (c)field distributions, respectively in pictorial and line graph forms for HPW.

Figure 5.9 shows the variation of grating period with propagation length with the grating period at constant duty cycle 0.57. Figure shows that when there is no grating is their the propagation length is 95 µm and modal propagation loss is 0.45 dB/µm and the effective mode area is 0.00063 /µm^2. With the variation of the grating period from 0 to 260 nm the propagation length increases from 95 µm to 2327 µm. Further from grating period 260 nm to 350 nm the propagation length decreases from 2327 µm to 132 µm and from the grating period 350 nm to 460 nm, the propagation length further increases from 132 µm to 1027 µm.

However from grating period 460 nm to 580 nm propagation length decreases from 1027 µm to 176 µm, from grating period 580 nm to 700 nm the propagation length increases as 176 µm to 3978 µm and finally from grating period 700 nm to 800 nm the propagation length decreases from 3978 µm to 195 µm. Further from grating period 800 nm to 840 nm the propagation length increases from 195 µm to 220 µm. From this figure it is concluded that at grating period 700 nm, the largest value of propagation length 3978 µm with lowest modal propagation loss 0.001 dB/µm and with nanoscale confinement the mode area as 0.00079/ μm^2 is obtained.

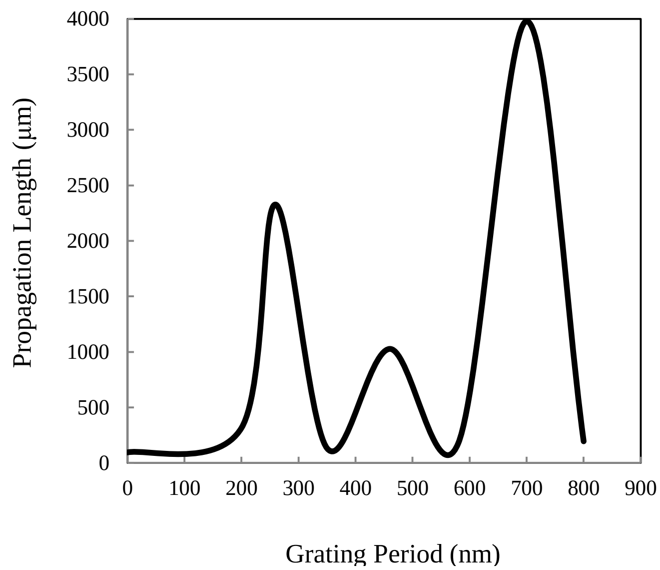

Figure 5.9 Variation of grating period with proagation Length at constant duty cycle 0.56.

Figure 5.10 Shows the variation of the grating period with duty cycle at constant grating period 700 nm. Figure shows that duty cucle 0.56, the largest value of the propagation length is obtained.From the duty cycle 0.14 to 0.28, the propagation length deacreases from 137 µm to 25 µm and from duty cycle 0.28 to 0.57 the propagation length increases from 25 µm to 3978 µm, further from 0.57 to 0.71 the propagation length decreases from 3878 µm to 61 µm and finally for the duty cycle from 0.71 to 0.85 the propagation length increases from 61 µm to 198 µm.

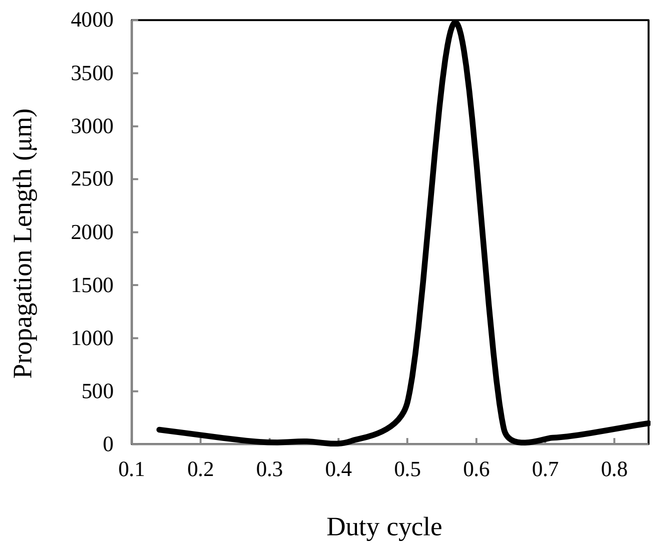

Figure 5.10 Variation of duty cycle with proagation Length at constant grating period 700 nm.

5.3.4 Variable air slot based HP Waveguide

In the preceding section of this chapter, various design for the modal characteristic of hybrid plasmonic waveguide is studied. In this section a variable air slot based hybrid plasmonic waveguide design is proposed. Figure 5.11 shows the proposed design for the nanoscale confinement. Above the substrate a Si crystalline with width = 3 μm with a height of Si h_{si} = 1μm is placed. In this region a variable air slot with variation of the width and thickness is placed. From this at width = 700 nm and height 200 nm of the air slot the lowest value of the modal propagation loss with tight mode confinement is obtained. So the slot with width = 700 nm and height 200 nm is inserted in the Si crystalline. Above the Si crystalline SiO_2 with width 200 nm and thickness 10 nm is placed and at top metal with width 200 nm and thickness 150 nm is placed. The confinement is there in the SiO_2 region with low loss. The air slot pushes the optical mode towards the plasmonic mode and leads to the formation of HP mode in SiO_2.

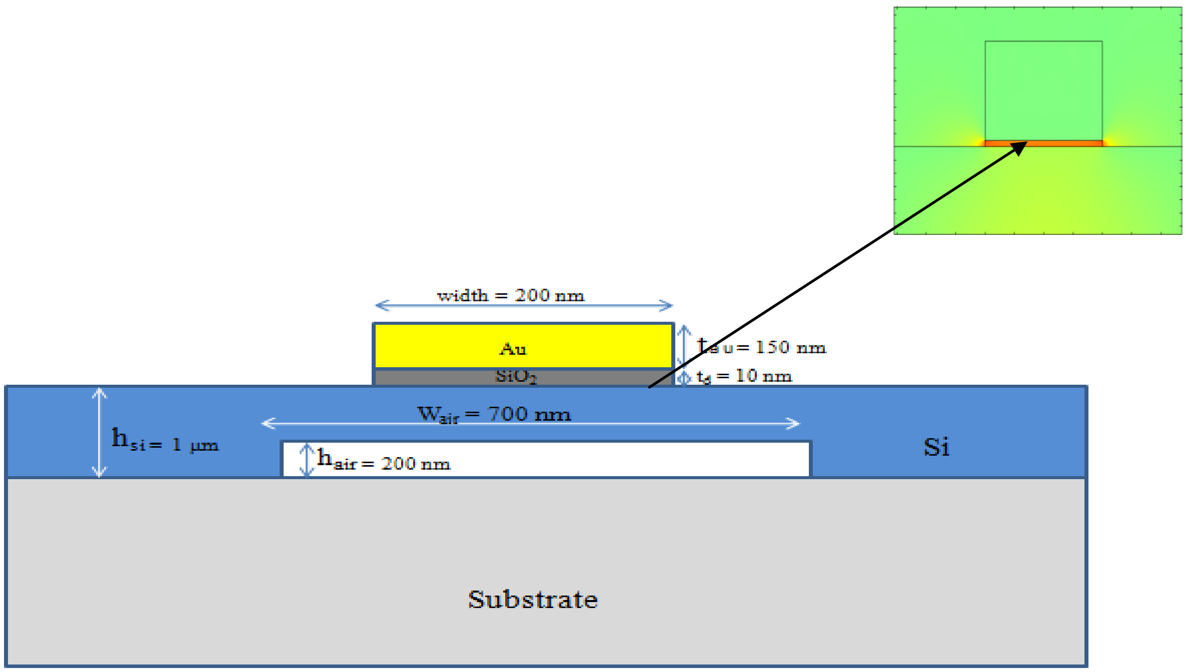

Figure 5.11 Design of Proposed Nanochannel with the air slot

Figure 5.12 shows the variation of the air slot height with the propagation length. With this figure it is shown that without air slot the propagation length is 102 µm with loss as,0.042 dB/µm. With the variation of the variation of the air slot height from 0 to 100 nm it found that there is decreases in the propagation length from 102 µm to 58 µm, and from air slot height to 100 nm to 200 nm increase in propagation length from 58 µm to 293 µm, and from 200 nm to 600 nm decrease in propagation length from 293 µm to 46 µm.

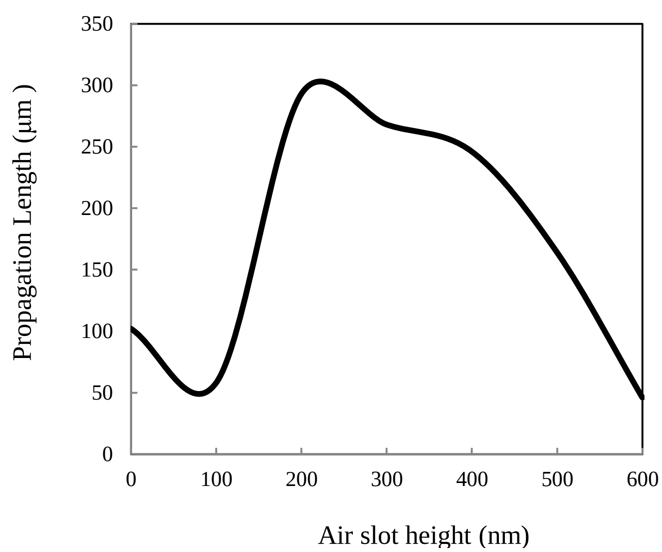

Figure 5.12 Variation of the air slot height with the Propagation Length at constant air slot width 700 nm.

So, with the air slot height 200 nm and width 700 nm the largest value of the propagation length 293 μm, with nanoscale mode area 0.00066 / μm^2 is obtained. Figure 5.13 shows the variation of the air slot height with the loss at constant air slot width is shown. It is shown that without air slot the loss as 0.042 dB/ μm, with the variation of air slot height from 0 to 100 nm loss increases from 0.042 dB/ μm to 0.073 dB/ μm, and with the variation of the air slot height from 100 nm to 200 nm loss decreases from 0.073 dB/μm to 0.014 dB/μm, and with air slot height variation from 200 nm to 600 nm increases in loss from 0.014 dB/μm to 0.095 dB/μm. After the air slot height 600 nm there is no confinement of the mode in the SiO_2 region.

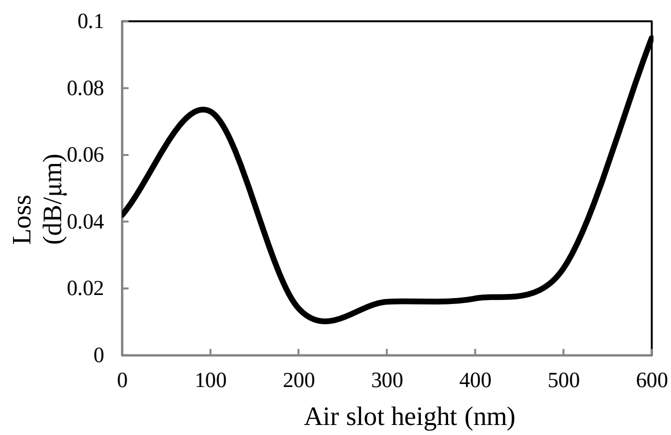

Figure 5.13 Variation of the air slot height with the Modal propagation Loss at constant air slot width 700 nm.

5.4 Summary

In this chapter a detailed study of various grating parameter like grating period, duty cycle, grating thickness and grating width on the different structure of the HPW is studied. In section 5.3.1 SiO_2 slot is inserted under the air slice which shows that air slice increases the propagation length with acceptable small propagation loss, in comparison to hybrid mode in the air slice. Further SiO_2 slot based waveguide have smaller mode area A_m = 0.00023 /μm^2, larger propagation Length L_p = 224 μm and lesser modal propagation loss L_m = 0.019 dB/μm at optimized value of the width and thickness. In the section 5.3.2 The garting is formed in the Si with Si/SiO_2 at fixed duty cycle is C = 0.96 and from this the obtained the grating period = 260 nm and thickness of each SiO_2 grating based slot is 10 nm and height of the slot is same as that of Si height. The presence of grating under core-dielectric causes a large propagation length of 1-mm with a low propagation loss of 4-dB/mm. The strong subwavelength optical confinement is evidenced from a very small mode area of 0.00017/ μm^2. The nonlinearity of grating based HPW is found to be $\gamma = 1.87 \times 10^8$ $km^{-1}w^{-1}$ which is almost ten times higher than that of other nanophotonic waveguides at the duty cycle 0.96. In the section 5.3.3 from this figure it is conclude that at grating period 700 nm, the largest value of propagation length 3978 μm with lowest modal propagation loss 0.001 dB/μm, with nanoscale confinement with the mode area 0.00079/μm^2 is obtained at duty cycle 0.57. And finally in the section 5.3.4 with air slot height 200 nm and width 700 nm the largest value of the propagation length 293 μm, with nanoscale mode area 0.00066 / μm^2 is obtained with very low loss 0.014 dB/μm is obtained. So, from the above discussion it is concluded that with the help of grating propagation length is increased upto 4mm with very low loss 1-dB/mm.

Chapter 6

Nanophotonics Coupler Based on Hybrid Plasmonic Waveguide

6.1 Introduction

The effect of high index layer and hybridization of plasmonic and photonic modes are discussed in the chapter 4 and 5. We found that there is increase in the propagation length with insertion of the grating in the high index contrast layer. Therefore in the present chapter we reported the effect of the garting on the nanophotonic vertical coupler coupling efficiency.

Nano silicon photonics carries the potential for large-scale integration of photonic and/or electronic devices on a single chip for applications in high-speed optical communications and in optical interconnects [106-108]. The emerging field of nanophotonics addresses the critical challenges in the path of optical manipulation at real nano scales. Recently there has been a keen interest in Hybrid Plasmonic Waveguides (HPW) for long-range propagation and subwavelength optical confinement [45, 74, 109-110]. A number of optical functionalities have been proposed based on HPW [101-102] . In HPW, a high index layer under the guiding dielectric layer can play a key role for tailoring the propagation characteristics which may be useful to enhance the coupling properties of the HPW based coupler. Besides realizing on-chip couplers, a grating based HPW can be a building block for making other nano photonic devices. Coupler is a basic component of photonic integrated circuit which are used in power splitting/combining, modulation, multiplexing and so on [67, 111-112]. For many applications it is sometimes needed to control the phase of the coupler which can be effectively done using grating and bragg reflectors.

Optical gratings and bragg reflectors are known for their filtering response and controlled coupling which have already been utilized in making many important optoelectronic functions [113-115]. As an alternative to Distributed Bragg Reflectors (DBRs), subwavelength gratings have recently created a deep interest because of its one-layer structure, broadband nature and large fabrication tolerance [116, 92-93]. High refractive index contrast and subwavelength nature of this grating can be used to tailor the guiding and coupling characteristics of on-chip photonic devices [62, 94-95, 117]. Vertical optical couplers being compact and high speed can enable monolithic 3D optoelectronic integration for optical interconnects [113].

A nanophotonic coupler based on HP waveguide is proposed which shows high-speed coupling caused by an ultra-short coupling length of 0.461-μm with a long propagation length of 123-μm. We found that the role of high-index layer under the guiding-dielectric in a HPW is significant to control guiding properties. The introduction of a Lateral Subwavelength Grating (LSG) into the high-index layer in the HPW results in efficient guiding and coupling characteristics. The lateral resonances in the LSG modify the vertical coupling of HP modes providing us an ultra-short coupling length of 0.461-μm resulting from large phase difference between even and odd HP modes. Further the proposed coupler exhibits acceptably large propagation lengths of 123-μm and 53-μm, respectively, for odd and even modes. The coupling performance, defined by the ratio of propagation length (of odd mode) to the coupling length which is the benchmark for a coupler, is reported to be 192. Introducing a disorder in the grating is also shown to enhance the coupling properties. In addition, the broadband nature of the LSG pushes the proposed coupler to show broadband coupling where coupling length remains acceptably small and the coupling performance remains high over a broad range of wavelength. The design and analysis of the proposed coupler are performed using Finite Element Method (FEM) and the results are validated with the Finite Difference Method (FDM). LSG introduced into the HP waveguide is shown to provide multifold benefit in the sense that the phases and optical confinement of the guided modes can be controlled with LSG. Besides increasing fabrication tolerance the presence of LSG makes the fabrication of the proposed coupler cost-effective because of the smaller grating width around 4 μm, which requires less time and cost to fabricate it. Also, the coupling regime, with respect to various coupler parameters gets expanded which again indicates larger fabrication tolerance.

6.2 Proposed Design of Nanophotonics Coupler

A schematic of the proposed nanophotonic coupler based on HPW is shown in figure 6.1, which consist of silica as substrate. It consists of a Si/SiO_2 subwavelength grating, we call it lateral subwavelength grating (LSG), distributed laterally on an SiO_2 substrate. The grating parameters are thickness t_g (= 200 nm), width w_g (= 4μm), grating period Λ, and duty cycle C. The hybrid plasmonic mode can be confined into the dielectric (SiO_2 of thickness 10 nm) layer sandwiched between LSG (in the bottom) and metal layer (gold on top). The HP mode is vertically coupled through gold layer into another dielectric (SiO_2 of same thickness 10 nm) layer. A layer of silicon with thickness equal to that of t_g (200 nm) is placed on top SiO_2 to maintain the symmetry of the structure [113]. The t_g is kept constant because only at this thickness even, odd mode beating occurs. The presence of top silicon provides large refractive index contrast in vertical direction for the tight odd-mode confinement. The LSG and the metal can efficiently control the coupling as well as guiding characteristics of the proposed nano-optical coupler.

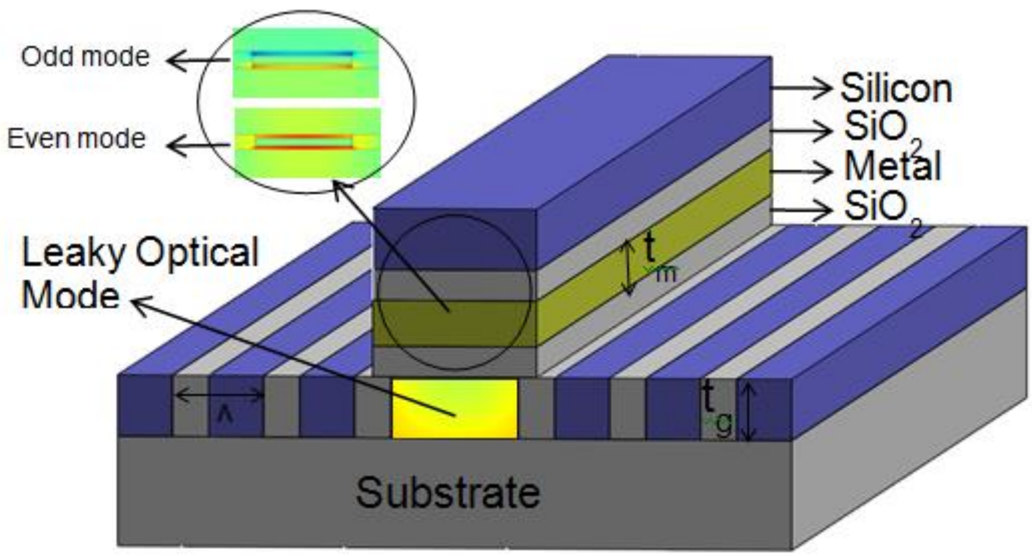

Figure 6.1 Schematic of the proposed design of nanophotonic vertical coupler based on hybrid plasmonic waveguide. The Si/SiO_2 grating is formed on the SiO_2 substrate. Inset shows the field distributions of the fundamental even and odd TM modes in the vertical coupler. The mode distribution shown in yellow color in the center of the grating (in the region of disorder) is the calculated leaky optical mode which control the vertical coupling of HP modes.

6.3 Analysis of Coupler Performance

The LSG increases the phase difference between odd and even HP modes leading to a lower coupling length as shown in figure 6.2. The phase difference is maintained by refractive index difference in even and odd mode. The propagation length given by $L_{p\ (\mu m)} = \frac{\lambda}{4\pi(n_{eff})imaginary}$ and coupling length, by $L_c = \frac{\lambda}{2|n_{eff(even)} - n_{eff(odd)}|}$ [113] are two important performance parameters, where L_c is defined as the distance at which maximum optical power is coupled between the two HP waveguides. The propagation length L_p describes the propagation loss of the HP mode. An important figure of merit is the coupling performance which is defined as the ratio, R= $\frac{L_{p(odd)}}{L_c}$. A good coupler performance requires larger L_p and smaller L_c , where L_c of the vertical coupler is estimated by the even and odd mode beating. The even and odd mode beating is done by separation of metal thickness(t_m) layer sandwiched between top and bottom SiO_2. The normalized odd mode power is given by f_{odd} = $1\text{-}e^{-1/R}$ [101], indicates the odd mode power loss after one coupling cycle. At dielectric thickness t_{sio2} = 10 nm, nanoscale optical confinement with very low loss is obtained [110-111] . So the dielectric layer below and above the metal layer is kept constant. Now proper choice of metal thickness has to be decided, which provides us the coupling between even and odd mode.

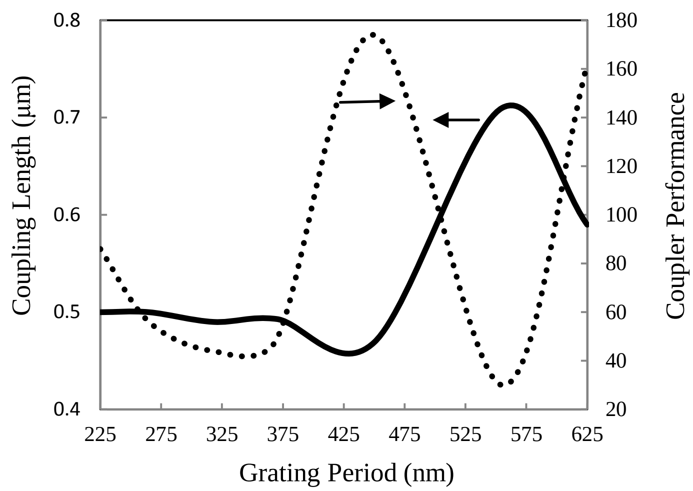

Figure 6.2 Effect of the grating period on coupling length (left y-axis) and on coupler performance (right y-axis) at constant duty cycle of 0.88.

By the variation of $t_{m,}$ from t_m= 10 nm onwards, when there is no grating in the high index region Si. At t_m 20 nm, with smallest ultra-short coupling length L_c = 0.484μm, larger coupler performance R= 52, reduced odd mode power loss f_{odd} = 1.9% and propagation length of the odd mode 25 μm is obtained. Therefore metal thickness as, t_m = 20 nm is kept constant, as after t_{au}= 50nm the mode starts decoupling. Now dielectric thickness 10 nm for both dielectric region above and below metal layer and t_m =20 nm as constant for the intersection of LSG in the high index region Si is with variable grating period (ʌ) and duty cycle C.

Figure 6.2 shows the variation of the grating periods at constant duty cycle 0.88. The left hand side shows coupling length and right hand side shows the coupler performance with variation of grating period. The variation of grating period with L_c is depicted by black line which shows that from grating period 225 nm to 450 nm coupling length decreases from 0.50 μm to 0.469 μm and further in grating period 450 nm to 550 nm coupling length increases from 0.469μm to 0.71 μm and finally in grating period 550 nm to 625 nm coupling length further decreases from 0.71 μm to 0.59 μm. Similarly the behavior of coupler performance depicted by dotted line, is found as at grating period 225 nm to 370 nm coupler performance decreases from 86 to 49. Further with grating period 370 nm to 450 nm coupler performance increases from 49 to 174 and from grating period 450 nm to 550 nm, coupler performance decreases from 174 to 30 and at last 550 nm to 625 nm, the increment in coupler performance was found from 30 to 162. The Vertical coupler characteristics in our analysis is studied at t_m 20 nm. Therefore in figure 2, at Λ = 450 nm, largest $L_{p(odd)}$ = 82 μm with lesser $L_{m(odd)}$ = 0.052 dB/ μm, with Ultrashort L_c = 0.469 μm with larger R = 174 and with very low f_{odd} = 0.5% is obtained. Figure 2 depicts the behavior of ordered grating and from this at grating period 450 nm and duty cycle 0.88, the best values of the coupler performance is obtained. By these garting period 450 nm and duty cycle 0.88, the grating with disorder is maintained by varying the gap under the coupler region. But at this grating period and duty cycle, the $L_{p(odd)}$ is not increased at different grating period for different grating with disorder length. But at grating period 550 nm and gap below the coupler is 250nm, for Grating with Disorder Length (GDL), enhancement in the odd mode propagation length is shown in figure3. It gives the variation of odd mode propagation length $L_{p(odd)}$ and coupling length for the grating with disorder length under coupler region. The left hand side and right hand side gives the behavior of $L_{p(odd)}$ and L_C, at grating with disorder period at Λ = 550 nm, the lower $L_{m(odd)}$ = 0.035 dB/μm with larger $L_{p(odd)}$ = 123 μm for this R is 192 and f_{odd} = 0.5% is obtained.

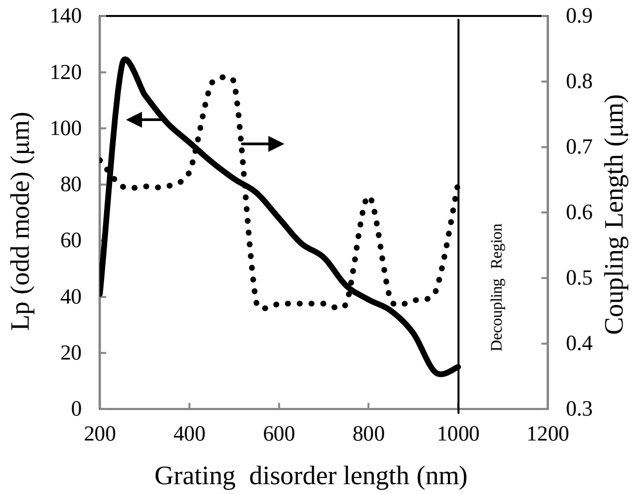

Figure 6.3 Effect of grating disorder length under the coupler region on $L_{p(odd)}$ (left y-axis) and on coupling length (right y- axis) at constant garting period of 550 nm.

The effect of variation of grating with disorder length under the coupler region from 200 nm to1100nm is shown in figure 6.3.This figure shows that at grating with disordered length from 200 nm to 250 nm the $L_{p(odd\ mode)}$ starts increasing from 41 µm to 123 µm and after 250 nm to 1000 nm, grating with disordered length mode odd propagation starts decreasing from 123 µm to 15 µm. After grating with disordered length 1000 nm the even and odd mode coupling is not there. Similarly behavior of coupling length is shown in figure3. It shows that for grating with disorder length from 200 nm to 350 nm the coupling length decreases from 0.68 µm to 0.64 µm and for grating with disorder length from 350 nm to 500 nm coupling length starts increasing from 0.64 µm to 0.798 µm and for grating with disorder length from 500 nm to 750 nm shows the constant behavior of coupling length i.e 0.461 µm. For grating with disorder length from 750 nm to 800 nm results in increase of coupling length from 0.461 µm to 0.625 µm and from grating with disorder length 800 nm to 900 nm, there is further decrease of coupling length from 0.625 µm to 0.466 µm. Later grating with disorder length from 900 nm to 1000 nm increases the coupling length from 0.466 µm to 0.645 µm. After this grating with disorder length coupling of odd mode with even mode is not there. Figure 6.3 shows the lateral subwavelength garting behavior. At the gap 250 nm with larger value of odd mode propagation length $L_{p(odd)}$ = 123µm and low loss 0.035 dB/µm with larger coupler performance 192, ultrashort coupling length of 0.461µm at specific point is also obtained.

After the detailed study of effect of grating period and grating with disordered length on coupling length, coupler performance and on the odd mode propagation length, we studied the effect of metal thickness on the coupler performance as the metal thickness plays a crucial role with the coupler performance. The effect of metal thickness without grating, grating with disorder length and ordered garting with the coupler performance(R) is shown in figure 6.4. Initially the effect of coupler performance without grating is studied. The black line shows the variation of coupler performance without grating with metal thickness. With the increases of metal thickness from t_m 10 nm to 20 nm there is a increase in coupler performance from 39 to 52, and from metal thickness t_m 20 nm to 30 nm, coupler performance decreases from 52 to 44 and from metal thickness t_m 30 nm to 50 nm there is further increase in coupler performance from 44 to 55. Black large dotted line in figure 6.4 shows the effect of grating with disorder length on coupler performance with the variation of metal thickness at constant Λ = 550 nm and C=0.88, with gap below the coupler is 250. With the increase in metal thickness from t_m 10 nm to 20 nm, there is increase in coupler performance 56 to 192 and from metal thickness t_m 20 nm to t_m 30 nm, coupler performance starts decreasing from 192 to 57. However from metal thickness t_m 30 nm to 40 nm there is slight increase in coupler performance from 57 to 64. Finally from metal thickness from t_m 40 nm to 50 nm, coupler performance is from 64 to 52. After the study of the without grating and grating with disorder length on the coupler performance, now the behavior of the ordered grating on the coupler performance is studied at constant grating period 450 nm with duty cycle 0.88. It is shown with the small dotted line. However with the increase in the metal thickness from t_m 10 nm to t_m 20 nm increases the coupler performance from 131 to 174, for metal thickness t_m 20 nm to 30 nm, there is decrease in coupler performance from 174 to 153 is observed. Further with metal thickness from t_{au} 30 nm to 50 nm, there is found increase in coupler performance from 153 to 164 and from metal thickness t_{au} 50 nm to 80 nm, decrease in coupler performance decreases from 164 to 47. One important feature of the intersection of the ordered grating is that it supports the metal thickness upto 80 nm for the coupling of the even and odd mode, whereas without grating and grating with disorder, supports the metal thickness upto 50 nm for the coupling of the even and odd mode. At t_m = 20 nm, largest coupler performance with all the three parameters is obtained i.e. without grating, with ordered grating and grating with disordered length, the $L_{p(odd)}$= 25 μm is smallest for the without grating and increased with ordered grating up to $L_{p(odd)}$= 82 μm and largest with grating with disordered length $L_{p(odd)}$= 123 μm.

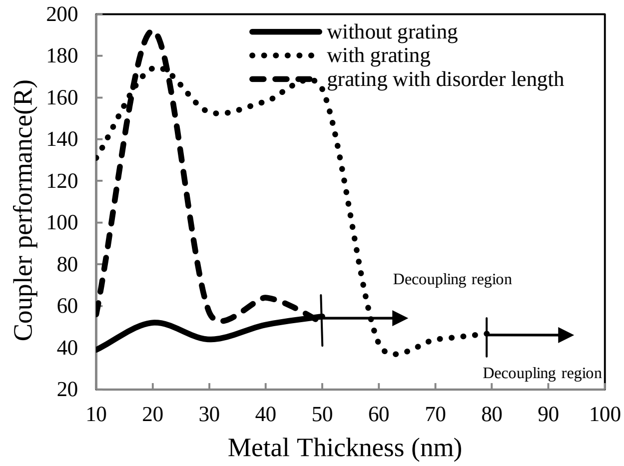

Figure 6.4 The variation of the metal thickness with the coupler performance is shown. The solid line for the without grating have L_c = 0.484 μm, the large dotted line shows the grating with disorder length for R with ʌ = 550 nm with gap below the coupler is 250 nm, at this specific ʌ with C =0.88, L_c= 0.64 μm. The third small dotted line show the variation of the metal thickness with ordered grating for R at constant ʌ = 450 nm and C= 0.88, at t_m = 20 nm, L_c = 0.469 μm.

6.4 Wavelength Dependence

After the detailed study of the coupler performance with the metal thickness, the wavelength dependence nature of the vertical directional coupler is studied. The wavelength selective operation of the vertical coupler is helpful for realization of the vertical coupler for the optical filter. The broadband nature of the vertical coupler for the different wavelength range is studied for without grating, ordered grating and grating with disorder. Figure5. shows the wavelength dependence of the vertical coupler at different wavelength range. Wavelength dependence with coupler performance without grating, with ordered grating and grating with disorder is studied with the variation of the wavelengths. At first stage, the effect of variation of wavelength on the coupler performance without grating is studied, it is shown with the small dotted line in figure 6.5. It shows that from wavelength λ = 1480 nm to 1530 nm there is a decrease in the coupler performance from 49 to 41 and with increase in λ = 1530 nm to 1550 nm, there is a increase in coupler performance from 41 to 52. With a further increase in wavelength from 1550 nm to 1600 nm, decrease in coupler performance from 52 to 27 is obtained. Secondly the solid line in figure 6.5 shows the variation of wavelength with the coupler performance for ordered grating. At grating period =450 nm and duty cycle =0.88, with ordered grating, the vertical coupler shows the broader wavelength coupling range. It shows that from wavelength 1420 nm to 1430 nm, there is a increase in the coupler performance from 19 to 65 and after increase in wavelength from 1430 nm to 1510 nm, there is a decrease in the coupler performance from 65 to 45. After this decrease, from wavelength 1510 nm to 1520 nm, there is slight increase in coupler performance from wavelength 1520 nm to 1530 nm. Coupler performance decreases from 58 to 56. As wavelength increases from 1530 nm to 1540 nm, a sharp increases is found in the coupler performance from 56 to 186, at last wavelength range from1540 nm to 1610 nm, there is decrease in coupler performance from 186 to 91. At third stage, the effect of the wavelength variation on the grating with disorder length is shown with the large dotted line at grating period 550 nm, duty cycle 0.88 and at gap below the coupler is 250 nm. For this study, as wavelength increases from 1480 nm to 1540 nm, coupler performance decreases from 71 to 53. Increase in wavelength from 1540 nm to 1560 nm, leads to increase in coupler performance from 53 to 194 and for wavelength from 1560 nm to 1590 nm, there is a decrease in coupler performance from 194 to 44. It is observed that for without grating and for grating with disordered length, coupling starts at 1480 nm wavelength and upto 1600 nm for without grating and upto 1590 nm for grating with disordered length.

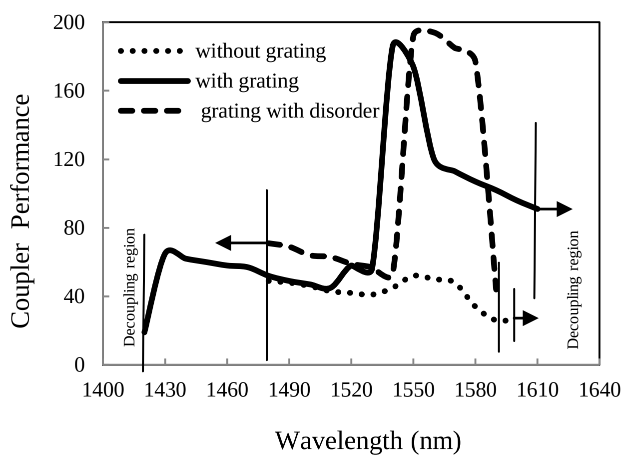

Figure 6.5 The effect of wavelength variation on the coupler performance. The small dotted line for the without grating, Solid line is with grating at ʌ = 450 nm and duty cycle =0.88.The large dotted line shows the grating with disordered length at ʌ =550 nm and duty cycle =0.88.

The ordered grating shows the coupling starts from wavelength 1420 nm and lasts upto 1610 nm. The arrow on the right and left hand side of the line shows the decoupling region where there is no even and odd mode beating.The figure 6.5, demonstrate the detailed study of the wavelength dependence on coupler performance. It shows that at wavelength 1550 nm for without grating, larger $L_{m(odd)}$ = 0.17 dB/μm, and lesser $L_{p(odd)}$ = 25 μm with larger L_c = 0.484 μm and odd mode power loss is $f_{(odd)}$ =0.5% is obtained. Similarly for ordered grating at wavelength 1550 nm the obtained value for L_p = 82 μm is larger as compared to without grating with reduced ultrashort coupling length L_c= 0.469 μm, with low odd mode loss = 0.052 dB/μm and odd mode power loss is found as $f_{(odd)}$ =0.5%. And finally, grating with disordered length the value as, larger L_p =123 μm and enhanced L_c= 0.64 μm with low loss = 0.035 dB/μm is obtained. The grating with disordered length gives us the flat response for coupler performance from 1550 nm to 1580 nm.

6.5 Summary

In conclusion a high-speed nano-photonic vertical coupler based on Hybrid Plasmonic (HP) waveguide with Lateral Subwavelength Grating (LSG) is proposed. High speed coupling is a result of an ultra-short coupling length 0.461 μm caused by the lateral resonances in the subwavelength grating. The combined effect of LSG and the metal layer sandwiched between the coupling regions makes it possible to realize efficient coupling and low-loss guiding of HP modes which corresponds to a propagation length of 123-μm. The lateral resonances strongly modify the vertical coupling resulting in a broadband coupling in terms of acceptably large coupling performance 192 over a broad range of wavelengths with very low normalized odd mode power loss 0.5%. In addition, the insertion of the LSG causes decoupling to occur at a larger value of metal thickness, upto 80-nm with a large value of coupler performance, which increases fabrication tolerance of the nano-coupler in terms of metal thickness. The proposed HP waveguide based nanophotonic coupler is capable of being integrated with/to-couple nano-optoelectronic devices into the silicon platform and it can find applications in optical interconnects with short response times.

Chapter 7
Conclusion and Future scope

7.1 Conclusion

The hybrid plasmonic are found to be superior in terms of the low loss and nanoscale confinement as compared to other types of the plasmonic waveguide. The HPW found application in the nanoscale photonics devices for the optical interconnect and biosensing. So, the main motivation in this thesis is to propose an HPW mechanism which has relatively low modal propagation loss with larger propagation length at nanoscale mode confinement as compared to the plasmonics waveguides. To achieve this, various types of HPW designs are proposed in this work. We also addressed the problem associated with the Plasmonic waveguides.

Plasmonic waveguides simultaneously cannot provide the tight mode confinement and low loss. For example, the metallic wire or stripe waveguides are not able to provide the subwavelength mode confinement even though these waveguides have larger modal propagation length of several hundred micrometer or even millimeters, however it is difficult for them to realize subwavelength mode confinement for plasmonic channel and slot waveguides with deep-subwavelength mode confinement, the propagation lengths are usually several micrometers. With large propagation length with a subwavelength mode confinement, the hybrid plasmonic waveguide is found to be relatively superior.

The objective of this thesis is to design and analyze the efficient HPW which shows the increases in the propagation length with tight mode confinement and high nonlinearity. The study of various types of the grating based devices, shows the effect of different grating parameters like (grating period, duty cycle, width, depth, length) on the waveguide characteristics. Further design of the nanophotonic coupler based on the proposed waveguide and to investigate the coupler performance of the HPW coupler is also studied.

The major findings obtained are summarized as follows:

1. The HPW consists of a high refractive index layer of semiconductor separated from a metal layer by a low index dielectric gap. The mode guiding in the HPW is in the dielectric gap which results from the coupling of a dielectric waveguide mode and a surface plasmonic mode.

2. The novel design with air gap between metal and semiconductor is proposed. The variation of the width and height of the air gap in between metal and semiconductor gives the tight mode confinement of HP mode in the air gap. The confinement of the HP mode in the air slice gives us nanoscale confinement with increased propagation length and simultaneously reduced mode area. This is due to low effective modal index in the lateral optical spread. The confinement of the HP mode with air gap gives lesser mode area $A_m = 0.0685/\mu m^2$ with larger propagation length $L_p = 142$ μm and low loss of 0.03 dB/μm for the certain value of width and height of the air as dielectric compared SiO_2 as dielectric.

3. Theoretical representation of the mode coupling between the plasmonic and optical mode which gives the HP mode is presented. The effect of the high index layer is also investigated. It is possible to guide and confine the light at real 'nanoscale' with the help of hybridization of the photonic mode and SPP mode. The hybridization is analytically decided by a parameter called mode character. It is further shown that that beyond a certain thickness of high- index region evanescent filed into dielectric begins to lose its coupling with SPP mode which disables the mode hybridization: the guided mode now becomes leaky photonic mode with larger field in the high-index layer. Thus the presence of high-index layer under the dielectric is crucial and can be used to mould the coupling of the free electrons of metal with the optical fields. The coupling strength for $Si/SiO_2/Ag$ system is 52%. Propagation length of HP mode with silicon is 154 μm at a 10 nm thick dielectric. The propagation loss for Si based HP waveguide is 0.028 $dB/\mu m$ and modal area for silicon is 0.0009 $/\mu m^2$. The nonlinear coefficient with the thickness of the dielectric at $t_d = 10$ nm is $\gamma = 3.8\times 10^7$ $km^{-1}w^{-1}$.

4. Further, some of the engineered designs of HPW are proposed by insertion of grating. Effect of different grating parameters like (grating period, duty cycle, width, depth, length) on the waveguide characteristics is calculated. Firstly we insert the SiO_2 slot below the hollow

hybrid plasmonic waveguide in the Si layer. With these increases in the propagation length is observed when slot is inserted below the hollow HPW, the L_p = 142 μm for air slice and it is L_p = 224 μm when slot is introduced and the loss is reduced from 0.03 dB/μm without air slice to 0.019 dB/μm for SiO_2 slot under the air slice. Nanoscale mode confinement is obtained in case of slot insertion 0.00023 /μm^2.In another design variation of garting period with the duty cycle is presented. The garting is inserted in high index region. The presence of grating under core-dielectric causes a large propagation length of 1-mm with a low propagation loss of 4-dB/mm. The strong subwavelength optical confinement is evidenced from a very small mode area of 0.00017/ μm^2. The nonlinearity of grating based HPW is found to be $\gamma = 1.87 \times 10^8$ km^{-1}w^{-1} which is almost ten times higher than that of other nanophotonic waveguides. Further for the increase of the propagation length another design is proposed which study the effect of high index region. It is observed that at grating period 700 nm and duty cycle 0.57, the largest value of propagation length is 3978 μm with lowest modal propagation loss 0.001dB/μm, with nanoscale confinement with the mode area 0.00079/ μm^2 is obtained. This is the highest value of the propagation length we obtained in our study with lowest loss.

5. It is found that a high index layer under the guiding dielectric layer can play a key role for tailoring the propagation characteristics which may be useful to enhance the coupling properties of the HPW based coupler. A nanophotonic coupler based on HP waveguide is proposed which shows high-speed coupling caused by an ultra-short coupling length 0.461 μm with a long propagation length 123 μm.The introduction of a lateral subwavelength grating (LSG) into the high-index layer in the HPW results in efficient coupling characteristics. Further the proposed coupler exhibits acceptably large propagation lengths for odd 123 μm and even modes 53 μm. In addition, the broadband nature of the LSG pushes the proposed coupler to show broadband coupling where coupling length remains acceptably small and the coupling performance remains high over a broad range of wavelength. The lateral resonances strongly modify the vertical coupling resulting in a broadband coupling in terms of acceptably large coupling performance 192 over a broad range of wavelengths with very low normalized odd mode power loss 0.5%. The proposed HP waveguide based nanophotonic coupler is capable of being integrated with/to-couple nano-optoelectronic devices into the silicon platform and it can find applications in optical interconnects with short response times.

The proposed work on the design, analysis and simulation of the HPW can be used to realize a nanophotonic platform with long range propagation with acceptably low-loss and nanoscale confinement.

7.2 Future Scope

The future scope of the Hybrid Plasmonic Waveguide from this thesis is drawn as

The hybrid plasmonic waveguide have scope in the field of telecommunication and biosensing. There is need of improvement for coupling efficiency of hybrid plasmonic waveguide with the standard photonic circuit. Our proposed work can be useful to enable an integrated platform based on hybrid plasmonic-photonic waveguide which can be promising for making photonic devices at real nano scales with flexible and variable nonlinearity.

The grating based devices have indicated the possible utilization of the proposed hybrid plasmonic waveguide in high density photonic integration and potential application in efficient nonlinear signal processing. For the further application in the field of the optical interconnects, the hybrid plasmonic waveguide coupling with nanophotonics circuits is necessary. The nanophotonic coupler can be used in the development of high speed optical switches. In integrated photonic circuits nanophotonic couplers are included for on chip integration. The proposed HP waveguide nanophotonic coupler is capable of being integrated with nano-optoelectronic devices. It can find applications in optical interconnects with short response time.

List of Publications:

[1] Tarun Sharma, Mukesh Kumar, "Hybridization of Plasmonic and Photonic Modes for Subwavelength Optical Confinement with Longer Propagation and Variable Nonlinearity", ***Elsevier,*** *Optics Communication*, vol.343, pp 85-90, 2015, **(IF 1.542).**

[2] Tarun Sharma, Mukesh Kumar," Hollow Hybrid Plasmonic Waveguide for Nanoscale Optical Confinement with Long Range Propagation," ***OSA****: Applied Optics*, vol. 53, no.9, pp 1954-1957, March 20, 2014,.**(IF: 1.649).**

[3] Tarun Sharma, Mukesh Kumar, "High-speed Nanophotonic Coupler Based on Hybrid Plasmonic Waveguide with Lateral Subwavelength Grating" Communicated to IEEE JLT.

[4] Tarun Sharma, Mukesh Kumar, "Air-slice and dielectric-slot Assisted Low Loss Hybrid Plasmonic Waveguide for Sub-wavelength Optical Confinement with Long Rang Propagation", accepted for international conference on optics and photonics, held from 18th Feb – 20th Feb2015, organized by Optical society of India association with Calcutta university**.**

[5] Tarun Sharma, Mukesh Kumar, "Subwavelength Optical Confinement and Long Propagation using Grating based Hybrid Plasmonic Waveguide with High Nonlinearity" at IISc, Bangalore in WRAP -2015, organized by IEEE photonics society on 16th and 17th Dec 2015.

[6] Tarun Sharma, Mukesh Kumar, "Grating based Hybrid Plasmonic Waveguide for Subwavelength Optical Confinement with Low Loss" SPIE EUROPE 3-7 April, 2016, held in Belgium.

References

[1] T.H. Maiman, "Stimulated Optical Radiation in Ruby Masers", *Nature*, vol. 187, pp.493-494, 1960.

[2] A. Barh, S. Ghosh, R. K. Varshney, B. P. Pal, "An efficient broad-band mid-wave IR fiber optic light source: design and performance simulation," *Optics Express*, vol. 21, no. 8, pp. 9547-9555, 2013.

[3] A Barh, S. Ghosh, R. K. Varshney, B. P. Pal, "A Tapered Chalcogenide Microstructured Optical Fiber for Mid-IR Parabolic Pulse Generation: Design and Performance Study", *IEEE Journal of Selected Topics in Quantum Electronics*, vol. 20, no. 5, p. 7500507, 2014.

[4] S. Sudha, T.ogasawara, Y.shoji, K.Kintaka, H.Kawashima, T.Hasama, H.Ishikawa, "optical nonlinear properties and carrier plasma effect at low carrier density in silicon wire waveguides" *IEEE Journal of Quantum Electronics*, vol. 47, no. 9, pp.1208-1213, 2011.

[5] Brajesh Kumar Kaushik, Saurabh Goel, Gaurav Rauthan, "Future VLSI Interconnects: Optical Fiber or Carbon Nanotube – a Review" *Microelectronics International*, vol. 24, no. 2, pp.53 – 63, 2007.

[6] K.Tanizawa, S.Suda, Y.Sukahipura, T.Kamei,R.Takei, H.Kawashiz,S.Nanini, M.Mori, H.Ishikawra, "observation of spontaneous raman scattering in hydrognted amorphous silicon wire waveguide at 1.55 μm" *Electron Letters*, vol. 49, no.9,pp.610-612, 2013.

[7] Y.Shoji, K.Kintaka, S.Suda, H.Kawashima, T.Hasama, H.Ishikawa, "four port optical switch having three connection states with Si waveguide" *IEEE Photonics Technology Letters,* vol 23,no. 1, pp.12-14, 2010.

[8] Paul O. Leisher, Chen Chen, Joshua D. Sulkin, Mohd Sharizal Bin Alias, Khairul Anuar Mat Sharif, Kent D. Choquette, "High Modulation Bandwidth Implant-Confined Photonic Crystal Vertical-Cavity Surface-Emitting Lasers", *IEEE Photonics Technology Letters,* vol. 19, no. 19,pp 1541-1543, 2007.

[9] S.Singh, R.S.Kaler, "Novel optical flat gain hybrid amplifier for dense wavelength division multiplexing system" *IEEE Photonics Technology Letters*, vol. 26, no.2, pp.173-176, 2014.

[10] S.P Mondal, S.K Ray, "Enhanced broadband photoresponse of Ge/Cds nanowire radial hetrostructure" *Applied Physics Lettrers*, vol.94, no.22, p.223119, 2009.

[11] VS Reddy , S.Karak, S K.Ray, A.Dhar, "Carrier transport mechanisem in aluminum nanoparticle embedded AlQ_3 structures for organic bistable memory devices" *Organic Electronics,* vol.10, no.01, pp. 1838-144, 2009.

[12] S K Ray, S. Maikap, W.Banerjee, S.Das , "Nanocrystals for Silicon based light emitting and memory devices", *J. physics D: Applied physics*, vol. 46, no.15, p.153001, 2013.

[13] M. T. Johnson, D. F. Siriani, Meng Peun Tan, K. D. Choquette, "High-Speed Beam Steering With Phased Vertical Cavity Laser Arrays," *IEEE Journal of Selected Topics in Quantum Electronics,* vol. 19, no. 4, pp. 1701006-1701006, 2013.

[14] S.E. Miller, "Integrated Optics: An Introduction", *The Bell System Technical Journal* vol.48, no.7, pp.2059–2068, 1969.

[15] S. Selvaraja, W. Bogaerts, D. Van "Throughout, Loss reduction in silicon nanophotonic waveguide micro-bends through etch profile improvement", *Optics Communications*, vol.284, no. 8, pp.2141-2144, 2011.

[16] S. Selvaraja, Erik Sleeckx, Marc Schaekers, W. Bogaerts, Dries Van, "Thourhout, Deposited amorphous silicon-on-insulator technology for nano-photonic integrated circuits", *Optics Communications*, vol. 313, no.3, pp. 210-216, 2014.

[17] Koos, C., Leuthold, J., Freude, W., Kippenberg, T. J., Pfeifle, J., Weimann, C. Schmogrow, "Terabit/s data transmission using optical frequency combs", International Society for Optics and Photonics, *SPIE LASE*, pp. 860009-860009, 2013.

[18] M Khorasaninejad, N Dhindsa, J Walia, S Patchett, SS Saini, "Highly enhanced Raman scattering from coupled vertical silicon nanowire arrays," *Applied Physics Letters,* vol. 101, no.17, p.173114, 2013

[19] M.Ohtsu, "Progress in Nano-Electro- Optics V", *Springer-Verlag Berlin,*1993.

[20] Vittorio M.N.Passaro, "Advances in Photonic Crystals", Publisher InTech, 2013.

[21] Alok Kumar Jha, T Sreenivasulu, Shafeek A Samad, T Srinivas, "Variation of Single waveguide modes with dielectric constant of line defect in 2D Photonic Crystals of dielectric rods in air: A Simulation based analysis" *Int. J. of Engineering Research & Technology*, vol. 1, no. 5, pp.1-10, 2012.

[22] Benjamin G. Griffin, Amir Arbabi, Meng Peun Tan, Ansas M. Kasten, Kent D. Choquette, Lynford L. Goddard,"Demonstration of enhanced side-mode suppression in metal-filled photonic crystal vertical cavity lasers", *Optics Letters,* vol. 38, no. 11,pp.1-3,2013.

[23] M. Tan, S.T.M. Fryslie, J.K. Guenter, J.A. Tatum, R.H. Johnson, K.D. Choquette, "Photonic crystal VCSELs with narrow spectral width and high bandwidth operating at low current density" *Electronics Letters*, vol. 49, no. 9, pp1-2, 2013.

[24] Fan, Shanhui, J. D. Joannopoulos,"Analysis of guided resonances in photonic crystal slabs", *Physical Review B, vol.* 65**,** no.23, pp.235112-235120, 2002.

[25] Vilson R. Almeida, Qianfan Xu, Carlos A. Barrios, Michal Lipson, "Guiding and confining light in void nanostructure" *Optics Letters,* vol.29, no.11,pp.1209-1211, 2004.

[26] C. A. Barrios, B. Sanchez, K. B. Gylfason, A. Griol, H. Sohlström, M. Holgado, R. Casquel, "Demonstration of slot-waveguide structures on silicon nitride / silicon oxide platform" Optics Express, Vol 15, no.11, pp.6846-6856, 2007.

[27] Allon I. Hochbaum, Rong Fan, Rongrui He, Peidong Yang, ""Controlled Growth of Si Nanowire Arrays for Device Integration" vol.5, no.3, pp. 457-460, vol. 5, no. 3, pp. 457-460, 2005.

[28] Mohammadreza Khorasaninejad, Simarjeet Singh Saini, "Silicon nanowire optical waveguide" *Optics Express*, vol.18, no,22, pp. 23442-23457,2010.

[29] William L. Barnes, Alain Dereux, Thomas W. Ebbesen, "Surface plasmon Subwavelength optics" *Nature,* vol. 424, pp.824-830, 2003.

[30] M Khorasaninejad, SM Raeis-Zadeh, S Jafarlou, MJ Wesolowski, CR Daley, JB Flannery, J Forrest, S Safavi-Naeini, SS Saini, "Highly Enhanced Raman Scattering of Graphene using Plasmonic Nano-Structure,"Scientific reports 3, article no.2936, 2013.

[31] A.E. Rider , K. Ostrikov, S.A. Furman, "Plasmas meet Plasmonics" *The European Physical Journal D*,66:226, PP.1-19, 2012.

[32] Sathish Malathi, Nivesh Mangal, Shafeek A. Samad, Rajini V. Honnungar, T. Srinivas "SOI strip waveguide microring resonator for homogeneous biosensing", *SPIE Proceedings*, vol 8129, Novel Optical Systems Design and Optimization XIV, 2011.

[33] M. K. Majumder, N. D. Pandya, B. K. Kaushik, S. K. Manhas, “Dynamic Crosstalk Effect in Mixed CNT Bundle Interconnects,” *Electronics Letters*, vol. 48, no.7, pp. 384-385, 2012.

[34] V. Ramesh Kumar, B. K. Kaushik, A. Patnaik, "An accurate model for dynamic crosstalk analysis of CMOS gate driven on-chip interconnects using FDTD method," *Microelectronics Journal*, vol.45,no.4, pp.441-448, 2014.

[35] S. A. Maier, P. E. Barclay, T. J. Johnson, M. D. Friedman, O. Painter, “Low-loss fiber accessible Plasmon waveguide for planar energy guiding and sensing”, *Applied Physics*, vol. 84, no. 20 , pp.3390-3392, 2004.

[36] R.Charbonneau, N.Lahoud, G.Mattiussi, P.Berini, “Demonstration of integrated elements based on long-ranging surface Plasmon polaritons”, *Optics Express,* vol.13 no.3, pp. 977–984, 2005.

[37] D.F.P.Pile, T.Ogawa, D.K.Gramotnev, T.Okamoto, M.Haraguchi, M.Fukui,S. Matsuo, “Theoretical and experimental investigation of strongly localized plasmons on triangular metal wedges for subwavelength waveguiding”, *Applied Physics,* vol. 87, no.6, pp.261114-261117, 2005.

[38] V.S.Volkov, E.Devaux, J.-Y.Lalue, T.W.Ebbesen, “Channel Plasmon subwavelength waveguide components including interferometers and ring resonators”. *Nature,* vol. 440, pp**.**508–511, 2006.

[39] M.Yan ,M.Qiu, “Guided Plasmon polariton at 2D metal corners”, *Journal of Optical Society of America B,* vol. 24, no.9, pp. 2333–2342, 2007.

[40] L.Chen, J.Shakya, M.Lipson, “Subwavelength confinement in integrated metal slot waveguide on silicon”, *Optics Letters,* vol 31,no.14, pp.2133–2135, 2006.

[41] A.V.Krasavin, A.V.Zayats, “Passive photonic elements based on dielectric-loaded surface Plasmon polariton waveguides”. *Applied Physics,* vol. 90, no. 21, pp. 211101-211103, 2007.

[42] Ajanta Barh, B. M. Azizur Rahman, Ravi K. Varshney, Bishnu P. Pal,“Design and Performance Study of a Compact SOI Polarization Rotator at 1.55 μm” Journal of Lightwave Technology, vol. 31, no. 23, pp. 3687-3693, 2013.

[43] T.Baehr-Jones, M.Hochberg, G.Wang, R.Lawson, Y.Liao, P.A.Sullivan, L.Dalton, “Optical modulation and detection in slotted Silicon waveguides”, *Optics Express,* vol. 13**,** no.14, pp.5216-5226, 2005.

[44] AF Roudsari, SS Saini, MP Anantram, "Junction-less phototransistor with nanowire channels, a modeling study," Optics Express, vol.22, no.6, pp.6391-6399, 2014.

[45] R.Slavador, A. Martinez, C. G-Meca, R.Ortuno, J. Marti, "Analysis of hybrid dielectric plasmonic waveguides", *IEEE Journal of Selected Topics in Quantum Electronics* ,vol. 14, no.6, pp.1496-1501, 2008.

[46] D.Dai, S.he, "A silicon-based hybrid plasmonic waveguide with a metal cap for a nano-scale light confinement", *Optics Express,* vol. 17, no. 19, pp.16646–16653, 2009.

[47] M. Z. Alam, J. Meier, J. S. Aitchison, M. Mojahedi, "Propagation characteristics of hybrid modes supported by metal-low-high index waveguides and bends", *Optics Express,* vol.18, no.12, pp.12971–12979, 2010.

[48] M. Z. Alam, J. Stewart Aitchison,Mo Mojahedi*, "Theoretical Analysis of Hybrid Plasmonic Waveguide"* IEEE Journal of Selected topics in quantum electronics, vol. 19, no. 3, p. 4602008, 2013.

[49] M. Z. Alam, J. Meier, J. S. Aitchison, M. Mojahedi, "Supermode propagation in low index medium," in conference on Laser and Electro-optics/ Quantum Electronics and Laser Science conference and Photonic Application systems Technologies,, paper JThD112, 2007.

[50] D. Sarid, "Long-range surface-plasma waves on very thin metal films," *Phys. Rev. Lett.*, vol. 47, no. 26, pp. 1927–1930, 1981.

[51] P. Berini, "Plasmon-polariton waves guided by thin lossy metal films of finite width: Bound modes of symmetric structures," *Phys. Rev. B*, vol. 61, no. 15, p. 10484, Apr. 2000.

[52] G. Veronis, S. Fan, "Bends and splitters in metal–dielectric–metal subwavelength plasmonic waveguides," *Appl. Phys. Lett.*, vol. 87, p. 131102, 2005.

[53] F.P.Kapron, D.B.Keck, R.D.Maurer, "Radiation losses in glass optical waveguides", *Applied Physics Letter*, vol.17**,** no. 10, pp**.**423-425, 1970.

[54] E Snitzer, "Cylindrical dielectric waveguide modes", *Journal of Optical Society of America*, vol. 51, no.5, pp.491-498, 1961.

[55] A.Yariv, "Optical Electronics in Modern Communications", Oxford Series in Electrical & Computer Engineering, Oxford *University Press, New York*, 5th edition, 1997.

[56] D. Marcuse. "Theory of Dielectric Optical Waveguides", *Academic Press, New York*, 2nd edition, 1974.

[57] S.Ramo, J.R.Whinnery Theodore, Van Duzer, "Fields and Waves in Communication Electronics", *Wiley New York,* 1st edition,1965.

[58] D. G. Peter, A.Yariv, "Interferometry and laser control with fabry-perot etalons", *Applied Optics*, vol.5, no.6, pp. 985-991, 1966.

[59] G. D. Boyd, J. P. Gordon, "Confocal multimode resonator for millimeter through optical wavelength masers", *Bell System Technical Journal*, vol. 40, no.2 **,** pp.453-488, 1961.

[60] W. Bogaerts, P. De Heyn, T. Van Vaerenbergh, K. De Vos, S. Selvaraja, T. Claes, P. Dumon, P. Bienstman, D. Van Thourhout, R. Baets, "Silicon Microring Resonators", *Lasers and Photonics Review*, vol. 6, no.1, pp.47-73, 2012.

[61] G.R.Bhatt, B.K.Das, "Improvement of polarization extinction in silicon waveguide devices," *Optics Communication*, vol. 285, no. 8, pp. 2067-2070, 2012.

[62] Jing Xiao, Jiansheng Liu, Yusheng Bian, GuanjunWang, "Design and analysis of a nanostructure grating based on a hybrid plasmonic slot waveguide", *Journal of Optics,* vol.13, no.10**,** pp.105001-105004, 2011.

[63] Yao Kou, Fangwei Ye, and Xianfeng Chen", Low-loss hybrid plasmonic waveguide for compact and high-efficient photonic integration", *Optics Express,* vol.19, no.12, pp.11746-11752, 2011.

[64] J. Volker Sorger1, Ziliang Ye1, Rupert F. Oulton, "Experimental demonstration of low-loss optical waveguiding at deep sub-wavelength scales", *Nature communications,* vol. 2, article no.3, pp.1315-1319, 2011.

[65] Yu Wakabayashi, Junji Yamauchi, Hamamatsu Nakano, "A TM-Pass/TE-Stop Polarizer Based on a Surface Plasmon Resonance", *Hindawi Publishing Corporation Advances in Optoelectronics,* vol.2011, Article ID 867271 ,pp.867271-867277, 2011.

[66] Hong-Son Chu, Ping Bai, Er-Ping Li, "Characterization of Planar Hybrid Dielectric loaded Plasmonic nano Waveguides used for nano-Photonic Circuits", *Microwave Symposium Digest (MTT)*IEEE MTT-S International, pp.1-4, 2011.

[67] Yi Song, Jing Wang, Min Yan, Min Qiu, "Efficient coupling between dielectric and hybrid plasmonic waveguides by multimode interference power splitter", *Journal of Optics,* vol. 13, no.7, pp.075002-075009, 2011.

[68] Lin Zhu, "Modal Properties of Hybrid Plasmonic Waveguides for Nanolaser Applications", *IEEE Photonics Technology Letters*, vol. 22, no. 8, pp.535-537, 2010.

[69] Yi Song, Jing Wang, Qiang Li, Min Yan, Min Qiu, " Broadband Coupler Between Silicon Waveguide And Hybrid Plasmonic Waveguide", *Optics Express,* vol 18, no. 12, pp.13173-13179, 2010.

[70] Jian-wei mu, Wei-ping huang, "A low loss Surface Plasmonics Bragg Grating", *IEEE Journal of light wave technology,* vol **27,** no. 4**,** pp.436-439, 2009.

[71] Hamed Dalir, Fumio Koyama, "Highly efficient out-of-plane optical coupler based on tapered hollow waveguide" *Japanese Journal of Applied Physics,* vol 53, no.4, p.048004, 2014.

[72] Qin Zhang, Xu-Guang Huang, Xian-Shi Lin, Jin Tao, Xiao-Ping Jin, "A subwavelength coupler-type metal-insulator-metal optical filter", *optics express,* vol.17, no.9, pp.7549-7555, 2009.

[73] K. Dmitri Gramotnev, Sergey Bozhevolnyi, "Plasmonics beyond the diffraction limit", *Nature photonics,* vol 4**,** pp.83-91, 2009.

[74] R.F.Oulton, V.J.Sorger, D.A.Genov, D.F.P.Pile, X.Zhang, "A hybrid plasmonic waveguide for subwavelength confinement and long-range propagation", *Nature Photonics*, vol.**2,** pp.496–500, 2008.

[75] R.F.Oulton, G.Bartal, D F P Pile and X Zhang, "Confinement and propagation characteristics of subwavelength plasmonic modes", *New Journal of Physics,* vol.10, pp.105018-105032, 2008.

[76] Georgios Veronis, Shanhui Fan, "Modes of Subwavelength Plasmonic Slot Waveguides", *IEEE Journal of Light Wave Technology* vol. 25**,** no.9,pp.2511-2521, 2007.

[77] A Stefan. Maier, "Plasmonics: The Promise of Highly Integrated Optical Devices'', *IEEE Journal of Selected Topics in Quantum Electronics,* vol.12**,** no. 6, pp.1671-1677, 2006.

[78] Amir Hosseini, Yehia massoud, "A low-loss metal-insulator-metal plasmonic Bragg reflector", *Optics Express,* vol.14, no. 23 , pp.318-323, 2006.

[79] Xiang-Tian Kong, Wei-Guo Yan, Zu-Bin Li, Jian-Guo Tian, "Optical properties of metal-multi-insulator metal plasmonic waveguides", *Optics Express,* vol. 20, no. 11, pp.12133-12146, 2012.

[80] Linfei Gao, Liangxiao Tang, Feifei Hu, Ruimin Guo, Xingjun Wang, Zhiping Zhou, "Active metal strip hybrid plasmonic waveguide with low critical material gain", *Optics express,* vol. 20, no.10, pp. 11487-11595, 2012.

[81] T. P. H. Sidiropoulos, S. A. Maier, R. F. Oulton, "Efficient low dispersion compact plasmonic-photonic coupler", *Optics express,* vol. 20, no. 11 , pp.12359-12365, 2012.

[82] Lin Chen, Tian Zhang, Xun Li, Weiping Huang, "Novel hybrid plasmonic waveguide consisting of two identical dielectric nanowires symmetrically placed on each side of a thin metal film", *Optics Express, vol.* 20, no. 18 , pp. 20535-20544, 2012.

[83] Mukesh Kumar, Takahiro Sakaguchi, Fumio Koyama "Tunable Three-Dimensional Nanostep Hollow Optical Waveguide with Low Polarization Dependence" *Applied Physics Express,* vol. 1, p.052002-3, 2008.

[84] Mukesh Kumar, "A hollow waveguide Bragg reflector: A tunable platform for integrated photonics" *Optics & Laser Technology*, vol. 65, pp. 5-13, 2015.

[85] I. G. Breukelaar, "Surface plasmon-polaritons in thin metal strips and slabs:Wave guiding andmode cutoff," Master Thesis, School Inf. Technol. Eng., University of Ottawa, Ottawa, Canada, 2004.

[86] J. T. Robinson, K. Preston, O. Painter, M. Lipson, "First-principle derivation of gain in high-index-contrast waveguides," *Optics Express* vol.16, no. 21, pp.16659–16669, 2008.

[87] P. Muellner, M. Wellenzohn, R. Hainberger, "Nonlinearity of optimized silicon photonic slot waveguides," *Optics Express*, vol.17, no. 11, pp.9282–9287, 2009.

[88] Y. Kou, F. Ye, X. Chen, "Low-loss hybrid plasmonic wave guide for compact and high-efficient photonic integration," *Optics Express,* vol. 19, no. 12, pp.11746–11752, 2011.

[89] X. Yang, Y. Liu, R. F. Oulton, X. Yin, X. Zhang, "Optical forces in hybrid plasmonic waveguides," *Nano Letters,* vol. 11, no.2, pp. 321–328, 2011.

[90] Johnson P. B., Christie R. W., "Optical constants of the noble metals" *Phys. Rev. B,* vol. *6,* no.12, pp. 4370–4379, 1972.

[91] P. D. Flammer, J. M. Banks, T. E. Furtak, C. G. Durfee, R. E. Hollingsworth, R. T. Collins, "Hybrid Plasmon/dielectric waveguide for Integrated Silicon-on-Insulator Optical Elements" *Optics Express,* vol. 18, no. 20, pp.21013-21014, 2010.

[92] Mukesh Kumar, Takahiro Sakaguchi, Fumio Koyama, "Polarization Insensitive and Low-Loss 3-D Nanostep Hollow Waveguide for Widely Tunable Photonic Devices" *Journal of Lightwave Technolology,* vol. 26, no. 11, pp. 1417-1422, 2008.

[93] Frank Trager, "Handbook of Laser and optics", Springer-Verlag publisher, 2012.

[94] Robert W. Boyd, "Nonlinear optics", San Diego, Academic Press 2008.

[95] A. Pitilakis, O. Tsilipakos, E. E. Kriezis, "Nonlinear effect in Hybrid Plasmonic Waveguide" *in Proceeding of IEEE,* 14th ICTON, pp. 1-4, 2012.

[96] A. Pitilakis, E. E. Kriezis, "Highly-nonlinear hybrid silicon-plasmonic waveguides: analysis and optimization" *Journal of Optical Society of America B.* vol 30, no.7, pp.1954-1965, 2013.

[97] M. Hossain, Mark D. Turner, Min Gu, "Ultrahigh Nonlinear nanoshell plasmonic waveguide with total energy confinement" *Optics Express,* vol. 19, no.24, pp.23800-23808, 2011.

[98] S. A. Maier, P. G. Kik, H. A. Atwater, S. Meltzer, E. Harel, B. E. Koel, A. A. G. Requicha, "Local detection of electromagnetic energy transport below the diffraction limit in metal nanoparticle plasmon waveguides," *Nature Material,* vol. **2**, no.4, pp. 229–232, 2003.

[99] C. Xiang, J. Wang, "Long-Range Hybrid Plasmonic Slot Waveguide", *IEEE Photonics,* vol.5, no.2, p.4800311, 2013.

[100] M. Z. Alam, J. Stewart Aitchison, M. Mojahedi, "Compact and silicon-on-insulator compatible hybrid plasmonic TE-pass polarizer" *Optics Letters,* vol. 37, no. 1, pp.55-57, 2012.

[101] Huang MCY, Zhou Y, Chang-Hasnain CJ. "A surface-emitting laser incorporating a high-index-contrast subwavelength grating", *Nature Photonics,* vol.1, pp.119-122, 2007.

[102] Shunya Inoue, Junichi Kashino, Akihiro Matsutani, Hideo Ohtsuki, Takahiro Miyashita, Fumio Koyama, "Highly angular dependent high-contrast grating mirror

and its application for transverse-mode control of VCSELs", *Japanese Journal of Applied Physics*, vol.53, no.9, p. 090306, 2014.

[103] Y. Zhou, Michael C. Y. Huang, Christopher Chase, Vadim Karagodsk, Michael Moewe, Bala Pesala, Forrest G. Sedgwick, Connie J. Chang-Hasnain, "High-Index-Contrast Grating (HCG) and Its Applications in Optoelectronic Devices" *IEEE Journal of Selected Topics in Quantum Electronics*, 1485, pp.1-15, 2009.

[104] M. Kumar, Chris Chase, Vadim Karagodsky, Takahiro Sakaguchi,Fumio Koyama, Connie J.Chang-Hasnain, "Low Birefringence and 2-D Optical Confinement of Hollow Waveguide With Distributed Bragg Reflector and High-Index-Contrast Grating", *IEEE Photonics*, vol.1, no.2, pp. 135-143, 2009.

[105] A.Hosseini, Hamid Nejati, Yehia Massoud, "Modeling and design methodology for metal-insulator-metal plasmonic Bragg reflectors" *Optics Express*, vol.16, no.3, pp. 13173-13179, 200

[106] Y.A.Vlasov, "Silicon CMOS-Integrated Nano-Photonics for Computer and Data Communications Beyond 100G", *IEEE Communication Magazine*, vol.50, no.2, pp-67-72, 2012.

[107] D. T. H. Tan, K. Ikeda, S. Zamek, A. Mizrahi, M. P. Nezhad, A. V. Krishnamoorthy, K. Raj, J. E. Cunningham, X. Zheng, I. Shubin, Y. Luo, Y. Fainman, "Wide bandwidth, low loss 1 by 4 wavelength division multiplexer on silicon for optical interconnects", *Optics Express*, vol. 19, no.3, pp. 2401-2409, 2011.

[108] R. Chen, Thai-Truong D. Tran, Kar Wei Ng, Wai Son Ko, Linus C. Chuang, Forrest G. Sedgwick, Connie Chang-Hasnain, "Nanolasers grown on silicon", *Nature Photonics*, vol. 5, pp. 70–75,2011.

[109] R. F. Oulton, Volker J. Sorger, Thomas Zentgraf, Ren-Min Ma, Christopher Gladden, Lun Dai, Guy Bartal, Xiang Zhang," Plasmon lasers at deep subwavelength scale," *Nature*, vol. 461, pp.629-632 ,2009.

[110] J. Hua Zhang, Ping Zhao, Eric Cassan, Xin Liang Zhang, "Phase regeneration of phase-shift keying signals in highly nonlinear hybrid plasmonic waveguides", *Optics Letters*, vol.38, no.6, pp.848–850, 2013.

[111] M.Yin, Qingzhong Deng, Yanping Li, Xingjun Wang, Hongbin Li, "Ultrashort and Low-Loss Polarization Rotators Utilizing Hybrid Plasmonic-Dielectric Couplers," *IEEE Photonics Technology Letters*, vol. 27, no. 3, pp. 229-232, 2015.

[112] M. Z. Alam, J.Niklas Caspers, J. S. Aitchison, M. Mojahedi, "Compact low loss and broadband hybrid plasmonic directional coupler" *Optics Express*, vol. 21, no. 13, pp.16029-16034, 2013.

[113] C.Han Du, Yih-Peng Chiou, "Vertical Directional Couplers With Ultra-Short Coupling Length Based on Hybrid Plasmonic Waveguides", *Journal of Lightwave Technology*, vol. 32, no.11,pp. 2065-2071, 2014.

[114] Tian, S. Q. Yu, W. Yan, M. Qiu, "Broadband high-efficiency surface plasmon-polariton coupler with silicon-metal interface" *Applied Physics Letters*, vol.95, p.013 504, 2009.

[115] Tohmori Y, Suematsu Y, TushimaY, Arai S. "Wavelength tuning of GaInAsP/InP integrated laser with butt-jointed built-in distributed Bragg reflector" *Electron Letters* vol,19, no.17, pp.656-657, 1983.

[116] M. Kumar, Takahiro Sakaguchi, Fumio Koyama, "Polarization-Insensitive and Low-Loss 3-D Nanostep Hollow Waveguide for Widely Tunable Photonic Devices", *Journal of Lightwave Technology*, vol. 26, no.11, pp. 1417-1422, 2008.

[117] Kumar M. "Narrow bandwidth and polarizationin dependent design of hollow waveguide in-plane mirror with ultra-wide tuning range", *Applied Optics*, vol. 52, no. 9, pp.1847–51, 2013.